

PTK7 protein localization and stability is affected by canonical Wnt ligands

Doctoral Thesis

In partial fulfillment of the requirements for the degree
“Doctor rerum naturalium (Dr. rer. nat.)”
in the GGNB program: “Genes and Development”
at the Georg August University Göttingen
Faculty of Biology

submitted by

Hanna Irena Berger
born in Katowice, Poland

Göttingen, Oktober 2015

Members of the Thesis Committee:

Supervisor:

Prof. Dr. Annette Borchers,
Molecular Embryology, Philipps University Marburg

Second member of the thesis committee:

Prof. Dr. Andreas Wodarz,
Institute I of Anatomy, University of Cologne

Third member of the thesis committee:

Prof. Dr. Renate Renkawitz-Pohl,
Animal developmental biology, Philipps University Marburg

Date of the oral examination:

Affidavit

Herewith I declare that I prepared the doctoral thesis “PTK7 protein localization and stability is affected by canonical Wnt ligands” on my own and with no other sources and aids as quoted.

Submission date

27.10.2015

Hanna Irena Berger

Table of Contents

Acknowledgements	VI
Abstract	VII
List of Figures	VIII
List of Tables	X
Abbreviations	XI
1 Introduction	1
1.1 Wnt signaling pathways	1
1.2 Core components of Wnt signaling pathways	3
1.2.1 Wnt proteins	3
1.2.2 Frizzled receptors	5
1.2.3 Dishevelled	6
1.3 Canonical Wnt signaling	7
1.3.1 Molecular mechanism of canonical Wnt signaling	7
1.3.2 Developmental processes regulated by canonical Wnt signaling	9
1.4 Planar cell polarity signaling	12
1.4.1 Molecular mechanism of planar cell polarity signaling (PCP)	12
1.4.2 Developmental processes regulated by PCP	15
1.5 Regulation of Wnt signaling by endocytosis.....	19
1.5.1 Endocytosis	19
1.5.2 Regulation of canonical Wnt signaling by receptor-mediated endocytosis	22
1.5.3 Regulation of non-canonical Wnt signaling by receptor-mediated endocytosis.....	25
1.6 Regulation of canonical Wnt signaling by caveolin-1, independent of endocytosis	26
1.7 PTK7	27
1.7.1 PTK7 functions in Wnt signaling	28
1.7.2 PTK7 is a target for proteolytic cleavage.....	31

1.8	The role of caveolin in early vertebrate development.....	33
1.8.1	Caveolae and the caveolin protein family.....	33
1.8.2	Phenotypes of caveolin-deficient vertebrates.....	35
1.9	Aim of this study.....	38
2	Materials and Methods	39
2.1	Model Organisms	39
2.2	Bacteria.....	39
2.3	Cell lines.....	39
2.4	Chemicals, Buffers and Media.....	39
2.4.1	Chemicals.....	39
2.4.2	Buffers and Media	39
2.5	Vectors and Constructs	43
2.5.1	Vectors	43
2.5.2	Expression constructs.....	44
2.5.3	Linearization of constructs for sense or antisense <i>in vitro</i> transcription.....	46
2.6	Oligonucleotides.....	46
2.6.1	Cloning primers	46
2.6.2	Sequencing primers.....	47
2.6.3	Morpholino oligonucleotides	47
2.7	Antibodies	47
2.8	DNA methods and cloning procedures	49
2.8.1	Isolation of plasmid DNA from <i>E.coli</i>	49
2.8.2	Polymerase chain reaction.....	49
2.8.3	Colony PCR.....	50
2.8.4	Agarose gel electrophoresis	50
2.8.5	Purification of DNA fragments from agarose gels	50
2.8.6	Restriction digestion of DNA.....	51
2.8.7	Ligation of DNA-fragments.....	51
2.8.8	Chemical transformation of E. coli cells	51

2.8.9 Sequencing of DNA	51
2.9 RNA methods.....	52
2.9.1 <i>In vitro</i> synthesis of capped sense RNA.....	52
2.9.2 <i>In vitro</i> synthesis of labeled antisense RNA	52
2.10 Cell culture techniques	53
2.10.1 Propagation of cell lines.....	53
2.10.2 Transfection of plasmid DNA into eukaryotic cells	53
2.10.3 Treatment of MCF7 cells with recombinant Wnt proteins and chemical inhibitors	54
2.11 <i>Xenopus laevis</i> techniques	54
2.11.1 Isolation of <i>Xenopus laevis</i> testis	54
2.11.2 <i>Xenopus</i> embryo microinjection and cultivation	55
2.11.3 Fixation and X-gal staining.....	55
2.11.4 <i>Xenopus</i> second axis assay	55
2.11.5 Embedding of <i>Xenopus</i> embryos for vibratome sectioning.....	56
2.11.6 Actin staining of <i>Xenopus</i> vibratome sections using phalloidin.....	56
2.12 Protein techniques.....	56
2.12.1 Preparation of protein extracts from MCF7 cells	56
2.12.2 Preparation of protein extracts from <i>Xenopus</i> embryos	56
2.12.3 SDS - polyacrylamide gel electrophoresis.....	57
2.12.4 Western blot	57
2.12.5 Co-Immunoprecipitation (Co-IP)	58
2.12.6 Cell surface biotinylation.....	58
2.12.7 <i>In vitro</i> coupled transcription/translation reactions	58
2.13 Whole-mount in situ hybridization (WISH)	59
2.14 Immunofluorescence	61
3 Results	63
3.1 PTK7 changes its cellular localization in response to canonical Wnt proteins	63
3.1.1 Wnt3a stimulation mediates PTK7 translocation	63

3.1.2	Wnt3a-dependent PTK7 internalization is independent of its kinase homology domain.....	65
3.1.3	Cell surface levels of PTK7 decrease in the presence of canonical Wnt ligands.....	67
3.2	Proteolytic cleavage of PTK7 is not induced in response to canonical Wnt proteins.....	68
3.3	PTK7 translocates from the membrane to the cytoplasm together with canonical Wnt2b.....	70
3.4	PTK7 is endocytosed via a caveolin-dependent pathway.....	72
3.4.1	PTK7 and caveolin-1 co-localize in vesicle-like structures in the cytoplasm in response to Wnt3a.....	72
3.4.2	Inhibition of caveolin-mediated endocytosis prevents PTK7 endocytosis.....	75
3.4.3	PTK7 interacts with caveolin-1.....	79
3.4.4	PTK7 endocytosis is independent of clathrin.....	80
3.4.5	PTK7 co-localizes with caveolin-1 but not with clathrin at the basal plasma membrane upon Wnt3a treatment.....	83
3.5	PTK7 is degraded in the lysosome in response to Wnt3a.....	85
3.5.1	PTK7 protein levels decrease upon Wnt3a treatment.....	85
3.5.2	Canonical Wnt proteins target PTK7 for proteasomal degradation via a caveolin-mediated pathway.....	86
3.6	Caveolin-1 loss-of-function decreases the inhibitory effect of PTK7 on canonical Wnt signaling.....	88
3.7	The function of caveolin-1 in <i>Xenopus</i> development.....	90
3.7.1	Caveolin-1 knockdown leads to swimming defects, eye defects and bended <i>Xenopus</i> embryos.....	90
3.7.2	Co-injection of caveolin-1 α mRNA rescues the caveolin-1 α knockdown swimming defect.....	92
3.7.3	Caveolin-1 α protein expression is inhibited by Cav-1 α MO, but not by Cav-1 β MO.....	93
3.7.4	Caveolin-1 α is localized to the notochord of <i>Xenopus</i> embryos.....	93
3.7.5	Caveolin-1 α knockdown causes disruption of the actin filaments.....	94

3.7.6 Caveolin-1 α depletion has no effect on Twist, Xbra or MyoD patterning, but leads to aberrant Pax2 expression.....	95
4 Discussion.....	98
4.1 PTK7 endocytosis and co-receptor context	98
4.2 PTK7 is endocytosed via a caveolin-mediated pathway in response to canonical Wnt proteins.....	99
4.3 Mutual inhibition of PTK7 and canonical Wnt proteins	100
4.4 PTK7 modulates Wnt signaling.....	102
4.5 Signaling function of PTK7	104
4.6 PTK7 regulates diverse signaling pathways	105
4.7 Function of caveolin-1 during <i>Xenopus</i> development.....	106
4.7.1 Caveolin-1 depletion leads to impaired swimming behavior in <i>Xenopus</i>	106
4.7.2 The loss of caveolin-1 leads to disrupted actin filaments in the somites.....	107
4.7.3 Caveolin-1 loss-of-function might lead to neuronal disorders	108
5 Conclusion.....	110
6 References.....	111

Acknowledgements

First of all, special thanks to my supervisor Prof. Dr. Annette Borchers for giving me the opportunity to work on this interesting project. Thanks for always taking the time to answer my questions, to motivate and encourage me during my work and to support me with all your knowledge and experience.

I would like to thank the members of my thesis committee, Prof. Dr. Andreas Wodarz and Prof. Dr. Renate Renkawitz-Pohl, for the helpful support, discussions and ideas during my thesis committee meetings and beyond.

Furthermore, I thank my former lab colleagues, Martina and Peter for all the help and support especially during the start of my PhD. Special thanks to Martina for the discussions about my project and for all the helpful advices. Thanks to my current lab members Ewa, Janina, Anita, Marlen, Barbara, Ingrid, Melanie and Christiane for the friendly and helpful atmosphere in our group. It is/was fun to work with all of you, making my PhD time really enjoyable.

Huge thanks to my friends that were always on my side to share happiness with me if things went good or to cheer me up if things went bad.

Special thanks to my family, my parents, grandparents, my sister Nina and Luis for your love and support, for always trusting in me and supported me during my PhD.

Abstract

Wnt co-receptors have been shown to be endocytosed in response to Wnt proteins. However, the role of Wnt receptor internalization for Wnt signaling is a topic of ongoing research. Here we show that the Wnt co-receptor PTK7 (protein tyrosine kinase 7) is internalized via a caveolin-mediated pathway upon stimulation with canonical Wnt ligands. PTK7 is an evolutionary conserved transmembrane receptor that regulates a broad range of processes including the determination of planar cell polarity and the regulation of cell migration. Previous data from our lab revealed that PTK7 acts as Wnt co-receptor activating non-canonical PCP/Wnt signaling through Dsh-recruitment to the plasma membrane. Further, our findings indicate that PTK7 binds canonical but not non-canonical Wnt proteins and inhibits canonical Wnt signaling. This study shows that the cellular PTK7 protein localization is affected by canonical Wnt ligands. PTK7 is translocated from the plasma membrane to the cytoplasm upon Wnt3a stimulation. Interestingly, PTK7 and canonical Wnt proteins are internalized together as a ligand/receptor complex. In contrast, non-canonical Wnt ligands, which do not interact with PTK7, do not affect PTK7 membrane localization. PTK7 internalization is mediated by a caveolin-dependent pathway and prevented by inhibitors of caveolin-mediated endocytosis. Furthermore, we found evidence that canonical Wnt ligands trigger lysosomal PTK7 degradation. PTK7 protein levels decrease in response to canonical Wnt ligands, which does not happen after inhibition of lysosomal degradation. These data suggest a model of PTK7 function, whereby PTK7 likely inhibits canonical Wnt signaling by binding canonical Wnt ligands. Thereby canonical Wnt ligands are trapped in a PTK7-complex in the cytoplasm and their interaction with Wnt receptors supporting canonical Wnt signaling is prevented. Conversely, canonical Wnt proteins trigger PTK7 lysosomal degradation, indicating a mutual inhibition between canonical Wnt signaling and PTK7 signaling.

In the context of caveolin-mediated internalization of PTK7, caveolin-1 depletion in *Xenopus* embryos was analyzed. Interestingly, caveolin-1 deficient embryos exhibit an impaired swimming behavior. Caveolin-1 is the best characterized member of the caveolin protein family, that includes three members in vertebrates, caveolin-1,-2 and -3. Here we show that caveolin-1 is strongly expressed in the notochord of *Xenopus* embryos and its depletion severely impairs swimming behavior. Co-injection of *caveolin-1* mRNA rescues this swimming defect. Morphological studies in caveolin-1 morphant embryos revealed disrupted actin filaments in muscle cells of the somites. These findings indicate that defects in muscle development upon caveolin-1 depletion might result in the observed abnormal swimming behavior of *Xenopus* embryos.

List of Figures

Figure 1: Wnt signaling pathways.	2
Figure 2: Posttranslational modifications and secretion of Wnt proteins.....	4
Figure 3: Structure of <i>Xenopus</i> Wnt8 in complex with Fz8.	5
Figure 4: Structure of Frizzled proteins	6
Figure 5: The conserved domains of Dishevelled.....	7
Figure 6: The canonical Wnt signaling pathway	9
Figure 7: Dorsal-ventral axis specification in <i>Xenopus</i>	11
Figure 8: Planar cell polarity.....	13
Figure 9: Molecular mechanism of PCP signaling.....	15
Figure 10: Examples of PCP phenotypes in <i>Drosophila</i> and mammals.....	16
Figure 11: PCP/convergent extension phenotype in the mouse	17
Figure 12: PCP signaling regulates neural crest cell migration.....	18
Figure 13: Endocytosis of ligand/receptor complexes	21
Figure 14: Regulation of Wnt signaling pathways by endocytosis	23
Figure 15: Dab2 directs LRP6 to different endocytic pathways	24
Figure 16: Regulation of non-canonical Wnt signaling by clathrin-mediated endocytosis	26
Figure 17: Protein structure of PTK7	27
Figure 18: PTK7 functions in Wnt signaling in vertebrates	30
Figure 19: Model of PTK7 with the MT1-MMP, ADAM and γ -secretase cleavage sites. .	32
Figure 20: Caveolae and caveolins	34
Figure 21: Phenotypes of caveolin-1 deficient zebrafish embryos.....	37
Figure 22: Canonical, but not non-canonical Wnt ligands, induce PTK7 internalization...64	
Figure 23: Quantification of PTK7 cellular localization in response to canonical or non-canonical Wnt proteins.....	65
Figure 24: Wnt3a-dependent Δ kPTK7 translocation is independent of its kinase domain	66
Figure 25: Quantification of Wnt3a-dependent Δ kPTK7 translocation	67
Figure 26: Cell surface PTK7 and Δ kPTK7 concentrations decrease after rhWnt3a treatment	68
Figure 27: rhWnt3a treatment does not induce PTK7 proteolysis.....	69
Figure 28: Wnt2b and PTK7 are translocated together to the cytoplasm.....	71
Figure 29: PTK7 endocytosis is mediated by caveolin-1	73
Figure 30: caveolin-1-mediated PTK7 endocytosis is independent of its kinase homology domain.....	74
Figure 31: PTK7 internalization is prevented by M β CD treatment.....	76
Figure 32: Δ kPTK7 internalization is prevented by M β CD treatment.....	78

Figure 33: PTK7 and Δ PTK7 interact with caveolin-1	79
Figure 34: PTK7 infrequently co-localizes with clathrin	81
Figure 35: Δ kPTK7 hardly co-localizes with clathrin	82
Figure 36: PTK7 and caveolin-1 co-localize at the basal plasma membrane after Wnt3a stimulation	84
Figure 37: PTK7 protein concentrations decrease in response to canonical Wnt proteins	86
Figure 38: Inhibition of lysosomal degradation prevents Wnt3a-induced decrease of PTK7 protein	87
Figure 39: Caveolin-1 α loss-of-function prevents PTK7-mediated inhibition of canonical Wnt signaling in <i>Xenopus</i> second axis assay	89
Figure 40: Caveolin-1 depletion leads to swimming defects, eye defects and bended embryos.....	91
Figure 41: <i>Caveolin-1α</i> mRNA rescues the Cav-1 α MO induced swimming defect	92
Figure 42: Cav-1 β MO does not affect caveolin-1 α protein expression	93
Figure 43: Caveolin-1 α is localized in the notochord in <i>Xenopus</i> embryos.....	94
Figure 44: Caveolin-1 depletion leads to the disruption of the actin cytoskeleton	95
Figure 45: Caveolin-1 α depletion has no effect on <i>Twist</i> patterning, but leads to aberrant <i>Pax2</i> expression	96
Figure 46: Caveolin-1 α depletion has no effect on <i>Xbra</i> or <i>MyoD</i> patterning.....	97
Figure 47: Molecular mechanism of PTK7 function	102

List of Tables

Table 1: Expression constructs used in this study	44
Table 2: Restriction enzymes for linearization of constructs and polymerases used for <i>in vitro</i> transcription	46
Table 3: Antisense Morpholino oligonucleotides.....	47
Table 4: Antibodies	47
Table 5: Temperature profile of the PCR reaction	50
Table 6: <i>In vitro</i> synthesis of antisense RNA	52
Table 7: Amounts of nucleic acids, Lipofectamin and medium are given according to the respective culture vessel.....	54
Table 8: Rehydration of embryos	59
Table 9: Proteinase K treatment	59
Table 10: Acetylation of embryos	60
Table 11: Washing steps and RNase treatment	60
Table 12: Blocking and antibody reaction	61
Table 13: Washing and staining reaction	61

Abbreviations

A	Adenine
AA	amino acid
ADAM	A Disintegrin and Metalloproteinase
AP	alkaline phosphatase
AP	adaptor protein
APC	adenomatosis polyposis coli
APS	Ammonium Persulfate
ATP	Adenosine triphosphate
Axin	axis inhibitor
BCIP	5-bromo-4-chloro-3-indolyl-phosphate
BMB	Boehringer Mannheim blocking reagent
Bp	base pairs
BSA	Bovine serum albumin
C	Cytosine
°C	Degrees Celsius
CCK-4	colon carcinoma kinase-4
CE	convergent extension
Celsr1	Cadherin, EGF LAG seven-pass G-type receptor 1
CKI	casein kinase I
cm	Centimeter
CRD	cysteine-rich domain
C-terminus	Carboxy-terminus
CTP	cytidine triphosphate
DAAM1	dishevelled-associated activator of morphogenesis 1
DAPI	4',6-Diamidino-2-Phenylindole
Dgo	Diego
Dsh	Dishevelled
dH ₂ O	distilled water
Dig	digoxigenin
DNA	deoxyribonucleic acid
DNase	deoxyribonuclease
dNTP	Deoxynucleotide triphosphate
DTT	Dithiothreitol
<i>E. coli</i>	<i>Escherichia coli</i>
EDTA	Ethylendiamin-tetra-acetic acid
EGTA	ethylen glycolel-bis(2-aminoethylether)-N,N'- tetraacetate
ER	endoplasmatic reticulum
et al.	<i>et alii</i>
EtOH	ethanol
Fmi	Flamingo

for	forward
Fz	Frizzled
g	gram
G	Guanine
GFP	green fluorescent protein
GTP	Guanosine triphosphate
GSK3 β	glycogen synthase kinase β
h	hour
HA	hemagglutinin-tag
HCG	human chorionic gonadotropin
Hyb-mix	Hybridization mix
ICD	intracellular domain
Ig	Immunoglobulin
k	kilo
kb	kilo base
kDa	kilo-Dalton
L	liter
LB	Luria-Bertani
LEF	lymphoid enhancer
LRP5/6	low density lipoprotein receptor-related protein 5/6
M	Molar
MAB	maleic acid buffer
mg	Milligram
MgCl ₂	Magnesium chloride
min	Minute
ml	Millilitre
mm	Millimeter
mM	Millimolar
mRNA	messenger RNA
MT	Myc-tag
MT1-MMP	membrane type-1 matrix metalloproteinase
MUSK	muscle-specific kinase
MVB	multi vesicular bodies
μ g	Microgram
μ l	Microlitre
μ m	Micrometer
μ M	Micromolar
NBT	nitro-blue-tetrazolium
nm	Nanometer
nM	Nanomolar
N-terminus	Amino-terminus
Otk	Off-track
PAGE	polyacrylamid gel elektrohoresis

PBS	Phosphate buffered saline
PCC	Pearson Correlation Coefficient
PCP	Planar cell polarity
PCR	Polymerase chain reaction
pH	<i>potentium hydrogenium</i>
Pk	Prickle
PKC1	Protein kinase C
Pol	Polymerase
PTK7	protein tyrosine kinase 7
Rac1	Ras-related C3 botulinum toxin substrate 1
RACK1	Receptor for activated C kinase 1
rev	reverse
RhoA	Ras homologue
RNA	Ribonucleic acid
Ror1/2	RAR-related orphan receptor 1/2
rpm	Rounds per minute
RT	Room temperature
RYK	receptor-like tyrosine kinase
Scrb1	Scribble
sec	Second
SDS	sodium dodecyl sulfate
SSC	Standard sodium citrate
st	stage
Stbm	Strabismus
T	Thymine
TAE	Tris-Acetate-EDTA
Taq	<i>Thermus aquaticus</i>
TBS(T)	Tris-buffered saline (with Tween)
TCF	T-cell factor
Temp.	Temperature
Tris	Tris-hydroxymethyl-aminomethane
U	Units
UTP	uridine triphosphate
UV	Ultra violet light
V	Volt
VANG(L)	van Gogh (Like)
v/v	Volume to volume
Wg	Wingless
Wls	Wintless
w/v	Weight to volume
wt	wild type
X-Gal	5-Bromo-4-chloro-3-indoxyl-D- galactopyranoside

1 Introduction

1.1 Wnt signaling pathways

Wnt signaling pathways control diverse biological processes, such as cell proliferation, cell polarity and cell fate specification during embryonic development and adult tissue homeostasis in all metazoan organisms. Misregulated activation of Wnt signaling pathways often results in birth defects, cancer and various other diseases (MacDonald et al., 2009; Clevers and Nusse, 2012; Sokol, 2015). The first identified and best characterized Wnt pathway is the canonical (β -catenin-dependent) Wnt signaling pathway. Later, further β -catenin-independent pathways were detected and called non-canonical Wnt signaling pathways, one of which is the planar-cell-polarity (PCP) pathway (Kikuchi et al., 2009; Niehrs, 2012). Although intracellular signal transduction differs between the distinct Wnt signaling pathways, some upstream core proteins are shared. These proteins include the Wnt ligands, the Frizzled (Fz) family receptors and the cytoplasmic adaptor protein Dishevelled (Dsh), which forms the branching point between the different Wnt signaling pathways (Figure 1) (MacDonald et al., 2009; Niehrs, 2012; Sokol, 2015). Canonical Wnt signaling is activated by the binding of a Wnt ligand to its Frizzled receptor. Downstream signaling of the canonical Wnt pathway leads to the stabilization of β -catenin in the cell and to a subsequent activation of β -catenin-dependent target gene expression, thereby regulating cell proliferation and differentiation (Figure 1 A). Non-canonical PCP/Wnt signaling acts through small GTPases of the Rac/Rho family, leading to changes in the cytoskeleton and subsequent determination of cell polarity (Figure 1 B) (MacDonald et al., 2009; Kikuchi et al., 2011; Clevers and Nusse, 2012).

Most Wnt proteins preferentially activate either canonical or non-canonical Wnt signaling pathways. However, Wnt proteins cannot be strictly classified as canonical or non-canonical activators, because the signaling outcome additionally relies on the receptors involved and the cellular context of a particular cell (Niehrs, 2012; Willert and Nusse, 2012). Beside the main Wnt receptor Frizzled, several other Wnt co-receptors have been identified, which bind Wnt and Frizzled simultaneously and are important regulatory determinants to direct downstream signaling to the different branches. Indeed, more than 15 receptors and co-receptors involved in Wnt signaling have been discovered until now, including the main Wnt receptor Frizzled (Frizzled 1-10), LRP5/6, ROR1/2, PTK7, RYK and MUSK (Verkaar and Zaman, 2010; Kikuchi et al., 2011; Niehrs, 2012). Interestingly, it still remains elusive if Frizzled can act without co-receptors. Frizzled co-receptors involved in the activation of canonical Wnt signaling are LRP5 or LRP6, whereas in PCP signaling Ror1, Ror2 or PTK7 serves as co-receptor (Niehrs, 2012). Considering the presence of

various Wnt ligands and receptors, it is of great interest to understand how signal specificity is achieved.

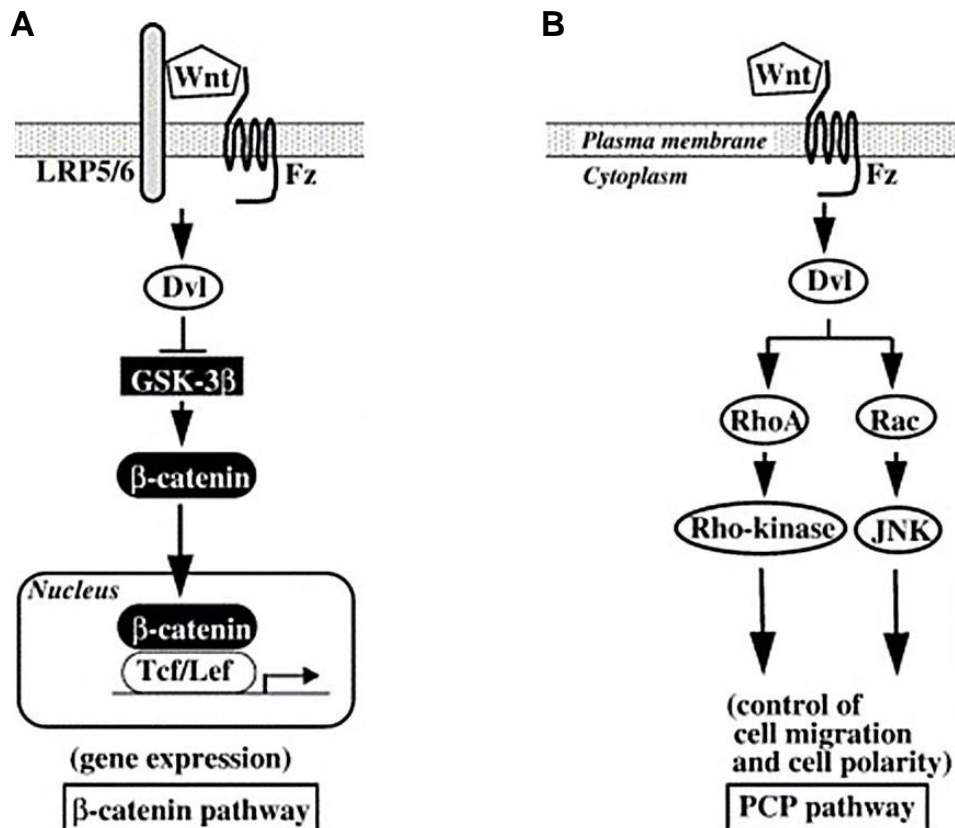


Figure 1: Wnt signaling pathways.

Wnt signaling pathways are regulated through some common key proteins, which are Wnt ligands, Fz receptors and Dsh (Dvl) proteins. **(A)** Activation of the canonical, β -catenin-dependent, Wnt pathway by Wnt ligand binding to its receptors Frizzled and LRP5/6, results in the inhibition of GSK3 β , leading to the accumulation and nuclear localization of β -catenin. β -catenin interacts with the transcription factors Tcf/Lef to induce target gene expression. **(B)** In PCP signaling Dsh activates Rac and Rho which in turn activate Rho-kinase and c-Jun-N-terminal kinase (JNK). Activation of PCP signaling leads to changes in the actin cytoskeleton and regulates cell polarity and cell migration (modified after Kikuchi et al., 2007).

1.2 Core components of Wnt signaling pathways

1.2.1 Wnt proteins

Wnt proteins are secreted hydrophobic cysteine-rich proteins that act as paracrine and autocrine ligands and are conserved in all metazoan animals (MacDonald et al., 2009; Feng and Gao, 2015). The first Wnt gene, *int-1*, now called *Wnt-1*, was isolated in the mouse in 1982 (Nusse and Varmus, 1982). So far 19 Wnt genes have been identified in most mammalian genomes, including humans (Clevers and Nusse, 2012; Willert and Nusse, 2012). Wnt proteins are composed of approximately 350-400 amino acids, contain up to 23 or 24 cysteine residues and at least one *N*-linked glycosylation site (Komekado et al., 2007). Glycosylation and lipidation/acylation are the main modifications of Wnt proteins. Moreover, the hydrophobicity of Wnt proteins is most likely established through posttranslational lipid modifications by the attachment of a mono-unsaturated fatty acid, palmitate and/or palmitoleic acid to one or more conserved serine or cysteine residues. These posttranslational modifications occur in the endoplasmic reticulum (ER) (Willert et al., 2003; Takada et al., 2006; Willert and Nusse, 2012). Glycosylation seems to be a crucial step for Wnt folding and secretion, as glycosylation mutants of Wnt3a and Wnt5a are not secreted into the extracellular matrix (ECM) (Komekado et al., 2007; Kurayoshi et al., 2007). Wnt modification by lipidation is essential for intracellular processing and Wnt activity (Willert et al., 2003; Takada et al., 2006; Clevers and Nusse, 2012). It has been shown that Wnt3a and Wnt5a palmitoylation mutants lose their ability to bind to their receptors and to activate signaling (Komekado et al., 2007; Kurayoshi et al., 2007). The multipass transmembrane O-acyltransferase Porcupine (Porcn), which resides in the ER, is supposed to catalyze the acylation of Wnt proteins (van den Heuvel et al., 1989b, 1989a, 1989b; Kadowaki et al., 1996; Hofmann, 2000). Mutation of Porcn results in the reduction of Wnt3a palmitoylation, its retention in the ER and thus the ablation of Wnt signaling (Tanaka et al., 2002; Barrott et al., 2011; Biechele et al., 2011). After Wnt proteins are processed, their secretion is regulated by the sorting receptor Wntless (Wls), also known as Evenness interrupted (Evi) or Sprinter (Srt) in *Drosophila*, which transports Wnt proteins to the plasma membrane (Banziger et al., 2006; Bartscherer et al., 2006; Goodman et al., 2006). After Wnt secretion Wls is recycled from endosomes to the Golgi mediated by the retromer complex which is composed of 5 subunits (Figure 2). Deficiency of the retromer complex leads to the degradation of Wls in the lysosome resulting in abolished Wnt secretion (Coudreuse et al., 2006; Belenkaya et al., 2008; Franch-Marro et al., 2008; Port et al., 2008).

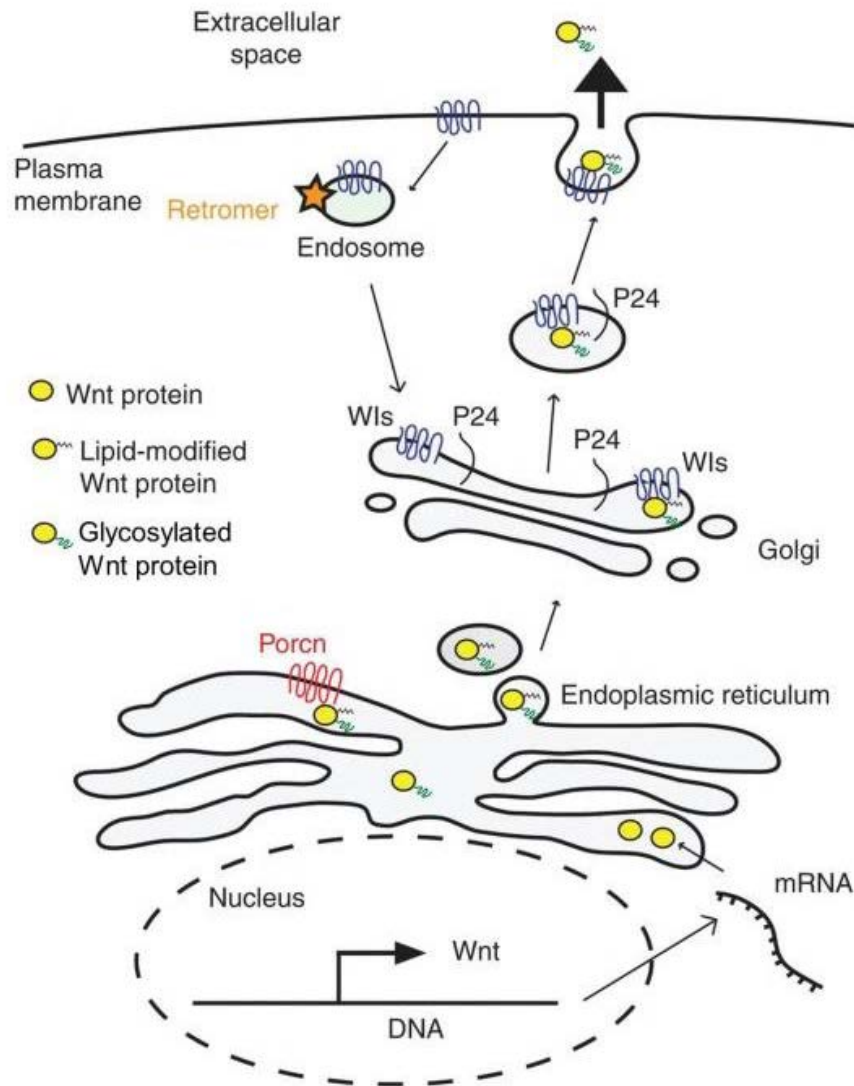


Figure 2: Posttranslational modifications and secretion of Wnt proteins.

After translation Wnt proteins enter the ER, where glycosylation and acylation through Porcupine (Porcn) occurs. Wnts are transported to the Golgi and interact with Wntless (Wls), which mediates its transport from the Golgi to the plasma membrane with the help of specific cargo proteins belonging to the p24 protein family. After release of the active Wnt protein, Wls is recycled back to the Golgi through clathrin-mediated endocytosis and the retromer complex (modified after Willert and Nusse, 2012).

Canonical and non-canonical Wnt proteins are proposed to activate the respective Wnt signaling pathway. However, no specific sequence or structure within the proteins has been found to categorize them as canonical or non-canonical. The cellular context defined by the expression of certain receptors and signal transducers is most crucial for Wnt proteins to act as canonical or non-canonical activators. This theory is supported by the fact that non-canonical Wnt5a and Wnt11 can activate canonical Wnt signaling under specific conditions (He et al., 1997; Tao et al., 2005; Cha et al., 2008; Willert and Nusse, 2012). Nevertheless, Wnt1, Wnt3a and Wnt8 are classified as typical canonical Wnt proteins, whereas Wnt5a and Wnt11 are mainly involved in non-canonical signaling. The

categorization of Wnt proteins as canonical or non-canonical activators is mainly based on their ability to induce a secondary axis in *Xenopus* embryos (Du et al., 1995) and/or to induce morphological transformation of C57MG mammary epithelial cells (Wong et al., 1994).

Interestingly, a high resolution structure achieved by crystallization of *Xenopus* Wnt8 in complex with the cysteine-rich domain (CRD) of mouse Frizzled8 was recently published. This crystallization revealed a structure which resembles a “hand” with a thumb extending from the N-terminal domain and an index finger from the C-terminal domain (CTD) that grasps Frizzled’s CRD at two binding sites. The thumb is modified with a palmitoleic acid at a highly conserved serine residue (Figure 3) (Janda et al., 2012).

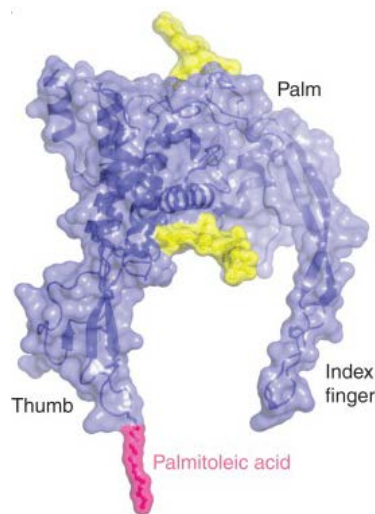


Figure 3: Structure of *Xenopus* Wnt8 in complex with Fz8.

Only the Wnt8 structure is shown. *Xenopus* Wnt8 protein structure resembles a “hand” with a thumb, a palm region and an index finger. The palmitoleic acid, shown in pink, extends from the thumb (Janda et al., 2012; Willert and Nusse, 2012).

1.2.2 Frizzled receptors

The *frizzled* gene was first identified in *Drosophila* in a screen for mutations that cause PCP phenotypes (Vinson and Adler, 1987a). Later Frizzled was found in diverse metazoan including humans, where ten family members have been identified. Frizzled proteins are the main Wnt receptors and regulate canonical and non-canonical Wnt signaling pathways (Huang and Klein, 2004; Clevers and Nusse, 2012). Frizzled is a seven transmembrane protein with a large extracellular N-terminal cysteine-rich domain (CRD). This CRD, containing ten cysteine residues, is conserved among the Frizzled protein family and is necessary and sufficient for Wnt ligand binding (Bhanot et al., 1996; Dann et al., 2001). Further, Frizzled has seven hydrophobic domains that form

transmembrane alpha-helices (Figure 4) (Wang et al., 1996; Huang and Klein, 2004). Via the intracellular domain (ICD) Frizzled binds cytoplasmic proteins, like the scaffold protein Dsh. The ICD has little homology between the Frizzled family proteins, despite of a conserved motif (KTXXXW) that is essential for Frizzled-Dsh protein interaction and thus, activation of canonical Wnt signaling (Umbhauer et al., 2000; Wong et al., 2003). It has been shown that a mutant Frizzled protein comprising a point mutation in one of the conserved amino acids lost its ability to activate canonical Wnt signaling (Umbhauer et al., 2000).

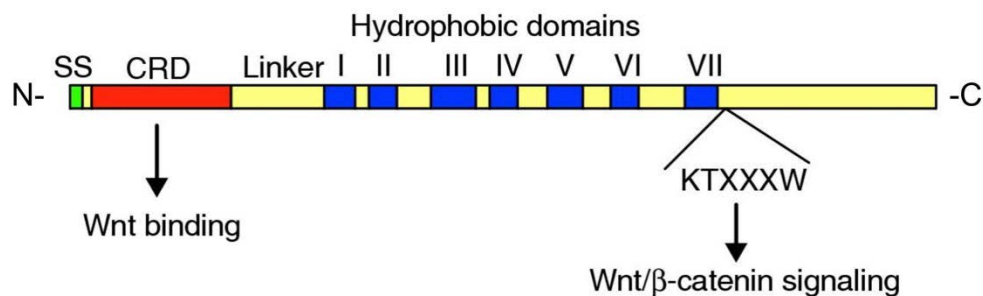


Figure 4: Structure of Frizzled proteins.

Frizzled proteins are about 500 to 700 amino acids in length containing an N-terminal signal sequence (SS). The large extracellular cysteine-rich domain (CRD) binds Wnt proteins and other ligands. Frizzled has seven hydrophobic transmembrane domains and a C-terminal intracellular domain including the conserved KTXXXW motif (modified after Huang and Klein, 2004).

1.2.3 Dishevelled

Dishevelled was first identified in *Drosophila* mutants and was named after the observed phenotype, as the mutation of the *dishevelled* gene leads to misoriented body and wing hairs (Fahmy and Fahmy, 1959). Highly homologous Dsh proteins were identified in mouse, *Xenopus* and humans (Sussman et al., 1994; Sokol et al., 1995; Pizzuti et al., 1996; Semenov and Snyder, 1997). Dsh is located downstream of the Wnt/Fz ligand-receptor complex and plays a crucial role in Wnt signaling as it is the branching point between canonical and non-canonical Wnt signaling (Axelrod et al., 1998; Boutros et al., 1998; Wallingford and Habas, 2005). The Dsh protein is composed of three highly conserved domains, the C-terminal DIX (Dishevelled/Axin), the central PDZ (Postsynaptic density 95, Discs Large, Zonula occludence-1) and the N-terminal DEP (Dishevelled, EGL-10, Pleckstrin) domain. These domains are important to direct Wnt signaling into the distinct downstream pathways. The DIX domain is involved in canonical Wnt signaling, whereas PCP signaling is transduced through the DEP domain. The central PDZ domain is essential for both Wnt signaling pathways and is often found to interact with Dsh binding partners (Figure 5) (Axelrod et al., 1998; Boutros et al., 1998; Rothbacher et al., 2000;

Wallingford et al., 2000; Capelluto et al., 2002). Thus, it is proposed to function as a switch between canonical and non-canonical PCP signaling.

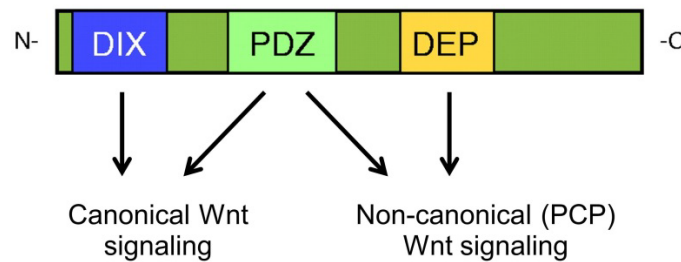


Figure 5: The conserved domains of Dishevelled.

Dsh contains three highly conserved domains, the N-terminal DIX domain, the central PDZ domain and the C-terminal DEP domain. The different domains are essential for the selective activation of different Wnt signaling pathways. The DIX and the PDZ domain are important for canonical Wnt signaling, while the DEP together with the PDZ domain function in PCP signaling (modified after Wallingford and Habas, 2005).

1.3 Canonical Wnt signaling

1.3.1 Molecular mechanism of canonical Wnt signaling

Canonical Wnt signaling or β -catenin-dependent Wnt signaling controls processes like cell proliferation and cell differentiation during embryogenesis and adult tissue homeostasis. Misregulation of canonical Wnt signaling results in various diseases, ranging from birth defects, several types of cancer including colon cancer and melanoma to neurodegenerative diseases (Niehrs, 2012; Acebron et al., 2014; Sokol, 2015). Active canonical Wnt signaling leads to the stabilization of β -catenin and to the transcription of β -catenin-dependent target genes in the cell. In the absence of Wnt ligands cytoplasmic β -catenin is constantly degraded. The degradation of β -catenin is regulated by the destruction complex, which is composed of the scaffolding protein axis inhibitor (Axin), the tumor suppressor adenomatosis polyposis coli (APC), casein kinase I (CKI) and glycogen synthase kinase 3 (GSK3). β -catenin interacts with Axin and APC and is thereby bound to the destruction complex (Aberle et al., 1997; Clevers and Nusse, 2012). The N-terminal region of β -catenin is sequentially phosphorylated by the kinases CKI and GSK3 (Yost et al., 1996; Amit et al., 2002; Liu et al., 2002; MacDonald et al., 2009). Phosphorylated β -catenin is recognized by the E3 ubiquitin ligase subunit β -TrCP resulting in β -catenin ubiquitination and rapid degradation in the proteasome (Jiang and Struhl, 1998; Marikawa and Elinson, 1998; Liu et al., 1999). In the absence of β -catenin, transcription of Wnt target genes is continuously repressed by the DNA-bound transcription factors T cell

factor/lymphoid enhancer (TCF/LEF). TCF/LEF interact with the transcriptional repressor Groucho (Transducin-like enhancer protein, TLE1 in human), which recruits histone deacetylases (HDAC) to mediate histone deacetylation and chromatin compaction (Figure 6 A) (Cavallo et al., 1998; Roose et al., 1998).

Canonical Wnt signaling is initiated by the binding of a canonical Wnt ligand to the membrane receptors Fz and low-density-lipoprotein receptor related protein 6 (LRP6) or LRP5. This ternary complex recruits Dsh to the membrane, which interacts with the cytoplasmic part of Fz. Dsh further recruits Axin together with the other components of the destruction complex to the membrane, including the kinases GSK3 and CKI (Mao et al., 2001; Clevers and Nusse, 2012). This recruitment induces rapid phosphorylation events at the intracellular domain of LRP6 by GSK3 and CKI. GSK3 phosphorylates LRP6 at Ser1490 in a PPPSP motif followed by CKI phosphorylation which occurs adjacent to the PPPSP motif at Thr1479 (Tamai et al., 2004; Davidson et al., 2005; Zeng et al., 2005). These dual phosphorylation events result in the formation of an axin docking site at the intracellular domain of LRP6, thereby strongly enhancing the recruitment of Axin and the destruction complex (Mao et al., 2001; Tamai et al., 2004; Davidson et al., 2005). Consequently, phosphorylated LRP6 inactivates the GSK3 β kinase through direct binding (Cselenyi et al., 2008; Piao et al., 2008; Wu et al., 2009). Signaling is further enhanced by the oligomerization of Dsh and Axin, which promotes the clustering of LRP6 to form the so-called LRP6 signalosome (Bilic et al., 2007). These processes stabilize β -catenin and prevent its phosphorylation by GSK3 β . Unphosphorylated β -catenin accumulates in the nucleus, binds to TCF/LEF, displaces Groucho and activates the expression of β -catenin dependent genes (Behrens et al., 1996; Molenaar et al., 1996), such as *c-Myc* (He et al., 1998), *cyclinD1* (Tetsu and McCormick, 1999) and *Axin2* (Jho et al., 2002) (Figure 6 B).

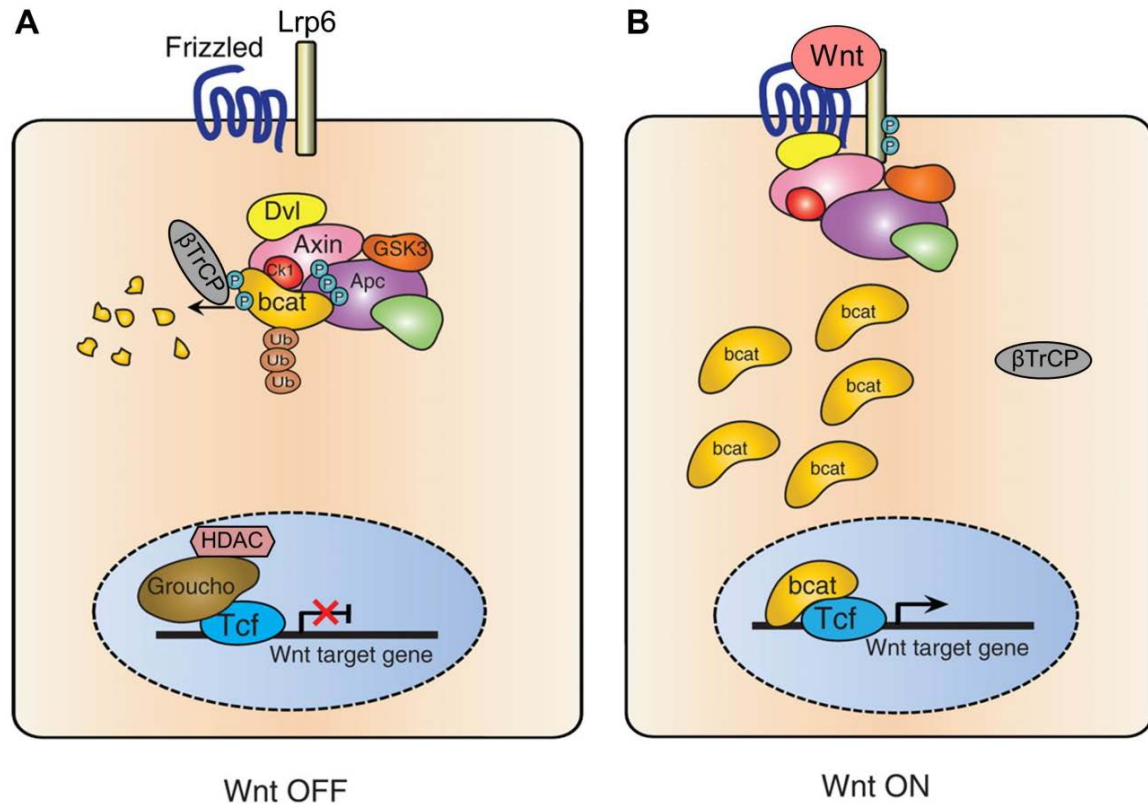


Figure 6: The canonical Wnt signaling pathway.

(A) In the absence of Wnt proteins, β -catenin is bound by the destruction complex composed of Axin, GSK3, APC and CKI leading to its constitutive phosphorylation. Phosphorylated β -catenin is recognized by the E3 ubiquitin ligase subunit β -TrCP, which mediates ubiquitination and proteasomal degradation of β -catenin. Wnt target gene transcription remains inactive due to the interaction of TCF with transcriptional co-repressors such as Groucho and histone deacetylases (HDAC). **(B)** Upon binding of a Wnt ligand to LRP6 the destruction complex associates with phosphorylated LRP6. This process leads to an inactivation of the destruction complex, so that β -catenin can accumulate and enter the nucleus, where it replaces Groucho and activates Wnt target gene transcription (modified after de Lau et al., 2012).

1.3.2 Developmental processes regulated by canonical Wnt signaling

During embryonic development canonical Wnt signaling regulates diverse processes including body axis specification and organogenesis (Niehrs, 2012; Acebron et al., 2014; Sokol, 2015). In vertebrates the specification of the first body axis, the dorsal-ventral (DV) axis, occurs directly after fertilization and subsequently also determines the orientation of the anterior-posterior (AP) axis. Our knowledge of how axis specification is determined mostly came from studies in *Xenopus laevis* (Weaver and Kimelman, 2004; Sokol, 2015). Sperm entry into the oocyte leads to an event called cortical rotation, which is a microtubule-dependent process. Through cortical rotation maternally deposited dorsalizing factors are actively transported from the vegetal towards the future dorsal pole, opposite to the point of sperm entry (Figure 7) (Gerhart et al., 1989; Houliston and Elinson, 1992;

Weaver and Kimelman, 2004; Hikasa and Sokol, 2013). These dorsalizing factors include maternally expressed Dsh, GSK3-binding protein (GBP) and Wnt11. At the future dorsal pole Dsh and GBP inactivate GSK3 β and Wnt11 further activates maternal canonical Wnt signaling (Figure 7). Inactivation of GSK3 β at the dorsal pole of the embryo leads to the accumulation of β -catenin, while β -catenin is degraded at the ventral pole (Miller et al., 1999; Weaver and Kimelman, 2004; Tao et al., 2005). Hence, cortical rotation leads to the local stabilization of β -catenin by the action of Dsh, GBP and Wnt11 and thus to the activation of canonical Wnt signaling in the nuclei of dorsal cells in early blastula *Xenopus* embryos. Asymmetric β -catenin distribution can already be observed soon after fertilization in 2- and 4-cell stage embryos (Larabell et al., 1997; Sokol, 1999). Subsequently, β -catenin activates the expression of several zygotic genes at the dorsal pole that are necessary for the formation of a signaling center known as the Spemann organizer in amphibians, the shield in zebrafish and the node in the mouse (Harland and Gerhart, 1997; Sokol, 1999; Schier and Talbot, 2005). In *Xenopus* these organizer inducing genes include the *Nodal* family genes, *Siamois* and *Twin* (Lemaire et al., 1995; Fan et al., 1998; Sokol, 1999). The importance of cortical rotation on dorsal-ventral axis specification has been demonstrated by disruption of microtubule-polymerization via UV irradiation or the microtubule-depolymerization agent nocodazole, which results in the development of ventralized *Xenopus* and zebrafish embryos (Chung and Malacinski, 1980; Scharf and Gerhart, 1980; Jesuthasan and Stahle, 1997).

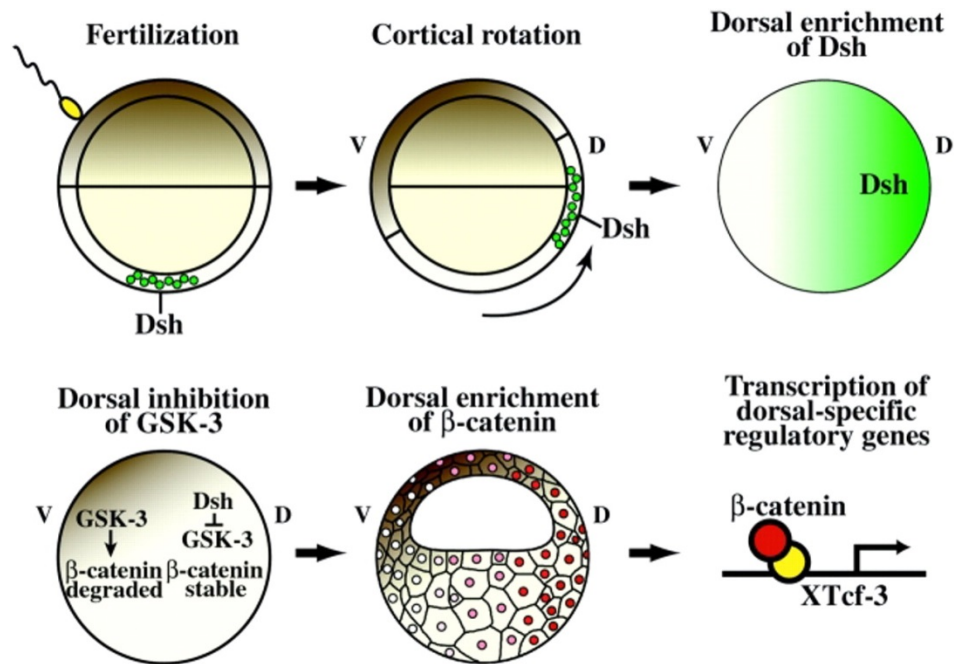


Figure 7: Dorsal-ventral axis specification in *Xenopus*.

Sperm entry induces cortical rotation, whereby vegetally localized Dsh and GBP are transported along microtubule arrays to the future dorsal pole of the embryo. Dsh and GBP inhibit GSK3 activity, thereby promoting the dorsal accumulation of β -catenin and the activation of the maternal Wnt signaling pathway. β -catenin enters the nuclei and activates together with XTcf-3 the transcription of dorsal-specific genes which in turn induce the formation of the Spemann organizer. V: ventral, D: dorsal (Miller et al., 1999).

The local stabilization of β -catenin at the future dorsal pole is the key step in organizer formation. Depletion of maternal β -catenin inhibits the development of dorsal and anterior structures, while overexpression of β -catenin on the ventral side of the embryo results in the formation of an ectopic dorsal axis (Heasman et al., 1994; Funayama et al., 1995; Larabell et al., 1997). For example, the activation of the canonical Wnt signaling pathway by ventral ectopic expression of Wnt1 or Wnt8 in *Xenopus* embryos leads to axis duplication through β -catenin activation and Spemann's organizer formation (Sokol et al., 1991; Sokol, 2015). Thus, modulation of canonical Wnt signaling by activation on the ventral or inhibition on the dorsal side of the embryo results in the generation of dorsalized (second axis) or ventralized embryos, respectively. Targeted injection into the ventral or dorsal blastomere of a *Xenopus* embryo has become a popular assay to study how a particular gene influences canonical Wnt signaling (Kuhl and Pandur, 2008). Based mainly on these assays, Wnt proteins have been categorized as canonical or non-canonical by their ability to induce secondary axis development when overexpressed ventrally (Du et al., 1995; Yamaguchi, 2001).

In addition to dorsal-ventral patterning, anterior-posterior patterning of neurectoderm has been shown to rely as well on canonical Wnt signaling in *Xenopus* and zebrafish. The neurectoderm gives rise to forebrain, midbrain, hindbrain and spinal cord precursor tissue

during gastrula stages. At these stages Wnt proteins are expressed in the posterior and Wnt inhibitors in the anterior regions, resulting in the establishment of a posterior to anterior gradient of β -catenin and Tcf-reporter activity (Glinka et al., 1998; McGrew et al., 1999; Kim et al., 2000; Kiecker and Niehrs, 2001; Schohl and Fagotto, 2002; Petersen and Reddien, 2009). Thus, canonical Wnt signaling needs to be inhibited in the anterior and activated in the posterior regions of the embryo to ensure correct anterior neural patterning and posterior tissue development. The importance of anterior Wnt signaling inhibition for head development was demonstrated in zebrafish *headless* (*hdl*) mutants. These mutants lack eyes, forebrain and part of the midbrain because of a null mutation in *Tcf3*, resulting in the loss of Tcf3 repressor activity (Kim et al., 2000). Hence, the establishment of a Wnt gradient from head to tail tissue in the developing embryo is crucial for appropriate anterior-posterior patterning.

1.4 Planar cell polarity signaling

1.4.1 Molecular mechanism of planar cell polarity signaling (PCP)

Planar cell polarity signaling regulates the coordinated polarization of cells and cellular structures along an axis within the plane of an epithelium, orthogonal to the apical-basal axis (Figure 8 A) (Vladar et al., 2009; Bayly and Axelrod, 2011; Sokol, 2015). However, after many years of studying PCP, it is now known that PCP regulates many processes in polarized cells and tissues and thus is not restricted to epithelial cells (Vladar et al., 2009). PCP controls diverse developmental processes such as convergent extension movements during gastrulation or neuronal and epithelial cell migration (Grumolato et al., 2010). Moreover, in vertebrates PCP was identified to regulate collective cell migration during epidermal wound repair, the orientation of cochlear sensory hair cells, multiciliated cells, cells of the developing long bones and cultured fibroblasts (Montcouquiol and Kelley, 2003; Guo et al., 2004; Caddy et al., 2010; Bayly and Axelrod, 2011; Wang et al., 2011; Wallingford, 2012). Since PCP controls such diverse developmental processes, the disruption of this signaling pathway leads to various diseases for instance deafness, neural tube, cardiac and renal developmental defects as well as polycystic kidney disease and metastatic cancer (Simons and Mlodzik, 2008; Vladar et al., 2009; Bayly and Axelrod, 2011; Wallingford, 2012). PCP was initially studied in insects, especially in the *Drosophila* wing, eye and abdomen. Thereby many evolutionary conserved PCP components have been identified, which are referred to as “core” PCP proteins. These “core” PCP proteins include the transmembrane proteins Van Gogh (Vang or Strabismus (Stbm) or Vang like

(Vangl) in vertebrates) (Taylor et al., 1998; Wolff and Rubin, 1998), Flamingo (Fmi or Starry Night or Celsr in vertebrates) (Chae et al., 1999; Usui et al., 1999), and Frizzled (Fz) (Vinson et al., 1989). Cytoplasmic proteins involved in PCP are Dsh (Klingensmith et al., 1989; Theisen et al., 1994), Prickle (Pk) (Gubb et al., 1999) and Diego (Dgo) (Feiguin et al., 2001; Das et al., 2004).

Interestingly, in *Drosophila* these core PCP proteins accumulate asymmetrically within the cell to distinct regions of the plasma membrane. Whereas Fmi is enriched at both, proximal and distal sides (Usui et al., 1999), Vang and Pk localize anteriorly opposite of Fz, Dsh and Dgo, which localize posteriorly (Figure 8 B). This polarized subcellular distribution of the core PCP proteins is important for cell-cell communication between adjacent cells and for the orientation of particular structures within the cell (Bayly and Axelrod, 2011; Gray et al., 2011; Wallingford, 2012)

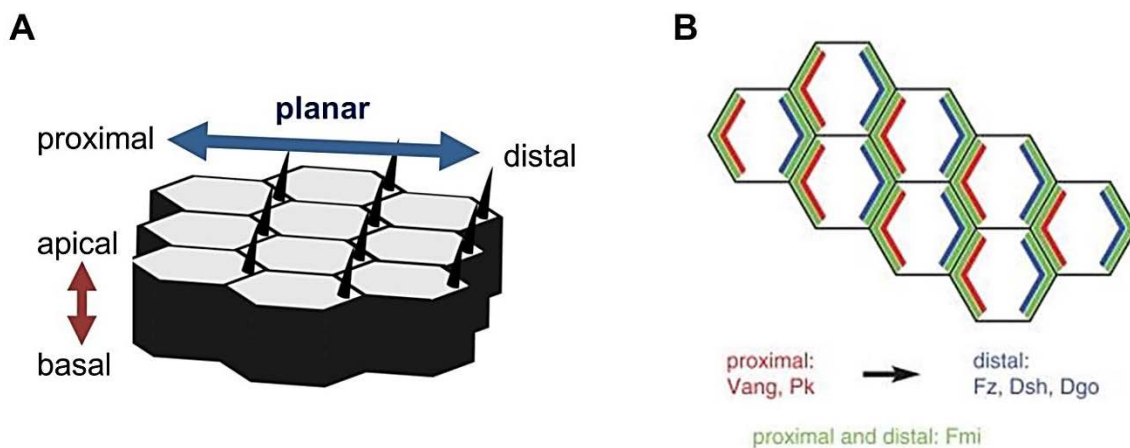


Figure 8: Planar cell polarity.

(A) Planar cell polarity regulates the planar, from proximal to distal, polarity, perpendicular to the apical-basal polarity. Scheme of PCP in epithelial cells where it controls the positioning of polarized hairs at the distal site of each cell (Marcinkevicius et al., 2009). **(B)** Polarity within the cell is established through the asymmetric distribution of core PCP proteins in many cell types undergoing PCP. Vang, and Pk are localized proximally, while Fz, Dsh and Dgo localize distally in each cell. Fmi is localized to both proximal and distal cell membranes (Vladar et al., 2009).

The subcellular asymmetry is additionally regulated by the mutual inhibition of Fz/Dsh/Dgo and Vang/Pk. Vang and Pk bind Dsh and inhibit its recruitment to the membrane, which is necessary for PCP pathway activation. Conversely, Dgo as well binds Dsh, thereby promoting its activity, thus antagonizing the inhibitory effect of Vang/Pk on Dsh (Feiguin et al., 2001; Tree et al., 2002; Bastock et al., 2003; Jenny et al., 2003; Das et al., 2004). Interestingly, Fmi is located on both sides, proximally and distally and forms homodimers between neighboring cells. Thus, Fmi binds both, Fz at one cell and Vang at the neighboring cell (Usui et al., 1999). Asymmetric distribution of core PCP proteins is not restricted to the fly, but was also observed in vertebrate sensory hair cells and the mouse

node (Vladar et al., 2009; Antic et al., 2010; Hashimoto et al., 2010) However, not every vertebrate tissue, which undergoes PCP, shows this asymmetric distribution, as for example Dsh and Vang localize together to basal bodies in vertebrate epithelial cells (Park and Moon, 2002; Vladar et al., 2009).

Regulation of cell polarity and cytoskeletal changes are induced by Frizzled-mediated membrane recruitment of Dsh. Dsh activates PCP effector proteins including the small GTPases Rac and Rho through two parallel pathways. In the first pathway Rho is activated by Dsh together with the cytoplasmic formin-related protein Daam1 and in turn activates the ROCK kinase that mediates cytoskeletal re-organization. The second pathway signals through Rac, which mediates the activation of the c-Jun-N-terminal kinase (JNK) leading to the activation of JNK-dependent transcription factors, like the activating transcription factor 2 (ATF2) and its target genes (Figure 9 A, B) (Habas et al., 2001; Winter et al., 2001; Rosso et al., 2005).

As Fz is a known receptor for Wnt ligands it seems likely that Wnt proteins act upstream of the PCP core proteins. However, in *Drosophila* the function of Wnt proteins in PCP establishment is not completely clarified and inconsistent findings exist. Although several studies implicated that Wnt proteins are not involved in *Drosophila* PCP, it has been reported recently that Wingless (Wg) and Wnt4a are necessary for PCP in the *Drosophila* wing (Wu et al., 2013; Lim et al., 2005; Chen et al., 2008). In vertebrates Wnt proteins have indeed important functions in the activation of PCP, which was shown in Wnt7a, Wnt11 and Wnt5a loss and gain of function experiments (Heisenberg et al., 2000; Tada and Smith, 2000; Wallingford et al., 2001; Dabdoub, 2003; Kilian et al., 2003). Beside Fz receptors, further Wnt co-receptors that function in PCP had been identified, including Ror1/2 and PTK7. Mutations of both receptors lead to typical PCP phenotypes in mouse and *Xenopus* (Oishi et al., 2003; Lu et al., 2004).

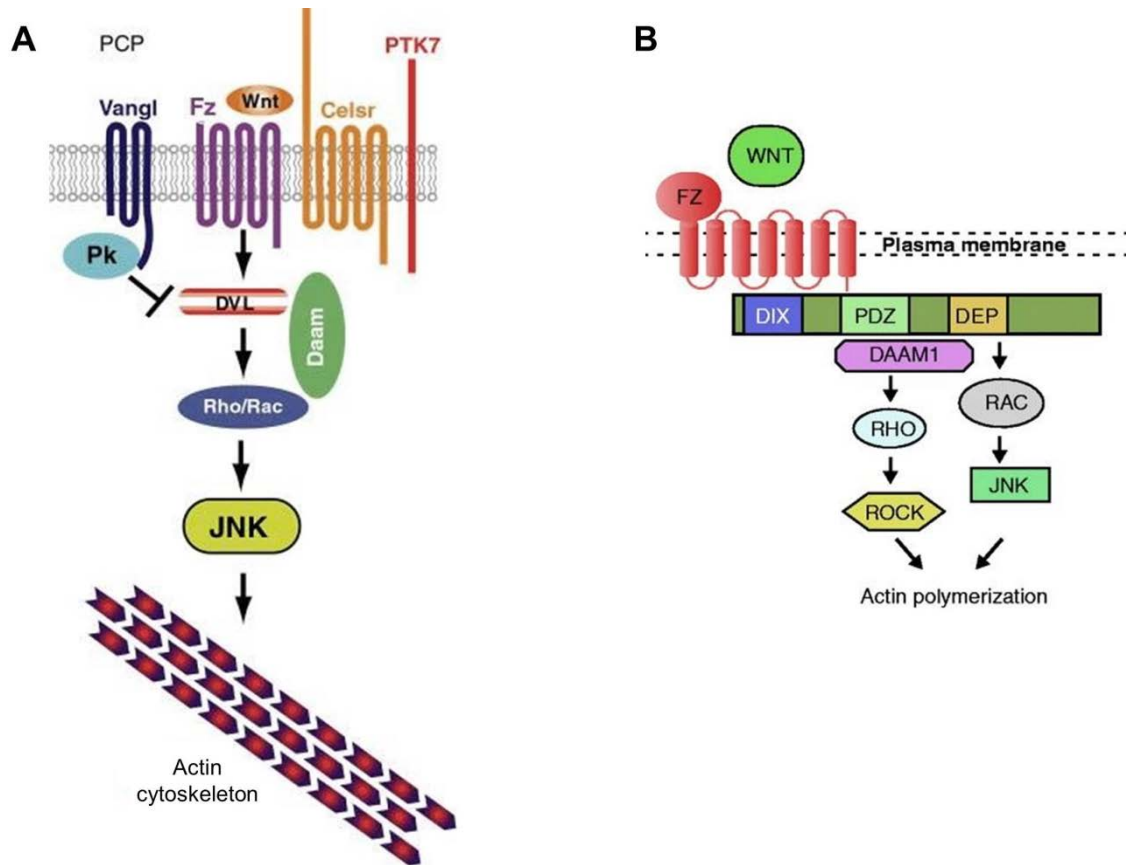


Figure 9: Molecular mechanism of PCP signaling.

(A) PCP is activated by the binding of Wnt proteins to its receptor Frizzled. Activation of Fz results in Dsh membrane recruitment and activation, which signals through the small GTPases Rho/Rac and c-Jun-N-terminal kinase (JNK) leading to a rearrangement of the actin cytoskeleton. Vangl and Pk inhibit Dsh membrane recruitment. Further receptors involved in PCP are Celsr (Fmi) and PTK7 (modified after Montcouquiol and Kelley, 2003). **(B)** PCP at the level of Dsh. The PDZ and the DEP domain of Dsh are important for transducing downstream PCP signaling to Rho and Rac, which further modulate the actin cytoskeleton via ROCK or JNK downstream signaling (modified after Wallingford and Habas, 2005).

1.4.2 Developmental processes regulated by PCP

PCP regulates the organization of cells in the plane of an epithelial tissue. Thus, mutations in PCP regulating genes result in disorganized surface appearance. Typical PCP phenotypes are observed in the orientation of the sensory bristles and cellular hairs (trichomes) on the wing, abdomen and thorax (notum) or photoreceptors in the *Drosophila* eye (Figure 10 A-D) (Vinson and Adler, 1987b; McNeill, 2010; Gray et al., 2011). Similar to the fly, mammalian epithelial tissue is polarized and a misorganization of the fur and the inner ear hair cells are typically found if PCP proteins are mutated. Depletion of Fz6 in the mouse results in disorganized hair on the back (swirls), strongly resembling the PCP phenotypes observed in the fly wing (Figure 10 E, F) (Guo et al., 2004). In mammals the inner ear sensory hair cells are the best studied example of PCP. These sensory hair cells

are located in the organ of Corti, in the cochlea, and are composed of actin-based stereocilia and a single tubulin-based kinocilium, which forms a V-shaped structure. These stereociliary bundles are polarized in a way that all cells point towards the periphery of the cochlea. Mutations of different components of the PCP pathway including *Wnt5a*, *Fz*, *Dsh*, *Vangl*, *Pk*, *Celsr* and *PTK7* results in misoriented inner ear hair cells in the mouse (Figure 10 G, H) (Klein and Mlodzik, 2004; Lu et al., 2004; Wang et al., 2006; Kelly and Chen, 2007; Grumolato et al., 2010).

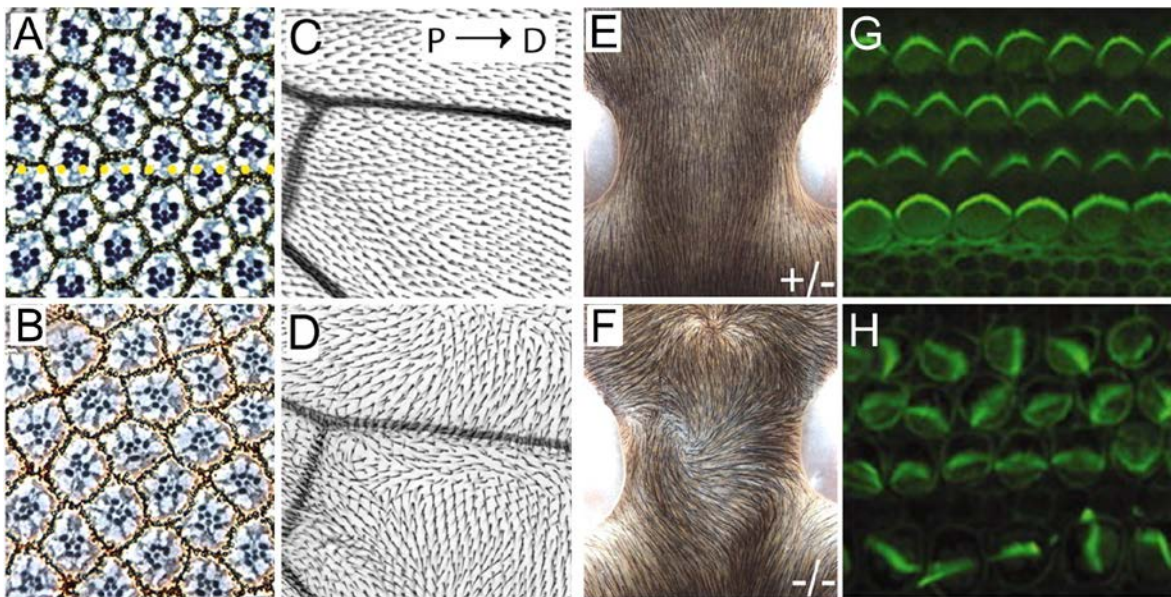


Figure 10: Examples of PCP phenotypes in *Drosophila* and mammals.

Wild type tissues are shown in the upper panel; PCP mutants in the lower panel. (A) Ommatidia in the *Drosophila* eye contain individual photoreceptor rhabdomeres that are located in each ommatidium in a specific arrangement. (B) In the PCP mutant eye the photoreceptor arrangement is defective. (C) The WT *Drosophila* wing shows parallel alignment of wing hairs from proximal to distal. (D) In the *vang* mutant wing hairs form swirls and are misorganized. (E) Mouse epidermal hairs are regularly oriented along the body axis. (F) The *frizzled6* mutant shows whorls and irregular waves. (G) Inner ear sensory hair cells of the mouse are arranged in a parallel fashion and show uniformly oriented stereocilia, but (H) this polarized arrangement gets lost in an *Fz* mutant, displaying misorganized stereocilia. P: proximal, D: distal (modified after Klein and Mlodzik, 2004; Wang and Nathans, 2007).

Mutations in PCP proteins in *Xenopus*, zebrafish and mouse revealed an important role of PCP signaling in the regulation of coordinated polarization of cells during convergent extension (CE) movements. CE is a process whereby cells intercalate between each other, leading to a narrowing and lengthening of the tissue along a particular axis (Figure 11 A). These movements are required for elongation of the body axis during gastrulation and neurulation (Bayly and Axelrod, 2011; Wallingford, 2012). Mutations in *Xenopus*, mouse and zebrafish PCP proteins results in the development of embryos having a short and wide body axis and neural tube defects. In the mouse mutations in PCP genes such as *vangl2*, *dishevelled*, *celsr1*, *fz* and *ptk7* (Djiane et al., 2000; Hamblet et al., 2002; Curtin

et al., 2003; Montcouquiol et al., 2003; Lu et al., 2004) lead to craniorachischisis a severe form of neural tube defects (NTD), whereby the neural tube remains open from the hindbrain to the tail (Figure 11 B) (Wallingford and Harland, 2002; Wang and Nathans, 2007). Interestingly, *VANGL1* and *VANGL2* mutations are also associated with neural tube closure defects in humans (Kibar et al., 2007).

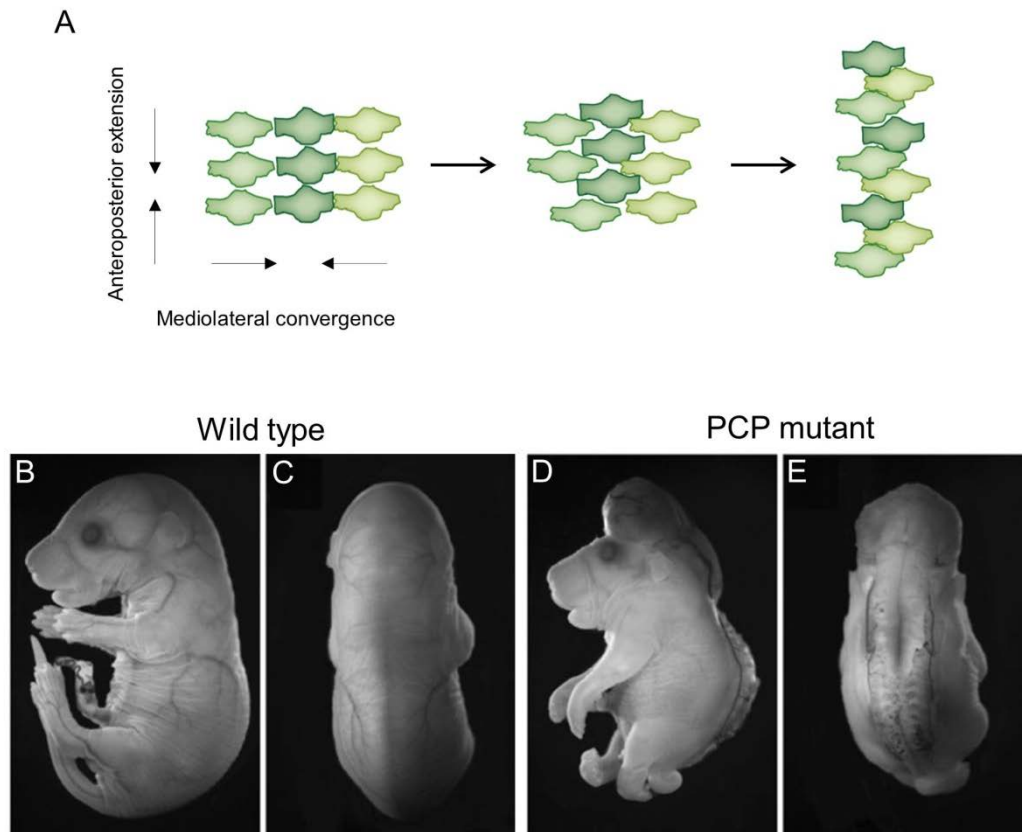


Figure 11: PCP/convergent extension phenotype in the mouse.

(A) Scheme of convergent extension movement. Cells intercalate leading to a mediolateral narrowing of the tissue and similarly to an anteroposterior extension (modified after (Wallingford, 2012)). (B, C) Lateral and dorsal view of a wild type mouse embryo with a closed neural tube, while (D, E) PCP mutants (Fz mutants) exhibit a completely open neural tube (craniorachischisis) from the head to the tail (modified after Wang et al., 2006).

Further processes regulated by PCP signaling are the directed migration of neurons and neural crest cells. Neural crest cells arise from the neural plate border during neurulation and migrate through the embryo in streams of high directionality to give rise to multiple cell types including neurons, glial cells, pigment cells and fibroblasts (Mayor and Theveneau, 2013). Interestingly, both canonical and non-canonical Wnt signaling pathways are involved in neural crest development. Canonical Wnt signaling is necessary for neural crest induction, whereas non-canonical Wnt signaling regulates the migration of neural crest cells (De Calisto et al., 2005). A number of experiments performed in

Xenopus, zebrafish and chick embryos demonstrate that distinct components of the PCP signaling pathway are essential for the migration of neural crest cells (De Calisto et al., 2005; Carmona-Fontaine et al., 2008; Matthews et al., 2008; Shnitsar and Borchers, 2008). For example, Dsh-DEP+, which is a dominant negative form of Dsh, blocks the non-canonical Wnt pathway without affecting the canonical Wnt signaling pathway, leads to a strong impairment in neural crest cell migration but not induction (Figure 12) (De Calisto et al., 2005), while Dsh mutants that block both canonical and non-canonical Wnt signaling inhibit neural crest cell induction (LaBonne and Bronner-Fraser, 1998; Bastidas et al., 2004).

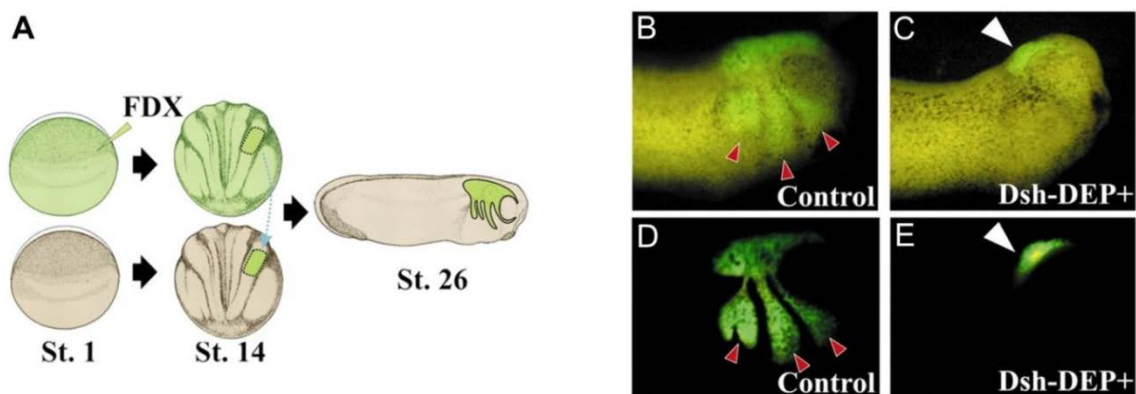


Figure 12: PCP signaling regulates neural crest cell migration.

(A) Neural crest cells from embryos injected with mRNA coding for Dsh-DEP+ (a dominant negative form of Dsh, which blocks exclusively the non-canonical Wnt pathway), were transplanted into a wild type embryo. FDX serves as lineage tracer (green). (B, D) In the control embryo neural crest cells migrate normally in typical streams. (C, E) In the embryo transplanted with the neural crest region taken from an embryo expressing Dsh-DEP+, neural crest cell migration is blocked (De Calisto et al., 2005).

1.5 Regulation of Wnt signaling by endocytosis

Wnt signaling pathways are selectively activated through specific combinations of Wnt ligands that bind to their receptors, thereby triggering different signaling outcomes by activating diverse intracellular cascades. However, the specificity of downstream signaling is additionally regulated by further molecular mechanisms. One of these regulatory mechanisms is the endocytosis of Wnt/receptor complexes and the sorting to different membrane-bound compartments (Kikuchi et al., 2009; Kikuchi et al., 2011). Ligand-induced trafficking of cell-surface receptors is a crucial step in the regulation of numerous signaling pathways. Traditionally endocytosis has been considered to be important for signal termination through receptor clearance from the cell surface, resulting in inaccessibility for ligands. However, today it is known that endocytosis is not only involved in signal termination but is indeed also required for signal transduction, maintenance and amplification, depending on the particular ligand-receptor complex (Yamamoto et al., 2006; Kikuchi et al., 2009; Niehrs, 2012; Willert and Nusse, 2012; Feng and Gao, 2015).

1.5.1 Endocytosis

Endocytosis is mediated through either clathrin-dependent or independent pathways (Figure 13). In the clathrin-dependent internalization pathway, membrane proteins are recognized by clathrin adaptor proteins (APs). Amongst these adaptor proteins the AP-2 complex is the major adaptor complex, which together with phospholipid phosphatidylinositol 4,5-bisphosphate (PtdIns(4,5)P₂) recruits the cytosolic coat protein clathrin to the membrane (Traub, 2009; Kikuchi et al., 2011). Clathrin deforms the plasma membrane and concentrates the appropriate transmembrane proteins, generally called “cargo”, into polygonal clathrin-coated pits (Traub, 2009; Kikuchi et al., 2011). The multidomain GTPase dynamin assembles at the necks of the pits and mediates the fission of the clathrin coated vesicles (CCVs) and their release into the cytoplasm. After vesicle release clathrin disassembles from the vesicles, which subsequently fuse with the early endosomes. Early endosomes regulate the membrane transport of the cargo between the plasma membrane and different intracellular components including the transport to late endosomes and lysosomes for degradation, the recycling back to the plasma membrane or the connection to the trans-golgi-network (TGN) (Yamamoto et al., 2006; Kikuchi et al., 2011; Feng and Gao, 2015). Vesicle trafficking is regulated by small GTP binding proteins, including Rab4, Rab5, Rab7, Rab9 and Rab11 (Figure 13) (Zerial and McBride, 2001; Kikuchi et al., 2011). The clathrin-mediated internalization pathway has been extensively analyzed and is well characterized. However, alternate endocytic pathways

exist that are independent of clathrin-coated vesicles. The best studied clathrin-independent endocytosis pathway is mediated through lipid raft microdomains and the caveolin family proteins (Figure 13). Lipid rafts are plasma membrane microdomains enriched in glycosphingolipids and cholesterol (Lajoie and Nabi, 2010; Kikuchi et al., 2011). In the lipid raft membranes caveolin proteins insert in a hairpin loop structure to induce the formation of flask-shaped membrane invaginations, called caveolae. Caveolin proteins form oligomers resulting in a striated caveolin form on the plasma membrane microdomains (Lajoie and Nabi, 2010; Kikuchi et al., 2011; Feng and Gao, 2015). In contrast to clathrin, which is dynamically associated with the plasma membrane, the binding of caveolin to the plasma membrane is stable. Caveolin-mediated endocytosis shares some features with clathrin-mediated endocytosis. Dynamin is also required for membrane fission and vesicle release (Oh et al., 1998), as this processes are inhibited after expression of a dominant-negative dynamin mutant (dynK44A) (Le and Nabi, 2003). Further, similar to clathrin coated vesicles, caveolin-vesicles has been reported to fuse with early endosomes, which is mediated by Rab-5, late endosomes or multivesicular bodies (MVBs) and they can be recycled back to the plasma membrane via a Rab11-dependent pathway (Kikuchi et al., 2011; Parton and del Pozo, 2013; Feng and Gao, 2015). Although several studies in the recent years contribute to a better understanding of the caveolin-mediated endocytosis, the trafficking pathway still remains to be unveiled in detail.

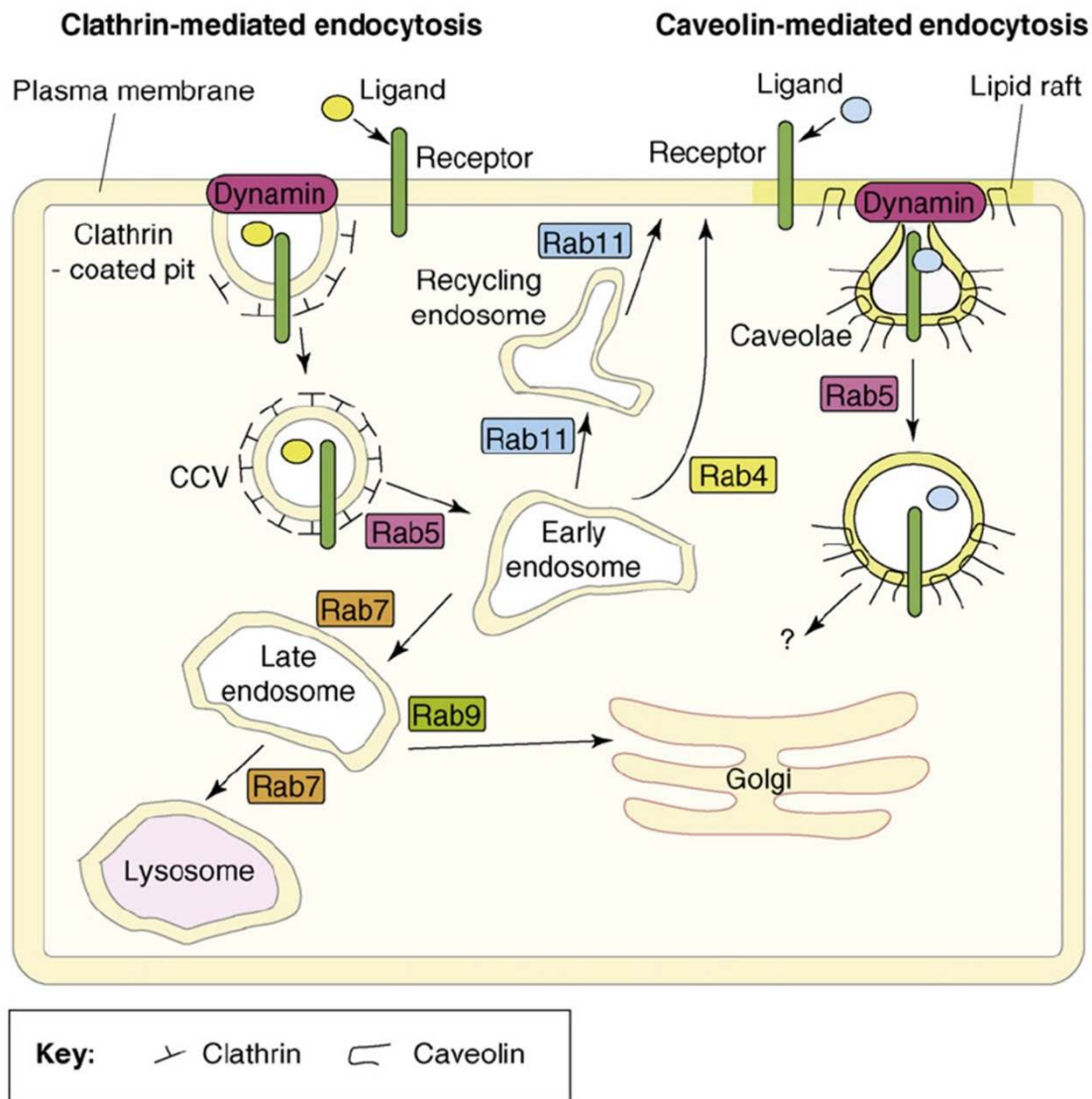


Figure 13: Endocytosis of ligand/receptor complexes.

The best characterized endocytosis pathway is mediated by clathrin, which assembles at the membrane to form a clathrin-coated pit. After internalization of the clathrin-coated vesicle (CCV), clathrin disassembles and the vesicle fuses with early endosomes. Early endosomes regulate the transport of the cargo, which can be recycled back to the plasma membrane, transported to late endosomes and lysosomes for degradation or to the trans-Golgi-network. Small GTP binding proteins belonging to the Rab family regulate vesicular trafficking. Rab5 mediates the fusion of CCVs with the early endosomes. Rab11 and Rab4 are involved in recycling. Rab7 regulates the transport to the lysosomes and Rab9 is involved in the trafficking of vesicles to the Golgi network. Caveolin-mediated endocytosis is restricted to specific plasma membrane microdomains, the lipid rafts. In the lipid rafts caveolae are formed with caveolin proteins as structural elements. Dynamin is also necessary for fission of caveolae and Rab5 mediates its trafficking. However, the trafficking pathway after internalization is yet not completely clear (Kikuchi et al., 2009).

1.5.2 Regulation of canonical Wnt signaling by receptor-mediated endocytosis

The internalization of Wnt proteins was first described in the wing imaginal disc of *Drosophila*. Antibody staining of Wingless (Wg, *Drosophila* Wnt protein) revealed an expression in cytoplasmic puncta in both Wg-expressing and Wg-responding cells. Inhibition of endocytosis prevented the formation of Wg cytoplasmic puncta. Electron microscopy analysis indicated that these cytoplasmic puncta are localized in small membrane-bound vesicles and in multivesicular bodies (van den Heuvel et al., 1989; Strigini and Cohen, 2000). MVB are endocytic compartments harboring many intraluminal vesicles, that form when a portion of the endosome membrane invaginates and buds into its own lumen (van den Heuvel et al., 1989b; Piper and Katzmann, 2007). Internalization of Wg proteins seems to be responsible for signal attenuation by ligand clearance, as it was shown that Wg is transported to the lysosome for degradation. Thus, it was suggested that in the *Drosophila* wing disc Wg endocytosis followed by degradation regulates the asymmetric Wnt signal along the anterior-posterior axis by the establishment of a Wnt gradient (Strigini and Cohen, 2000; Dubois et al., 2001; Feng and Gao, 2015).

In contrast to internalization of Wnt proteins, receptor endocytosis of LRP6 results in activation of canonical Wnt signaling in HEK293 and HeLaS3 cells. LRP6 binds to caveolin and is internalized in response to Wnt3a. Internalized LRP6 co-localizes not only with caveolin but also with EEA1, a marker for the early endosome. Caveolin depletion inhibits Wnt3a induced Tcf transcriptional activation. Moreover, inhibition of endocytosis by overexpression of dominant-negative forms of Rab5 or dynamin blocks LRP6 internalization and nuclear β -catenin accumulation. The interaction of LRP6 and caveolin leads to Axin recruitment and to the dissociation of β -catenin from Axin, thus promoting canonical Wnt signaling (Yamamoto et al., 2006; Bilic et al., 2007; Kikuchi et al., 2011; Feng and Gao, 2015). These data support a model whereby upon binding of Wnt3a to Fz and LRP6 in lipid rafts, the ligand-receptor complex is internalized via a caveolin-mediated pathway. This internalization is regulated by dynamin and the vesicles fuse in a Rab5-dependent manner with early endosomes (Figure 14 A). However, the mechanism by which β -catenin is stabilized through this process is not completely clear. The complex on the vesicle might be altered leading to an inhibition of Axin and GSK3 β (Yamamoto et al., 2006; Kikuchi et al., 2009; Kikuchi et al., 2011). Another model proposes that the receptor complexes including GSK3 β are further sequestered into intraluminal vesicles of MVBs. Thus, GSK3 β is captured in MVBs and β -catenin is protected from degradation leading to its accumulation and activation of canonical Wnt signaling (Yamamoto et al., 2006; Bilic et al., 2007; Taelman et al., 2010; Kikuchi et al., 2011; Niehrs, 2012). Interestingly, a role of clathrin-mediated endocytosis in the inhibition of canonical Wnt signaling was described.

The Wnt antagonist Dkk1 binds to LRP6 and Kremen2, thereby inducing a rapid clathrin-mediated internalization of this ternary complex (Figure 14 B). The removal of LRP6 from the membrane and possibly subsequent degradation inhibits canonical Wnt signaling (Yamamoto et al., 2008; Sakane et al., 2010). Considering these findings, Wnt3a as an activator of canonical Wnt signaling and Dkk1 as an inhibitor of canonical Wnt signaling might direct LRP6 to distinct internalization routes in order to activate or inhibit canonical Wnt signaling.

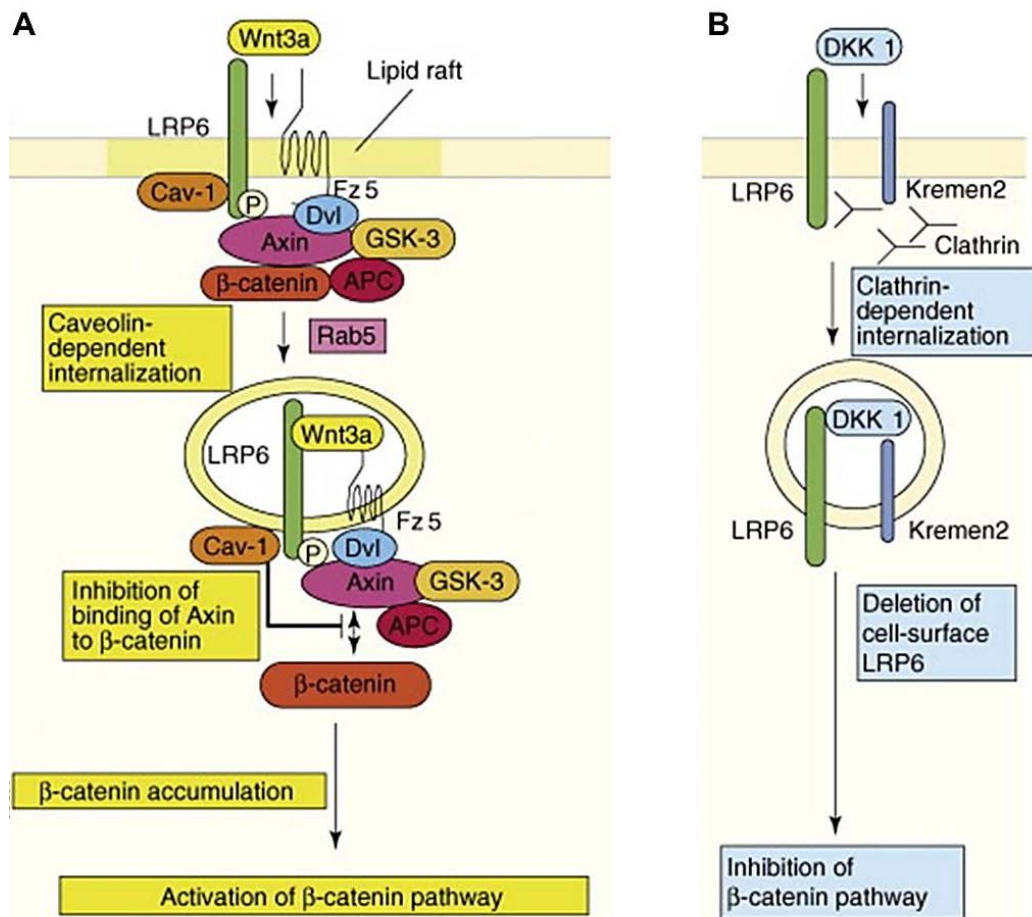


Figure 14: Regulation of Wnt signaling pathways by endocytosis.

(A) After a canonical Wnt ligand binds to LRP6 and Fz, the ligand-receptor complex, together with the components of the destruction complex, is internalized via a caveolin-dependent pathway. This internalization stabilizes β -catenin, possibly through the inactivation of Axin subsequently leading to an activation of the canonical/ β -catenin Wnt signaling pathway. **(B)** The binding of Dkk1 to LRP6 and Kremen induces a clathrin-dependent internalization of the ligand-receptor complex. LRP6 is removed from the cell surface resulting in an inhibition of the canonical/ β -catenin Wnt signaling pathway (modified after Kikuchi et al., 2009).

Further studies confirmed the model of distinct internalization pathways of LRP6 to activate or inhibit canonical Wnt signaling. In mouse F9 cells the endocytic adaptor protein disabled-2 (Dab2) regulates whether LRP6 is internalized via a caveolin- or clathrin-

mediated route. In the absence of Dab2 LRP6 is internalized via a caveolin-dependent manner, thus promoting canonical Wnt signaling. However, in the presence of Dab2, Wnt stimulation directs LRP6 to clathrin-dependent internalization, thereby inhibiting canonical Wnt signaling (Figure 15) (Jiang et al., 2012).

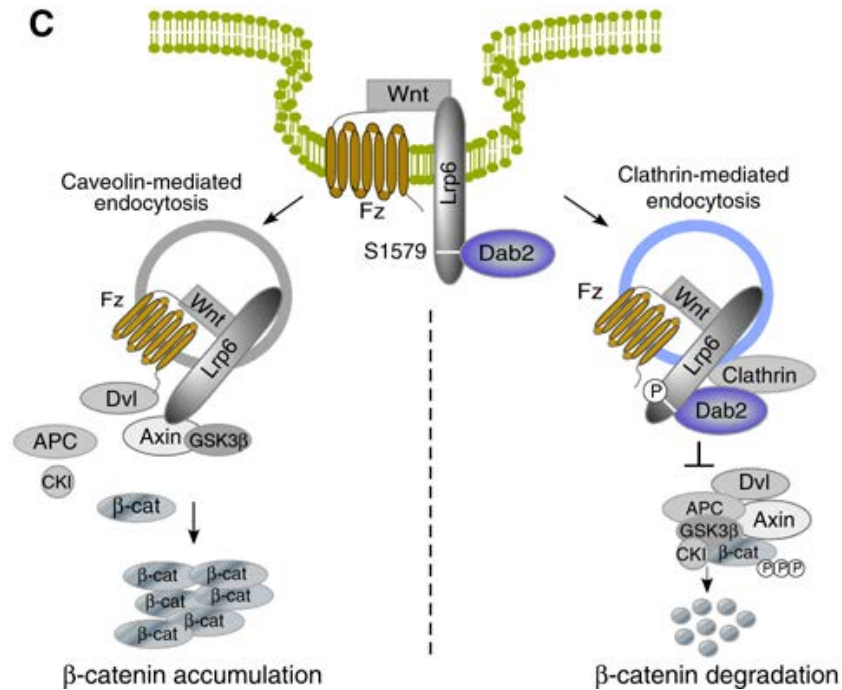


Figure 15: Dab2 directs LRP6 to different endocytic pathways.

Upon Wnt3a stimulation LRP is internalized via a caveolin-mediated pathway, in the absence of Dab2, triggering the activation of canonical Wnt signaling. In the presence of Dab2 LRP6 is internalized through the clathrin-dependent pathway promoting β -catenin degradation and inhibition of canonical Wnt signaling (Jiang et al., 2012).

Contrary to these data some findings indicate a function of clathrin in the activation of canonical Wnt signaling. In mouse fibroblast L-cells inhibition of clathrin-mediated endocytosis by pharmacological reagents blocks Wnt3a-mediated β -catenin stabilization (Chen et al., 2001; Blitzer and Nusse, 2006). Additionally β -arrestin, a clathrin adaptor was detected to bind Dsh and thereby promote Tcf transcriptional activation in cultured cells (HEK293, NIH 3T3 and L cells) (Chen et al., 2001). Knockdown of β -arrestin results in the inhibition of both Dsh phosphorylation and stabilization of β -catenin in response to Wnt3a (Bryja et al., 2007). These findings indicate a function of clathrin-mediated endocytosis in the activation of canonical Wnt signaling. However, if LRP6 and Fz are internalized via a clathrin-dependent pathway remains to be clarified (Kikuchi et al., 2009). Hence, contradictory data exist about the activation of canonical Wnt signaling through endocytosis. These inconsistent data might rely on different cell types, model organisms or different experimental conditions. Furthermore, pharmacological and molecular tools

that are used to study endocytic processes by blocking certain endocytic routes might have pleiotropic effects, which makes the interpretation of the results difficult (Kikuchi et al., 2009; MacDonald et al., 2009).

1.5.3 Regulation of non-canonical Wnt signaling by receptor-mediated endocytosis

Although the findings about the regulation of canonical Wnt signaling by endocytosis are controversial, non-canonical Wnt signaling has been clearly shown to be activated by clathrin-mediated endocytosis. In HEK293 cells Fz4 was found to be endocytosed upon Wnt5a stimulation. Fz4 endocytosis is mediated by the recruitment of Dsh2 and the clathrin adaptor, β -arrestin-2, which binds clathrin and further adaptor proteins to promote clathrin-mediated endocytosis. This endocytosis process results in enhanced non-canonical Wnt signaling (Chen et al., 2003; Feng and Gao, 2015). Further, the binding of Dsh2 to another clathrin-binding protein, called μ 2-adaptin, which is a subunit of adaptor protein 2 (AP2), was found to be required for Fz4 internalization and activation of PCP (Figure 16).

In addition the importance of clathrin-mediated endocytosis on PCP activation was shown in *Xenopus* animal cap explants. These mesodermal explants elongate via convergent extension movements activated by PCP signaling after treatment with activin protein. A Dsh mutant, unable to bind μ 2-adaptin, abolished animal cap explant elongation and was deficient in inducing JNK activation in *Xenopus* embryos (Yu et al., 2007). These findings show that upon binding of Wnt5a, Fz4 interacts with the Dsh2/ β -arrestin complex, which leads to the internalization of Fz4 via a clathrin-mediated route and thus activates PCP signaling (Kikuchi et al., 2009). Not only Fz4 but also Fz2 was demonstrated to be internalized by a clathrin-mediated route in response to Wnt5a in HeLaS3 cells. Inhibition of endocytosis abolished Wnt5a function to activate PCP signaling through Rac (Sato et al., 2010). Thus, Wnt5a stimulates the clathrin-mediated internalization of Fz4 and Fz5 to promote non-canonical Wnt/PCP signaling.

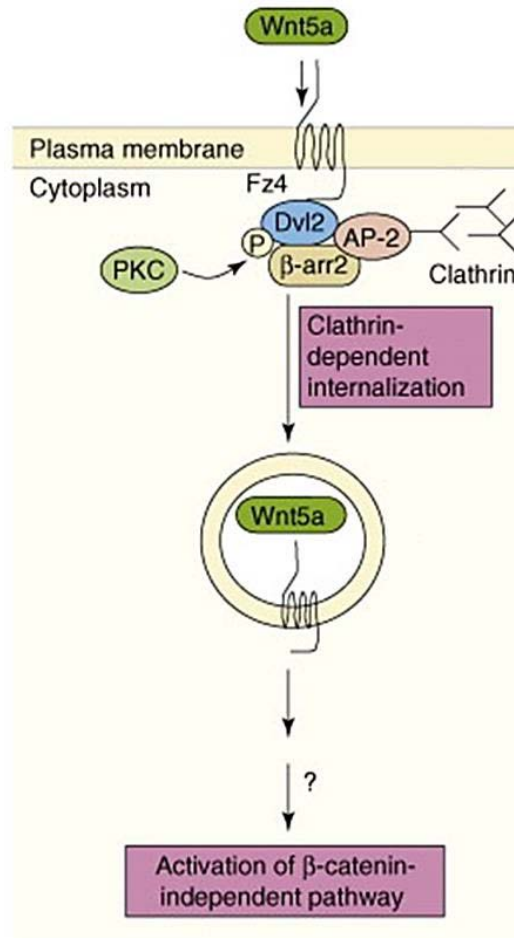


Figure 16: Regulation of non-canonical Wnt signaling by clathrin-mediated endocytosis.

Wnt5a stimulation induces the internalization of Fz via a clathrin-dependent pathway. The internalization depends on the phosphorylation of Dsh by PKC and the interaction of Dsh with β -arrestin and μ 2-adaptin, a subunit of the AP2 complex (modified after Kikuchi et al., 2009).

1.6 Regulation of canonical Wnt signaling by caveolin-1, independent of endocytosis

Several studies described a function of caveolin-mediated endocytosis in the activation of canonical Wnt signaling (Bilic et al., 2007; Yamamoto et al., 2008; Sakane et al., 2010; Jiang et al., 2012). Interestingly, canonical Wnt signaling was reported to be regulated by caveolin-1 in an endocytosis-independent manner in NIH 3T3 cells and zebrafish embryos (Galbiati et al., 2000; Mo et al., 2010). In NIH 3T3 cells caveolin-1 binds β -catenin and recruits it to membrane-bound caveolae, thus preventing its nuclear localization. The inhibitory effect of caveolin-1 on canonical Wnt signaling has been demonstrated by luciferase reporter assays. In these assays the ectopic expression of caveolin-1 blocks Wnt1- or β -catenin-mediated activation of canonical Wnt signaling (Galbiati et al., 2000). Similar findings in zebrafish embryos indicate that caveolin-1 contributes to dorsoventral

axis formation by inhibiting β -catenin nuclear localization. Ectopic expression of caveolin-1 results in the development of ventralized zebrafish embryos. Ventralized embryos are typically observed when maternal canonical Wnt signaling is blocked. Consistently loss of caveolin-1 led to the induction of ventral marker genes at the expense of dorsal marker genes. Similar to the results obtained in NIH 3T3 cells overexpression of caveolin-1 in zebrafish was found to inhibit β -catenin-mediated activation of canonical Wnt signaling in luciferase reporter assays (Mo et al., 2010). These findings suggest that caveolin-1 might additionally function without mediating endocytosis in the regulation of Wnt signaling.

1.7 PTK7

The evolutionary conserved transmembrane receptor protein tyrosine kinase 7 (PTK7) is involved in the regulation of diverse processes including embryonic morphogenesis and wound repair in adult organisms (Peradziryi et al., 2012). PTK7 was first identified in colon carcinoma cells and was accordingly named colon carcinoma kinase-4 (CCK-4) in humans (Mossie et al., 1995). In addition to colon carcinoma cells PTK7 expression is also upregulated in acute myeloid leukemia (AML) and various other cancer cell types (Easty et al., 1997; Muller-Tidow et al., 2004). Further orthologs of PTK7 were found in different organisms, including Lemon in Hydra (Miller and Steele, 2000), Off-track (Otk) in *Drosophila* (Pulido et al., 1992; Winberg et al., 2001), Kinase-like gene (KLG) in chicken (Chou and Hayman, 1991) and PTK7 in mouse (Chou and Hayman, 1991; Mossie et al., 1995; Park et al., 1996; Miller and Steele, 2000; Winberg et al., 2001; Jung et al., 2004). The PTK7 protein contains an N-terminal signal peptide, seven extracellular immunoglobulin domains, a single transmembrane domain and an intracellular tyrosine kinase homology domain (Figure 17) (Mossie et al., 1995; Park et al., 1996). However, PTK7 is catalytically inactive, due to a mutation in the DFG triplet within the kinase homology domain, which is necessary for kinase activity. Interestingly, the kinase homology domain is conserved from hydra to human, indicating that this domain is indeed important for PTK7 function (Mossie et al., 1995; Miller and Steele, 2000; Jung et al., 2004).

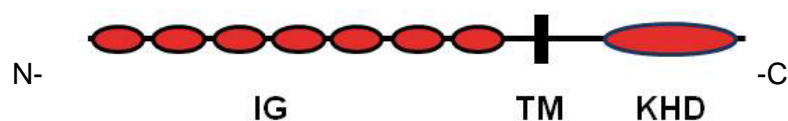


Figure 17: Protein structure of PTK7.

IG: immunoglobulin domains, TM: transmembrane domain, KHD: Kinase homology domain.

1.7.1 PTK7 functions in Wnt signaling

In vertebrates PTK7 loss-of-function leads to the development of animals showing classical PCP phenotypes. PTK7 knockout mice exhibit severe neural tube closure defects (craniorachischisis), with a completely open neural tube from the midbrain-hindbrain boundary to the base of the spine (Figure 18 A) (Lu et al., 2004). Additionally, PTK7 mutant mice have a shortened body axis and a broader floor plate. These phenotypes are typical for disruption of convergent extension movements. Moreover, PTK7 depletion affects the orientation of sensory hair cells of the ear, leading to the disruption of the stereociliary bundle orientation (Figure 18 A) (Lu et al., 2004; Paudyal et al., 2010). Typical PCP phenotypes were additionally observed in *Xenopus* and zebrafish embryos, where the knockdown of PTK7 as well results in neural tube closure and convergent extension defects (Figure 18 B) (Lu et al., 2004; Hayes et al., 2013). Another PCP regulated process, migration of neural crest cells, was also demonstrated to be controlled by PTK7. Loss-of-function of PTK7 in *Xenopus* leads to an inhibition of neural crest cell migration (Figure 18 C, D) (Shnitsar and Borchers 2008). PTK7 is expressed in the neuroectoderm in developing *Xenopus* embryos from late gastrula through all neurula stages, thus seems to regulate neural morphogenesis, including neural tube closure and migration of neural crest cells in these tissues (Lu et al., 2004).

Analyses in *Xenopus* embryos indicate a molecular mechanism by which PTK7 might promote PCP signaling. PTK7 recruits Dsh to the plasma membrane, which is a prerequisite for the activation of vertebrate PCP (Rothbacher et al., 2000; Wallingford et al., 2000; Shnitsar and Borchers, 2008). In *Xenopus* PTK7-Dsh interaction is mediated by the adaptor protein RACK1 (receptor of activated protein kinase C) which is recruited to the membrane by binding to the kinase domain of PTK7. RACK1 further interacts with PKC δ 1 thereby supporting Dsh recruitment (Figure 18 E) (Wehner et al., 2011). PTK7 function in activating PCP was demonstrated by the finding that its overexpression in *Xenopus* leads to nuclear localization of JNK (Shnitsar and Borchers, 2008) and transcriptional activation of ATF2 in luciferase reporter assays (Peradziryi et al., 2011). Surprisingly, although PTK7 was implicated to function in non-canonical Wnt/PCP signaling, it selectively interacts with canonical Wnt proteins via its extracellular domain, but not with non-canonical Wnt ligands. This interaction is mediated by Fz7, suggesting that PTK7 is a Fz co-receptor (Peradziryi et al., 2011; Linnemannstöns et al., 2014). These data suggest that PTK7 functions in non-canonical PCP/Wnt signaling and canonical Wnt signaling simultaneously. Double axis and luciferase reporter assays demonstrated an inhibitory effect of PTK7 on canonical Wnt signaling in *Xenopus*, zebrafish, *Drosophila* and mammalian cells, whereas depletion of PTK7 results in increased Wnt/ β -catenin target gene expression (Peradziryi et al., 2011; Hayes et al.,

2013). These data indicate a model of PTK7 function through receptor competition. PTK7 might compete with canonical Wnt co-receptors for Fz and Wnt binding. By displacing LRP6 from the ternary complex, PTK7 might prevent the activation of canonical Wnt signaling (Peradziryi et al., 2012).

For the *Drosophila* ortholog of PTK7, Otk, contradictory data have been reported. PTK7 depletion has been shown to result in defective epidermal patterning. As Otk was found to interact with Wnt4, it was suggested that Otk is a Wnt4 receptor and necessary for epidermal patterning (Peradziryi et al., 2012). However, in a later study, functions of Otk in epidermal patterning could not be confirmed and no PCP defects were observed for Otk knockout or knockout of its paralog Otk2 (Linnemannstöns et al., 2014), suggesting that the previously reported phenotypes might result from off-target effects. Interestingly the interaction with Fz and Wnt2 was confirmed (Linnemannstöns et al., 2014), further supporting the role of Otk/PTK7 as a Wnt-co-receptor, but likely with different functions in vertebrates and flies.

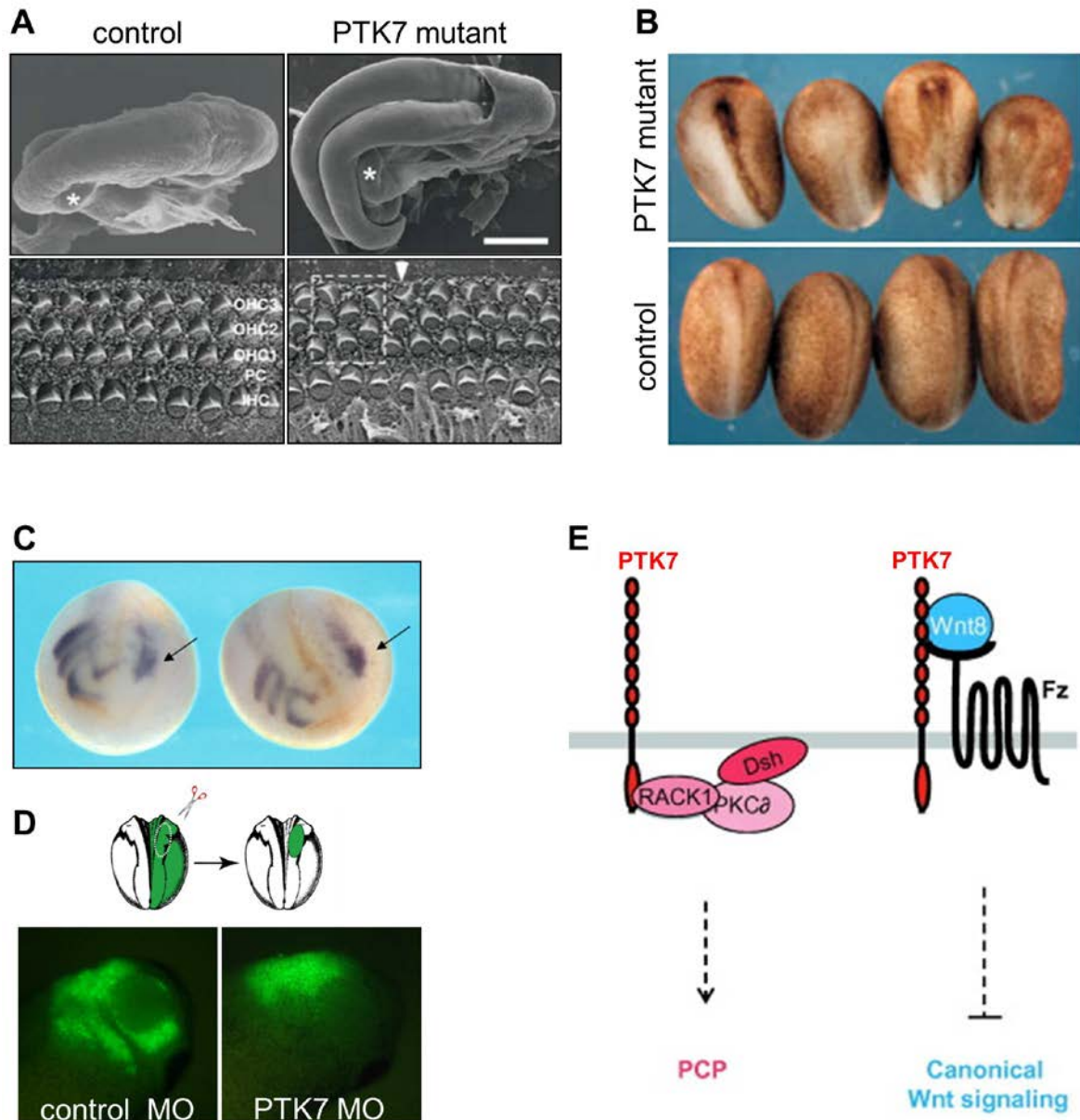


Figure 18: PTK7 functions in Wnt signaling in vertebrates.

(A) PTK7 knockout mouse exhibits a completely open neural tube (craniorachischisis) and misoriented stereociliary bundles of hair cells in the inner ear compared to the control mouse. In the cochlea one row of inner hair cells (IHC) and three rows of outer hair cells (OHC) are found separated by pillar cells (PC). The strongest bundle misorientation in the PTK7 mutant is found in the third row of OHC. (B) Knockdown of PTK7 by morpholino (MO) injections leads to open neural tubes in *Xenopus* embryos. Control morpholino injected embryos show closed neural tubes (Lu et al., 2004). (C) At the PTK7 MO injected side of the embryos (indicated by arrows) neural crest cells fail to migrate as they do at the non-injected side. (D) Neural crest migration defects are also observed in transplanted neural crest cells. Control MO or PTK7 MO was injected together with GFP as a lineage tracer and premigratory neural crest cells were transplanted into a wild type embryo. Control MO injected neural crest cells migrate in typical streams, while PTK7 MO injected neural crest cells fail to migrate (Shnitsar and Borchers, 2008). (E) Model of PTK7 function in Wnt signaling: PTK7 activates non-canonical Wnt signaling through the recruitment of Dsh via its kinase homology domain. The Dsh recruitment is supported by RACK1 and PKC δ 1. PTK7 is a Fz co-receptor and binds canonical Wnt ligands, thereby inhibiting canonical Wnt signaling, possibly through capturing Wnt ligands in a PCP signaling complex (modified after Peradziryi et al., 2012).

In contrast to these findings, a different study described an activating function of PTK7 in canonical Wnt signaling. PTK7 was shown to interact with β -catenin, thereby activating the transcription of β -catenin-dependent genes in mammalian cells and *Xenopus* embryos. Moreover, PTK7 was reported to be required for Spemann's organizer formation and *Siamois* promoter activation, both events depend on canonical Wnt signaling (Lhoumeau et al., 2011; Puppo et al., 2011). However, in zebrafish PTK7 requirement for Spemann's organizer formation could not be verified. In contrast, mRNA levels of *chordin* (*chd*) and *bozozok* (*boz*), which are both required for organizer formation in zebrafish, were upregulated in PTK7 knockout embryos, indicating an inhibitory effect of PTK7 on organizer formation (Hayes et al., 2013).

Moreover, PTK7 was reported to interact with the canonical key receptor LRP6. PTK7 depletion reduces LRP6 protein levels, thus PTK7 positively modulates canonical Wnt signaling through regulating LRP6 in this study (Bin-Nun et al., 2014).

1.7.2 PTK7 is a target for proteolytic cleavage

PTK7 is a target for proteolytic processing by several distinct membrane proteases (Figure 19). The first cleavage in the seventh immunoglobulin domain by membrane type-1 matrix metalloproteinase (MT1-MMP) releases a secreted extracellular PTK7 fragment. A second cleavage in the extracellular domain of PTK7 is performed by ADAMs. The proteolysis by MT1-MMP and ADAM is followed by a third cleavage by the γ -secretase in the C-terminal membrane region of PTK7. This cleavage generates a soluble cytoplasmic PTK7 fragment (Golubkov and Strongin, 2012). Interestingly, PTK7 proteolysis is necessary for its function on PCP signaling. Inhibition of MT1-MMP phenocopies PTK7 loss-of-function defects in convergent extension in zebrafish (Coyle et al., 2008; Golubkov et al., 2010). Moreover, a mouse PCP mutant, called *chuhzoi* (*chz*) was identified that shows typical PCP phenotypes like an open neural tube, convergent extension defects and misoriented inner ear hair cells. This mutant carries a splice site mutation in the *ptk7* gene, leading to the insertion of an additional MT1-MMP cleavage site between the fifth and sixth extracellular domain of PTK7 (Paudyal et al., 2010; Golubkov et al., 2011). Thus, proper PTK7 proteolysis by MT1-MMP seems to be essential for PTK7 function in PCP signaling.

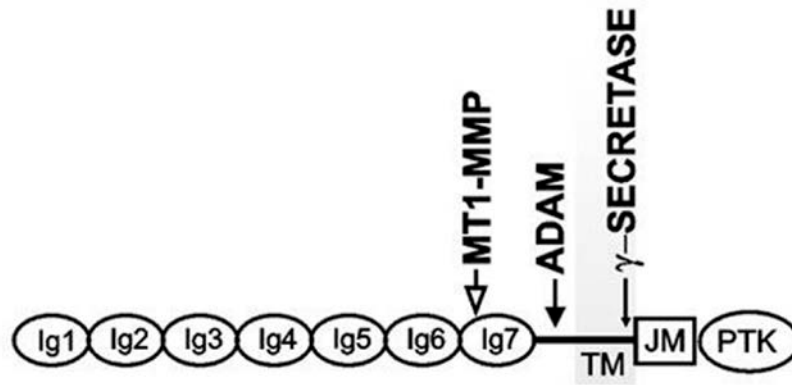


Figure 19: Model of PTK7 with the MT1-MMP, ADAM and γ -secretase cleavage sites.

Cleavage in the seventh Ig-like domain by MT1-MMP (open arrow) generates a soluble N-terminal PTK7 fragment and a C-terminal membrane-bound fragment. ADAM cleaves a peptide sequence proximal to the plasma membrane (solid arrow). Intramembrane cleavage by γ -secretase (thin arrow) leads to the generation of a cytoplasmic PTK7 fragment. Ig: immunoglobulin-like domains 1–7. TM: transmembrane domain. JM: juxtamembrane region. PTK: catalytically inactive pseudokinase domain (modified after Golubkov and Strongin, 2012).

1.8 The role of caveolin in early vertebrate development

1.8.1 Caveolae and the caveolin protein family

Caveolae (“little caves”) are flask-shaped invaginations of the plasma membrane with 60-80 nm in diameter, that were first identified by electron microscopy (Palade, 1953; Williams and Lisanti, 2004; Parton and Simons, 2007). Caveolae are located in lipid rafts, which are plasma membrane microdomains enriched in sphingolipids and cholesterol. Thus, caveolae are mainly localized in the plasma membrane but are also found in the cytoplasm as single vesicles or exist as higher-ordered multi-caveolae structures, called rosettes or caveolar clusters (Figure 20 A, B) (Parton and del Pozo, 2013). The structural components of caveolae are caveolin proteins, which together with a second group of proteins, namely cavins, are essential for caveolae formation (Figure 20 C) (Rothberg et al., 1992; Vinten et al., 2005; Parton and Simons, 2007; Hill et al., 2008; Parton and del Pozo, 2013).

The caveolin protein family includes two members (caveolin-1 and caveolin-2) in the nematode *C. elegans* (Tang et al., 1997) and three members in vertebrates, caveolin-1, caveolin-2 and caveolin-3 (Rothberg et al., 1992; Way and Parton, 1995; Scherer et al., 1996; Tang et al., 1996; Williams and Lisanti, 2004), indicating that caveolins are evolutionary conserved from worm to human. Two isoforms of caveolin-1 (caveolin-1 α and -1 β) have been identified, that arise by alternate splicing and so that they differ in the length of their N-terminus. Caveolin-1 β has an internal translation start site and thus is truncated by 31 residues (Scherer et al., 1995; Navarro et al., 2004).

The small caveolin proteins (18-24 kDa) are co-translationally inserted into the ER membranes, processed in the Golgi and transported to the plasma membrane to form caveolae (Liu et al., 2002b; Hayer et al., 2010). Thus, intracellularly caveolins are mostly found at the plasma membrane, in the Golgi, the ER and additionally in vesicles throughout the cytoplasm (Schlegel and Lisanti, 2000; Williams and Lisanti, 2004). The expression of the caveolin proteins varies between different tissues. Caveolin-1 (also called CAV-1 or VIP21) is broadly expressed in distinct cell types, with an abundant expression in smooth muscles, endothelial cells, adipocytes, fibroblasts and type I pneumocytes. Caveolin-2 (CAV-2) requires the formation of heterooligomers with caveolin-1 for proper membrane targeting and thus is co-expressed with caveolin-1 in same tissues (Scherer et al., 1997; Parolini et al., 1999; Parton and Simons, 2007; Parton and del Pozo, 2013; Shvets et al., 2014). Caveolin-3 (CAV-3) is specifically expressed in muscle cells, like smooth, skeletal and cardiac myocytes (Way and Parton, 1995; Tang et al., 1996). Depletion of caveolin-1 or caveolin-3 leads to a loss of caveolae formation in

the respective cell types (Drab et al., 2001; Galbiati et al., 2001), whereas caveolin-2 ablation has no effect on caveolae formation (Razani et al., 2002b). The levels of caveolin expression strongly differ from tissue to tissue with differences of about thousand-fold for example between adipocytes and hepatocytes. Nevertheless, also very low expression levels of caveolin are still functionally important, which has been shown in lymphocytes, neurons and hepatocytes (Parton and del Pozo, 2013).

The unusual structure of all three caveolin proteins is similar, with a short hydrophobic intramembrane domain forming a hairpin loop and their N- and C- termini facing the cytoplasm (Parton and Simons, 2007). The N-terminally localized scaffolding domain is highly conserved and binds cholesterol, fatty acids and various proteins including receptors, G-proteins and small GTPases to regulate their activity. The C-terminal domain is modified by palmitoyl groups, which insert into the plasma membrane (Figure 20 D) (Dietzen et al., 1995; Navarro et al., 2004; Williams and Lisanti, 2004; Parton and Simons, 2007). Caveolins form high molecular weight homo- or hetero-oligomeric complexes by interacting via their N-terminal domains. These complexes consist of 14-16 caveolin molecules (Monier et al., 1995; Pelkmans and Zerial, 2005; Parton and Simons, 2007). Caveolin-oligomerization and the specific interaction with cholesterol are required for caveolae formation as cholesterol depletion results in the disruption of caveolae (Smart and Anderson, 2002; Fridolfsson et al., 2014).

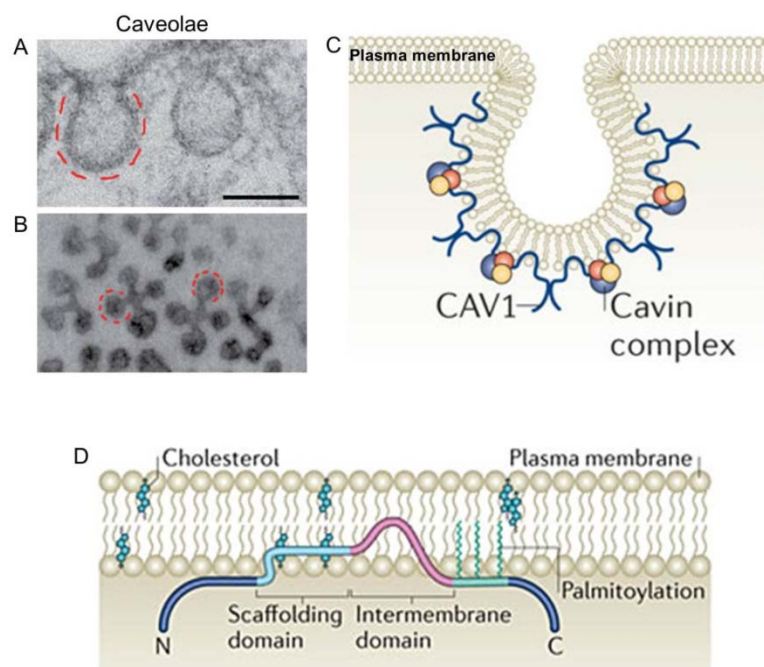


Figure 20: Caveolae and caveolins.

(A, B) Electron micrographs of single caveolae in fibroblasts (A) and clustered caveolae in the skeletal muscle (B) Scale bar: 100 nm. (C) Scheme of caveolae with membrane inserted caveolin proteins, which are stabilized by cavin complexes. (D) The structure of caveolin proteins, with the intermembrane domain forming a hairpin structure and the N- and C-termini facing the cytoplasm. Caveolin is modified C-terminally by palmitoyl groups that insert into the plasma membrane. The N-terminal scaffolding domain interacts with cholesterol (modified after Parton and del Pozo, 2013).

Caveolins play important roles during different cellular processes, including vesicular transport (Pelkmans and Helenius, 2002), cholesterol homeostasis, signal transduction and tumor suppression (Williams and Lisanti, 2004). Lipid raft concentrated caveolae were found to serve as cellular signaling platforms by compartmentalization and concentration of signaling molecules. The scaffolding domain of caveolin was identified to bind many signaling proteins, thereby activating or inhibiting downstream signaling (Nabi and Le, 2003; Williams and Lisanti, 2004).

In humans, misregulation of caveolins has been associated with several diseases, including lipodystrophy, cardiac diseases, muscular dystrophies and cancer (Parton and del Pozo, 2013). A caveolin-1 dominant negative mutant form (P132L), which has an impaired membrane localization, was found in up to 16% of human breast cancers (Hayashi et al., 2001; Lee et al., 2002). Moreover, mutation of caveolin-3 leads to a number of muscle disorders, for instance limb girdle muscular dystrophy (Woodman et al., 2004).

1.8.2 Phenotypes of caveolin-deficient vertebrates

Studying the phenotypes of caveolin-deficient animals gave insights into the function of caveolin *in vivo* (Le Lay and Kurzchalia, 2005). Interestingly, the single knockout of any caveolin gene (*caveolin-1*, *caveolin-2* or *caveolin-3*) and even the *caveolin-1/caveolin-3* double knockout in the mouse results in the development of viable and fertile animals. However, various defects such as muscle, pulmonary or lipid disorders have been reported (Le Lay and Kurzchalia, 2005). The knockdown of caveolin-1 in mice leads to a complete absence of caveolae in non-muscle tissues (Razani et al., 2001; Park et al., 2003). Moreover, a variety of diseases was reported including lipid disorders leading phenotypically to lean mice, cardiac diseases as hypertrophic cardiomyopathy (Le Lay and Kurzchalia, 2005), pulmonary defects due to thickening of the alveolar wall (Drab et al., 2001) and a higher tumorigenicity when exposed to carcinogens (Razani et al., 2001; Capozza et al., 2003). Caveolin-1 is required for proper membrane targeting of caveolin-2. Thus, after caveolin-1 depletion, caveolin-2 remains in the Golgi and is subsequently degraded. Hence, the caveolin-1 knockout mice can be regarded as caveolin-1/caveolin-2 double-knockouts (Razani et al., 2001). However, the single knockout of caveolin-2 only leads to pulmonary dysfunctions, indicating a specific role of caveolin-2 in lung function (Razani et al., 2002b).

Ablation of the muscle specific caveolin-3 protein results in the loss of caveolae in skeletal muscle fibers without affecting caveolae formation in non-muscle tissues. Interestingly, muscle degeneration with defects similar to those described in patients suffering from

limb-girdle muscular dystrophy, which is caused by a dominant-negative mutation of the human *caveolin-3* gene, were reported (Hagiwara et al., 2000). Furthermore, these mice have a disorganized T-tubule system (Galbiati et al., 2001). Thus, caveolin-3 is important for normal muscle function in the mouse.

Interestingly, even caveolin-1/caveolin-3 double knockout mice, which lack all caveolae in muscle and non-muscle tissues, are still viable and fertile. These mice exhibit defects similar to their single knockout counterparts, but show more severe cardiomyopathy, indicating a crucial role of caveolae in the heart (Park et al., 2002; Le Lay and Kurzchalia, 2005). In contrast to the mouse model organism, depletion of either caveolin-1 isoform (α or β) in zebrafish leads to morphological defects and embryonic lethality after approximately 5 days post fertilization. These defects include curved tails, eye development defects, heart defects, a deformed notochord, misorganized somites with disrupted actin microfilaments and disrupted vascular endothelial tissue (Figure 21) (Fang et al., 2006; Nixon et al., 2007). Interestingly, the two caveolin-1 isoforms seem to exhibit distinct functions in zebrafish development. Although the phenotypes are quite similar, caveolin-1 α affects neural and tail tissue development, whereas caveolin-1 β exclusively affects neural tissue. Furthermore rescue experiments revealed that the isoforms exhibit non-redundant roles during zebrafish development as caveolin-1 α was not able to rescue the phenotype caused by caveolin-1 β depletion and *vice versa* (Fang et al., 2006). In the chick, mouse and zebrafish a high caveolin-1 expression was detected in the notochord. Further, in zebrafish caveolin-1 ablation leads to the disruption of the notochord, indicating a conserved role of caveolin in notochord development and/or function (Nixon et al., 2007).

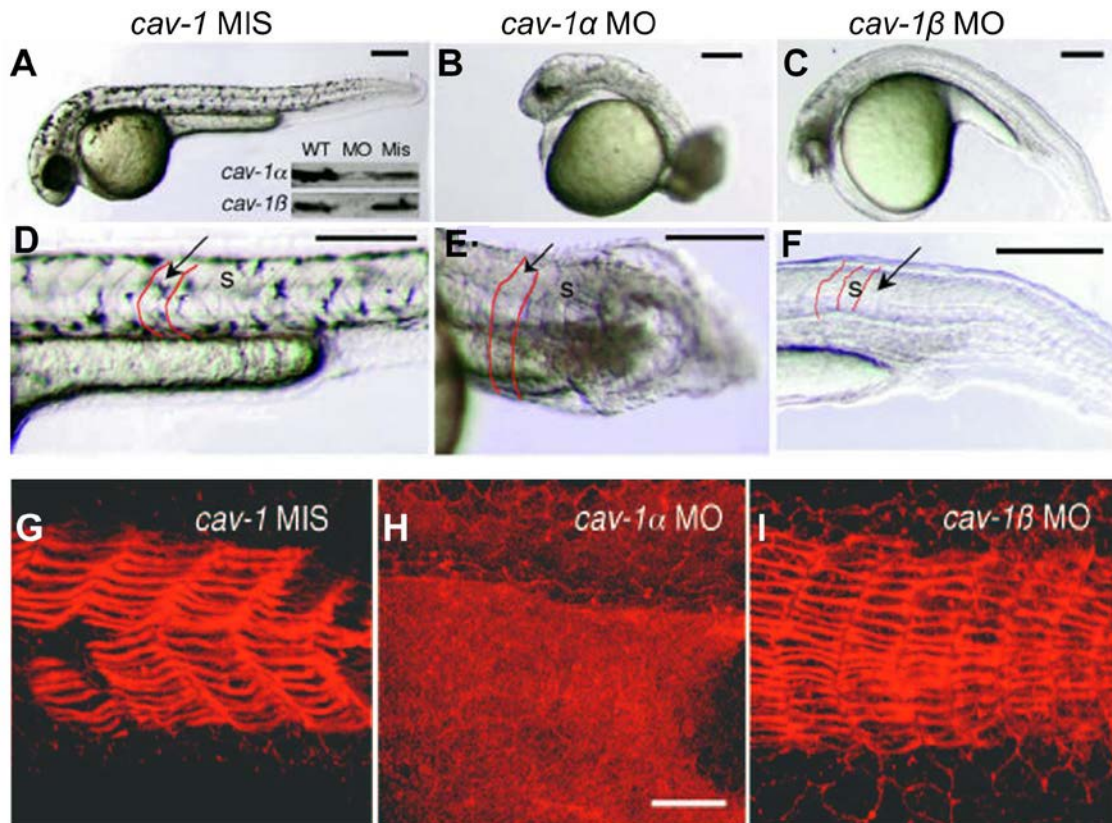


Figure 21: Phenotypes of caveolin-1 deficient zebrafish embryos.

(A, D) Mismatch control morpholino injected zebrafish embryos show normal morphological development. (B, E) Caveolin-1 α depleted zebrafish embryos exhibit curved or kinked tails, eye developmental defects and impaired somite patterning. (C, F) Caveolin-1 β depleted embryos show the same but less severe phenotypes as caveolin-1 α morphants and have additionally a flattened head. (G) Normal organization of the actin cytoskeleton in control embryos. (H) Misorganized and disrupted actin cytoskeleton of the somites in caveolin-1 α morphant embryo and (I) slight disruption in caveolin-1 β morphant embryos (Fang et al., 2006).

1.9 Aim of this study

PTK7 is a Wnt co-receptor that is involved in both canonical and non-canonical Wnt signaling pathways. PTK7 activates non-canonical PCP/Wnt signaling but inhibits canonical Wnt signaling. Wnt signaling pathways have been shown to be regulated by endocytosis, which plays a role in both, signal termination or activation. This endocytosis processes are often induced by the binding of different Wnt ligands to their respective receptors. Interestingly, previous findings from our lab revealed that PTK7 binds exclusively canonical Wnt ligands (Peradziryi et al., 2011). However, it remains unclear how canonical Wnt ligands affect the function of PTK7. Preliminary data suggest that PTK7 may be endocytosed in response to Wnt ligands. Thus, the aim of this study is to characterize the effect of canonical Wnt ligands on the localization and stability of the PTK7 protein and consequently on its function regarding Wnt signaling. Therefore, the localization and stability of the PTK7 protein in response to Wnt proteins will be analyzed. It will be studied if the binding of canonical and non-canonical Wnt ligands to PTK7 induces its endocytosis as reported for other Wnt co-receptors. If we confirm that PTK7 is endocytosed in the presence of Wnt we will determine if this process is caveolin- or clathrin-dependent and if the kinase domain of PTK7, which is catalytically non-active, but relevant for its function in PCP signaling, is required. Moreover, using inhibitors of endocytosis we will determine how endocytosis affects the function/s of PTK7 in Wnt signaling.

2 Materials and Methods

2.1 Model Organisms

During this study the African clawed frog *Xenopus laevis* (*X. laevis*) served as a model organism. Adult frogs were obtained from Nasco (Ft. Atkinson, USA).

2.2 Bacteria

E. coli strain XL1-Blue *recA1 endA1 gyrA96 thi-1 hsdR17 supE44 relA1 lac* [F' *proABlacIqZΔM15 Tn10* (Tetr)] (Stratagene) was used for cloning procedures.

2.3 Cell lines

MCF7 (Michigan Cancer Foundation-7), breast adenocarcinoma cells, ATCC No (HTB-22).

2.4 Chemicals, Buffers and Media

2.4.1 Chemicals

Chemicals for the preparation of buffers, solutions and media were obtained from the following companies: Carl Roth (Karlsruhe), Thermo Fisher Scientific (Waltham, MA, USA), Roche (Mannheim), Sigma-Aldrich (Munich), Applichem (Darmstadt), Merck (Darmstadt), Merck Millipore (Berlin).

2.4.2 Buffers and Media

Alkaline phosphatase buffer (APB)	100 mM Tris-HCl (pH 9.5) 50 mM MgCl ₂ 100 mM NaCl 0.1% Tween20
Blocking buffer (Western blot)	5% (w/v) dry, non-fat milk powder in TBST
Blocking solution (immunostaining)	1% bovine serum albumin (BSA) in 1x PBS

Cell culture Medium	<p>RPMI 1640 (Merck Millipore)</p> <p>10% (v/v) FCS</p> <p>100 U/ml penicillin</p> <p>100 µg/ml streptomycin</p> <p>Opti-MEM® Reduced Serum Medium</p> <p>GlutaMAX™ Supplement (Thermo Fisher Scientific)</p>
Co-IP buffer	<p>50 mM Tris pH 7.5</p> <p>150 mM NaCl</p> <p>0.5% (v/v) NP-40</p>
Co-IP lysis buffer	<p>50 mM Tris-HCl, pH 7.5</p> <p>150 mM NaCl</p> <p>0.5% NP-40</p> <p>Complete Protease inhibitor mix EDTA free (1 tablet / 50 ml, Roche)</p>
Cysteinhydrochloride-solution	<p>2% L-Cysteinhydrochloride, pH 8.0, adjusted with NaOH</p>
Gelatin/albumin embedding medium	<p>4,4% gelatin</p> <p>27% bovine serum albumin (BSA)</p> <p>18% saccharose</p> <p>in 1x PBS</p>
Hybridization mix (Hyb-mix)	<p>50% (v/v) Formamid</p> <p>5xSSC</p> <p>1 mg/ml Torula RNA (Sigma)</p> <p>100 µg/ml Heparin</p> <p>1x Denhardts</p> <p>0.1% (v/v) Tween20</p> <p>0.1% (w/v) CHAPS (Sigma)</p>
Injection buffer	<p>1x MBS, 2% Ficoll 400 (Sigma)</p>
Laemmli running buffer (10x)	<p>250 mM Tris-base</p> <p>2.5 M Glycine</p> <p>0.1% SDS</p>

Laemmli loading buffer (6x)	350 mM Tris-HCl, pH 6.8 9.3% Dithiotreitol 30% (v/v) Glycerol 10% SDS 0.02% Bromphenolblue
Luria-Bertani (LB)-Medium	1% (w/v) Bacto-Trypton (Carl Roth) 0.5% (w/v) yeast extract (Carl Roth) 1% (w/v) NaCl, pH 7.5
LB-Agar	2% (w/v) agar (Carl Roth) in liquid LB-medium
MAB	100 mM Maleic acid 150 mM NaCl, pH 7.5
MBS Buffer	10 mM Hepes pH 7.4 88 mM NaCl 1 mM KCl 2.4 mM NaHCO ₃ 0.2 mM MgSO ₄ 0.41 mM CaCl ₂ 0.66 mM KNO ₃
MEM	100 mM MOPS, 2 mM EGTA, 1 mM MgSO ₄
MEMFA	1x MEM with 4% (v/v) Formaldehyde
Moviol embedding solution	5 gr Moviol 10 ml Glycerol 20 ml 1x PBS
Nile blue	0.5 M Na ₂ HPO ₄ 1 M NaH ₂ PO ₄ 0.01% Nile Blue Chloride
PBS (10x)	8% (w/v) NaCl 2% (w/v) KCl 65 mM Na ₂ HPO ₄ 18 mM KH ₂ PO ₄ , pH 7.4

PonceauS solution	0.2% PonceauS, 3% trichloro acetic acid
PTw buffer	1x PBS with 0.1% Tween20
SSC	150 mM NaCl 15 mM Sodiumcitrate, pH 7.4
TAE (Tris/Acetate/EDTA)	40 mM Tris-Acetate (pH 8.5) 2 mM EDTA
TE-Buffer	10 mM Tris pH 8.0 1 mM EDTA
TBS	50 mM Tris-HCl pH 7.5, 150 mM NaCl
TBST	TBS + 0.5% (v/v) Tween 20
Transfer buffer	25 mM Tris 192 mM Glycine 20% (v/v) Methanol
Tris HCl (pH 6.8, 7.5, 8.8)	1/1.5 M Tris-HCl, pH adjusted with 32% HCl
X-gal staining solution	1 mg/ml X-gal 5 mM $K_3Fe(CN)_6$ 5 mM $K_4Fe(CN)_6$ 2 mM $MgCl_2$

2.5 Vectors and Constructs

2.5.1 Vectors

pCS2+ is a multipurpose expression vector, used for the expression of proteins in *Xenopus*, zebrafish and mammalian cells. It contains a strong enhancer/promoter (simian CMV IE94), a polylinker and a SV40 late polyadenylation site. This vector includes an SP6 promoter, allowing *in vitro* transcription of sense polyadenylated mRNA and a T7 promoter in reverse orientation for synthesis of antisense mRNA for *in situ* hybridization. The ampicillin resistance gene is present for selection of transformants (Rupp et al., 1994).

pCS2+/MT contains six copies of the Myc-tag (MT) sequence inserted into BamHI/Clal sites of the pCS2+vector to allow for expression of Myc-tagged proteins (Klisch et al., 2006).

pCS2+/HA contains the hemagglutinin (HA) epitope tag inserted into the pCS2+ vector at the XbaI site to allow for expression of HA-tagged proteins (Damianitsch et al., 2009).

pCS2+/GFP contains the GFP sequence inserted into XbaI/XhoI sites for the expression of GFP-tagged proteins.

pEGFP-N1 is used for the expression of EGFP fusion proteins in mammalian cells. The neomycin resistance gene is present for selection of transformants (Clonetechn).

pcDNA5TM/O contains a CMV IE promoter and a tetracycline operator for tetracycline inducible gene expression in mammalian cells (Hillen et al., 1983; Hillen and Berens, 1994) (Thermo Fisher Scientific).

pcDNA6TM/R contains the tetracycline resistance gene. It is used for tetracycline inducible gene expression in mammalian cells (Hillen et al., 1983; Hillen and Berens, 1994) (Thermo Fisher Scientific).

pGL3 is a luciferase reporter vector containing the firefly luciferase gene. This vector is used for the quantitative analysis of factors that regulate mammalian gene expression (Promega).

pRL-TK is a control reporter vector that is used in combination with a firefly luciferase vector to co-transfect eukaryotic cells. This vector contains the *Renilla* luciferase gene under the control of the herpes simplex virus thymidine kinase (HSV-TK) promoter (Promega).

pCMV-Sport6 is used for eukaryotic protein expression (Thermo Fisher Scientific).

pGEM-T is used as a cloning vector (Promega).

2.5.2 Expression constructs

Table 1: Expression constructs used in this study

Name	Vector	Description	Reference/ Cloning Strategy
Caveolin-1 α -HA	pCS2+/HA	<i>Xenopus laevis</i> caveolin-1 α with a HA-tag	Hanna Peradziryi, PhD thesis
Caveolin-1 α -HA shifted ATG	pCS2+/HA	<i>Xenopus laevis</i> caveolin-1 α with a 5' truncated region of 24 base pairs to shift the ATG. Contains a HA-tag.	The caveolin-1 α -HA plasmid was amplified using the primers <i>Cav1a new ATG NheI for</i> and <i>Cav1a new ATG NheI rev</i> to generate a 5' truncated caveolin-1 α construct.
lacZ	pCS2+	Bacterial β -galactosidase	(Smith and Harland, 1991)
MyoD	pSP73	<i>Xenopus laevis</i> myogenic differentiation (MyoD)	(Hopwood et al., 1989b)
Pax-2	pT7TS	<i>Xenopus laevis</i> paired box 2 (Pax-2)	Kind gift from Pieler lab, Göttingen
PTK7	pCMVSPORT6	<i>Xenopus laevis</i> full length PTK7	(Shnitsar and Borchers, 2008)
PTK7-EGFP	pcDNA5 T/O	EGFP-tagged human full length PTK7	Martina Podleschny, PhD thesis
Δ kPTK7-EGFP	pcDNA5 T/O	EGFP-tagged human PTK7 with deleted kinase homology domain	Martina Podleschny, PhD thesis

PTK7-RFP	pCS2+	RFP-tagged <i>Xenopus laevis</i> full-length PTK7	Iryna Shnitsar, unpublished
PTK7-MT	pCS2+/MT	<i>Xenopus laevis</i> full length PTK7 with a Myc tag	(Shnitsar and Borchers, 2008)
Δ kPTK7-MT	pCS2+/MT	<i>Xenopus laevis</i> PTK7 with deleted kinase homology domain and a Myc tag	(Shnitsar and Borchers, 2008)
Renilla Reporter	pRL-TK	contains the Renilla luciferase gene under the control of the herpes simplex virus thymidine kinase (HSV-TK) promoter	Promega
Siamois Reporter	pGL3	<i>Xenopus laevis</i> Siamois promoter upstream of Firefly luciferase	(Brannon et al., 1997)
Wnt2b-EGFP	pCS2+	EGFP-tagged <i>Xenopus laevis</i> Wnt2b	(Holzer et al., 2012)
Wnt5a-EGFP	pCS2+	EGFP-tagged <i>Xenopus laevis</i> Wnt5a	(Wallkamm et al., 2014)
Wnt8	pCS2+	<i>Xenopus laevis</i> Wnt8	(Peradziryi et al., 2011)
Xbra	pSP72	<i>Xenopus laevis</i> homolog of Brachyury (T)	(Smith et al., 1991)
xTwist	pGEM-T	<i>Xenopus laevis</i> Twist	(Hopwood et al., 1989a)

2.5.3 Linearization of constructs for sense or antisense *in vitro* transcription

Table 2: Restriction enzymes for linearization of constructs and polymerases used for *in vitro* transcription

Name	Sense RNA		Antisense RNA	
	Restriction enzyme	Polymerase	Restriction enzyme	Polymerase
Caveolin-1 α -HA	NotI	SP6		
Caveolin-1 α -HA shifted ATG	NotI	SP6		
lacZ	NotI	SP6		
MyoD			BamHI	Sp6
Pax-2			EcoRI	T3
PTK7	NotI	SP6		
PTK7-MT	NotI	SP6		
Δ kPTK7-MT	NotI	SP6		
Wnt8	NotI	SP6		
Xbra			HindIII	T7
xTwist			EcoRI	T7

2.6 Oligonucleotides

2.6.1 Cloning primers

Oligonucleotides for cloning procedures were purchased from Sigma-Aldrich (Munich). The primer sequence is given in 5'→3' direction. The enzyme restriction sites are indicated in bold letters.

Cav1a new ATG NheI for
Cav1a new ATG NheI rev

AT**GCTAGC**ATGGAAGAGGGTGTCTCTACAC
 AT**GCTAGC**GAATCGATGGGATCCTGCAAA

2.6.2 Sequencing primers

The following primers were used for sequencing of expression constructs in pCS2+ vectors. The primer sequence is given in 5'→3' direction.

SP6	TTAGGTGACACTATAGAATAC
T3	AATTAACCCTCACTAAAGGG
T7	TCTACGTAATACGACTCACTATAG

2.6.3 Morpholino oligonucleotides

Morpholino oligonucleotides used in this study were purchased from GeneTools, LLC (Philomath, Oregon, USA).

Table 3: Antisense Morpholino oligonucleotides

Morpholino name	Target gene	Sequence in 5'→3' direction	Concentration/embryo
Cav1 α -MO	<i>Xenopus laevis</i> <i>caveolin-1α</i>	CATCTATGTATTTGCCACCAGACAT	5 -20 ng
Cav1 β -MO	<i>Xenopus laevis</i> <i>caveolin-1β</i>	CGTCAGTCAGCATATCATCTGCCAT	5 -20 ng
Control MO	No target	CCTCTTACCTCAGTTACAATTTATA	5 -20 ng

2.7 Antibodies

Table 4: Antibodies

Name	Company, catalog number	Description	Dilution		
			WB	IF	IP
Actin	Merck Millipore, MAB1501	Primary mouse monoclonal IgG, recognizes F- and G-actin	1:2000		

Name	Company, catalog number	Description	Dilution		
			WB	IF	IP
MT (9E10)	Sigma, M4439	Primary mouse monoclonal IgG, recognizes MT epitope corresponding to residues 408-439 of the human c-Myc protein	1:5000	1:500	
MT-Cy3 (9E10)	Sigma, C6594	9E10 MT antibody directly coupled to Cy3		1:100	
MT	Abcam ab19234	Primary goat polyclonal IgG, against MT epitope, recognizes peptide sequence EQKLISEEDL	1:10000		1:250
GFP	Abcam, ab290	Primary rabbit polyclonal IgG, recognizes GFP	1:2000	1:1000	
GFP	Roche, 11814460001	Primary mouse monoclonal IgG, recognizes GFP	1:1000		
HA.11	Covance, MMS-101P	Primary mouse monoclonal IgG, recognizes hemagglutinin epitope (YPYDVPDYA)	1:1000	1:100	1:150
Caveolin	Abcam, ab2910	Primary rabbit polyclonal IgG against caveolin-1 protein	1:1000	1:500	
Clathrin	Abcam, ab144409	Primary mouse monoclonal IgG against clathrin light chain protein		1:500	
EEA1	Abcam, ab2900	Primary rabbit polyclonal IgG against EEA1 protein		1:500	
PTK7 (CCK-4)	R&D systems, AF4499	Primary polyclonal goat IgG, recognizes human, mouse, rat PTK7 (CCK-4) protein	1:1000	1:200	
Wnt3a	Cell signaling, 2721	Primary monoclonal rabbit IgG, recognizes human, mouse, rat Wnt3a protein	1:1000		
α -mouse-Alexa 488	Thermo Fisher Scientific, A-11029	Secondary goat polyclonal IgG, conjugated with Alexa Fluor® 488		1:400	
α -mouse-Alexa 594	Thermo Fisher Scientific, A-11005	Secondary goat polyclonal IgG, conjugated with Alexa Fluor® 596		1:400	

Name	Company, catalog number	Description	Dilution		
			WB	IF	IP
α -rabbit-Alexa 488	Thermo Fisher Scientific, A-11008	Secondary goat polyclonal IgG, conjugated with Alexa Fluor® 488		1:400	
α -rabbit-Alexa 594	Thermo Fisher Scientific, A-11012	Secondary goat polyclonal IgG, conjugated with Alexa Fluor® 596		1:400	
α -rabbit-HRP	CellSignaling, 7074	Secondary goat polyclonal IgG coupled with HRP	1:2000		
α -mouse-HRP	Santa Cruz	Secondary goat polyclonal IgG coupled with HRP	1:5000		
α -goat-HRP	Santa Cruz	Secondary donkey polyclonal IgG coupled with HRP	1:10000		

2.8 DNA methods and cloning procedures

2.8.1 Isolation of plasmid DNA from *E. coli*

To isolate plasmid DNA from *E. coli* cultures in analytical amounts the GeneJET Plasmid Miniprep Kit (Thermo Scientific) was used. Isolation of preparative amounts was carried out using the NucleoBond Xtra Midi Kit (Macherey and Nagel). Plasmid DNA isolation was performed after the manufacturer's instructions. Isolated plasmid DNA concentration was quantified using the NanoDrop 2000c spectrophotometer (Thermo Fisher Scientific).

2.8.2 Polymerase chain reaction

For the *in vitro* amplification of DNA fragments the polymerase chain reaction (PCR) was applied (Saiki et al., 1988). The amplification reaction was carried out by either the DreamTaq™ DNA Polymerase (Thermo Scientific) for analytical PCR reactions or the Phusion™ High-Fidelity DNA Polymerase (Thermo Scientific) for subsequent cloning procedures. To perform a standard PCR reaction 10 - 100 ng of the DNA template and oligonucleotides in a final concentration of 10 μ M were used. Deoxynucleotide triphosphates (dNTPs), the polymerase and the respective reaction buffer were added after the instructions of the manufacturer. The PCR programs and the temperature profiles

were chosen according to the used oligonucleotides and the expected DNA fragment size. Optionally, PCR reactions were purified using the GeneJET PCR Purification kit (Thermo Scientific).

Table 5: Temperature profile of the PCR reaction

	Phusion™-polymerase	DreamTaq™-polymerase
1. Initial heat-denaturation	98 °C, 25 sec	95 °C, 25 sec
2. heat-denaturation	98 °C, 10 sec	95 °C, 10 sec
3. Annealing	specific annealing temperature, 25 sec	
4. Elongation	72 °C, 20 sec/kb	72 °C, 1 minutes/kb
5. Final step of synthesis	72 °C, 5 minutes	72 °C, 5 minutes

2.8.3 Colony PCR

To test whether a cloning process was successful colony PCR was performed. Therefore, single *E. coli* colonies from a transformation plate were picked using a sterile toothpick and put into a 0.5 ml reaction tube. Each single colony was used as a template for the following PCR reaction. Primers amplifying the inserted fragment were used. Amplification was performed using the DreamTaq™ DNA Polymerase.

2.8.4 Agarose gel electrophoresis

To separate DNA fragments according to their size in an electrical field, agarose gel electrophoresis was performed (Sharp et al., 1973). Samples mixed with DNA loading dye (6x, Thermo Fisher Scientific) were loaded on 1% (w/v) agarose gels, prepared in 1x TAE buffer containing 0.5 µg/ml ethidium bromide or 1x GelRed™ fluorescent nucleic acid dye (GeneOn, Ludwigshafen). Electrophoresis was run in horizontal electrophoresis chambers containing 1x TAE buffer at 90-120 V. The DNA bands were detected in a UV - transilluminator at $\lambda = 254$ nm.

2.8.5 Purification of DNA fragments from agarose gels

The desired DNA bands, which were separated by gel electrophoresis, were cut out under UV - light from the agarose gel using a scalpel. DNA purification was performed using the GeneJET Gel Extraction Kit (Thermo Scientific) or to yield high concentrations in minimal

volumes the Zymoclean™ Gel DNA Recovery Kit (Zymo Research, Irvine, CA, USA) according to the manufacturer's instructions. The DNA concentrations were measured using the NanoDrop 2000c spectrophotometer (Thermo Fisher Scientific).

2.8.6 Restriction digestion of DNA

Restriction enzymes were purchased from Thermo Fisher Scientific. The restriction digestion was prepared according to the instructions of the manufacturer. Restriction digestion reactions were either purified using the GeneJET PCR Purification kit (Thermo Fisher Scientific) or purified from the gel after agarose gel electrophoresis.

2.8.7 Ligation of DNA-fragments

Linearized DNA fragments were incubated in a reaction volume of 10 µl containing 5 U T4 - DNA-ligase (Thermo Scientific) according to the manufacturer's protocol. The reaction was allowed to proceed overnight at 16 °C or 1 hour at room temperature. DNA concentrations of 50 - 200 ng/µl were used in a molar concentration ratio of 1:3 between vector and insert DNA. The T4 ligase was inactivated by incubation at 65 °C for 10 minutes and subsequently transformed using competent *E. coli* cells.

2.8.8 Chemical transformation of *E. coli* cells

For transformation of *E. coli* XL1blue cells, chemical competent cells were thawed on ice. 100 ng plasmid DNA or 5- 10 µl ligation mix were added to 200 µl of the bacterial cells and incubated for 30 minutes on ice. After a heat-shock for 2 minutes at 42 °C, the cells were cooled down on ice for 5 minutes prior to the addition of 800 µl warm LB Medium. The samples were incubated for 30 minutes up to 1 hour at 37 °C on a shaker (Inoue *et al.*, 1990). The transformed cells were pelleted and plated with the aid of sterile glass beads or a sterilized Drigalski spatula on LB plates containing ampicillin or kanamycin at a final concentration of 100 µg/ml or 50 µg/ml, respectively. Transformation plates were incubated overnight at 37 °C.

2.8.9 Sequencing of DNA

Sequencing of DNA was done using the Dye-termination method, modified from the Sanger chain-termination sequencing method (Sanger *et al.*, 1977) with the use of the Big Dye™ Terminator Kit (Applied Biosystems) according to the manufacturer's instructions.

The sequencing analysis was performed with the ABI 3100 Automated Capillary DNA Sequencer (Applied Biosystems). Alternatively, DNA samples were sent to GATC Biotech (Konstanz) for sequencing analysis.

2.9 RNA methods

2.9.1 *In vitro* synthesis of capped sense RNA

Capped sense mRNAs for microinjection into *Xenopus laevis* embryos were synthesized *in vitro* using the SP6 or T7 mMessage mMachine kit™ (Ambion/Thermo Fisher Scientific) according to the manufacturer's protocol. 1.2 µg linearized DNA was used in a total reaction volume of 20 µl and the reaction was incubated for 2 hours at 37 °C. TURBO DNase I (Ambion/Thermo Fisher Scientific) treatment was performed for 15 minutes at 37 °C to digest the DNA template. The Illustra™ RNAspin Mini RNA Isolation Kit (GE Healthcare) was used for mRNA clean-up. Synthesized mRNA was quantified using the NanoDrop 2000c spectrophotometer (Thermo Fisher Scientific).

2.9.2 *In vitro* synthesis of labeled antisense RNA

Synthesis of digoxigenin labeled antisense RNA probes for whole mount *in situ* hybridization of *Xenopus* embryos was carried out as follows:

Table 6: *In vitro* synthesis of antisense RNA

volume/concentration	reagents
1 µg	Template DNA
5 µl	5x transcription buffer (Invitrogen)
1 µl	10 mM each of rATP, rCTP, rGTP (Thermo Scientific)
0.64 µl	10 mM rUTP (Thermo Scientific)
0.36 µl	10 mM digoxigenin-rUTP (Roche)
1 µl	0.75 M DTT
0.5 µl	RNAseOut (Invitrogen)
1 µl	T7 polymerase (20U/µl, Invitrogen)

RNAse-free water (Amresco) was added to a final volume of 25 µl.

The reaction mix was incubated at 37 °C for 2 hours. Afterwards the DNA template was digested using Turbo DNaseI (Ambion/Thermo Fisher Scientific). Synthesized antisense RNA was purified using the RNeasy™ mini Kit (Qiagen) after the manufacturer's protocol.

2.10 Cell culture techniques

2.10.1 Propagation of cell lines

Human cell lines were cultured in cell culture flasks (Greiner bio-one/Sarstedt) in a sterile incubator at 37 °C, 5% (v/v) CO₂ and 95% humidity. RPMI 1640 medium (Merck Millipore), supplemented with 10% (v/v) fetal calf serum (FCS), 100 U/ml penicillin (Merck Millipore) and 100 µg/ml streptomycin (Merck Millipore) was used for cultivating MCF7 cells. The cells were split once per week with a subcultivation ratio of 1:10. Therefore, trypsin-EDTA (0.025% (w/v) Trypsin, 0.53 mM EDTA) was added to the cells for 5 - 10 minutes at 37 °C to break the adhesion and detach the cells from the flask. Trypsin was inactivated by the addition of 5 - 10 ml RPMI 1640 medium and the appropriate volume of the cell suspension was transferred into a new cell culture flask containing medium. For long term storage cells were frozen in FCS supplemented with 10% (v/v) DMSO in cryotubes (Nunc™, Thermo Scientific) and kept in liquid nitrogen.

2.10.2 Transfection of plasmid DNA into eukaryotic cells

Lipofectamine®2000 Transfection Reagent (Life Technologies) was used for DNA transfection of mammalian cells according to the manufacturer's protocol. One day before transfection cells were plated in medium without antibiotics, supplemented with 10% FCS into the particular well plates to reach a confluence of 70 - 90% at the time of transfection. Cells were cultivated in 6-well plates, for co-immunoprecipitation experiments or preparation of cell lysates. Alternatively, cells were seeded on glass dishes in 24-well plates for immunostaining. In dependence of the used culture vessel, DNA and Lipofectamin reagent were diluted in Opti-MEM medium as indicated in the following table.

Table 7: Amounts of nucleic acids, Lipofectamin and medium are given according to the respective culture vessel

Culture vessel	Volume of plating medium	Volume of dilution medium	DNA	Lipofectamin	RNA	Lipofectamin
96-well	100 µl	2 x 25 µl	0.2 µg	0.5 µl	5 pmol	0.25 µl
24-well	500 µl	2 x 50 µl	0.8 µg	2.0 µl	20 pmol	1.0 µl
6-well	2 ml	2 x 250 µl	4.0 µg	10 µl	100	5 µl
10-cm	15 ml	2 x 1.5 ml	24 µg	60 µl	600	30 µl

2.10.3 Treatment of MCF7 cells with recombinant Wnt proteins and chemical inhibitors

For treatment with Wnt proteins, cells were seeded on six-well plates prior to Western blotting or 10 mm glass coverslips in 24-well plates prior to fluorescence analysis. Cells were washed three times with PBS and rhWnt3a or rhWnt5a (R&D systems) diluted in RPMI medium were added to the cells in concentrations ranging from 25 – 200 ng in a final volume of 500 µl in six-well plates and 250 µl in 24-well plates, for 1 to 15 hours. Afterwards, cells were washed again for three times with PBS before preparation of protein extracts for Western blot analysis or fixation for immunofluorescence staining. For inhibition of caveolin-mediated endocytosis or lysosomal degradation, cells were incubated in 5 mM methyl- β -cyclodextrin (Sigma-Aldrich) or 100 µM chloroquine (Sigma-Aldrich), respectively, four hours before Wnt treatment.

2.11 *Xenopus laevis* techniques

2.11.1 Isolation of *Xenopus laevis* testis

Male frog was sacrificed by putting it in 0.05% benzocaine (Sigma-Aldrich) in water for 30 minutes at room temperature and subsequently cutting the cervical spine using scissors or a scalpel. For isolation of the testis, the frog was put on its back and the skin at the belly and the muscles were cut with scissors to get access to the abdominal cavity. The fat body was pulled out and the attached testes were isolated. Testes were washed 3 times in 1x MBS and stored in 1x MBS at 4 °C.

2.11.2 *Xenopus* embryo microinjection and cultivation

To stimulate ovulation in female *Xenopus laevis* frogs, 500 – 1000 units human chorionic gonadotropin (hCG) (Sigma-Aldrich, Prospec) were injected into the dorsal lymph sack. hCG-stimulation was done approximately 12 hours before eggs were retrieved. Eggs were *in vitro* fertilized with 50 – 150 μ l macerated testis tissue in 0.1x MBS according to the size of the batch. The jelly coat was removed by gentle shaking of the embryos in 2% cysteinhydrochloride-solution. Subsequently, the embryos were washed six times in 0.1x MBS and incubated at 12 °C until the appropriate stage for injection. Albino embryos were stained with Nile blue vital dye to distinguish between the animal and vegetal pole and later for classification of the developmental stages. Injections were performed using glass needles prepared with a needle puller (Narishige, Japan). The injection procedure was carried out in injection buffer at 12 °C using a microinjection system (PV820 Pneumatic Pump, M3301 Micromanipulator, World Precision Instruments). Embryos were kept on a cooling plate (12 °C) prior and directly after injection or injected directly on a cooling plate. 1 hour after injection embryos were washed three times in 0.1xMBS and cultured in 0.1x MBS at 12 – 18 °C in an incubator. The developmental stages were classified according to Nieuwkoop and Faber, normal table of *Xenopus laevis* (Nieuwkoop and Faber, 1956).

2.11.3 Fixation and X-gal staining

For lineage tracing using X-gal staining β -galactosidase (*lacZ*) mRNA was co-injected into the embryos. This method is used to distinguish between injected versus non-injected regions of the embryo. Embryos were fixed in MEMFA for 45 minutes and washed 3 times for 10 minutes in 1x PBS. Embryos were incubated in X-gal solution in the dark until a blue staining was visible. The solution was removed and embryos were washed for 3 times with 1x PBS for 10 minutes. Re-fixation of the embryos was performed using MEMFA for at least 1 hour at room temperature or overnight at 4 °C. For long-term storage, embryos were transferred in 100% ethanol and stored at -20 °C.

2.11.4 *Xenopus* second axis assay

For the generation of a secondary axis, 5 pg *Wnt8* mRNA was injected marginally into one ventral blastomere of a 4-cell stage *Xenopus* embryo together with 75 pg *lacZ* RNA as lineage tracer. 250 pg *PTK7* mRNA, 10 ng control morpholino or 10 ng caveolin-1 α morpholino were co-injected. Second axis induction phenotypes were counted at stage 18 – 23.

2.11.5 Embedding of *Xenopus* embryos for vibratome sectioning

Embryos were embedded in gelatin/albumin prior to sectioning. 1.5 ml thawed gelatin/albumin embedding solution was mixed with 150 μ l 25% glutaraldehyde on ice and filled in a plastic mold. After the solution got solid, embryos were placed on the solidified block and covered with another 1.5 ml aliquot of gelatin/albumin + glutaraldehyde medium. Embryos were stored in a humid chamber at 4 °C until sectioning. 30-50 μ m sections were made using the Leica VT1000 S vibratome and collected on an object slide.

2.11.6 Actin staining of *Xenopus* vibratome sections using phalloidin

The vibratome sections were washed 3 times with 1x PBS on the object slide. Tetramethylrhodamine (TRITC)-conjugated phalloidin (Sigma-Aldrich) at a concentration of 1 μ g/ml was used to stain the actin cytoskeleton. The sections were incubated in phalloidin-TRITC for 1 hour at room temperature. Afterwards, the section were washed 3 times with 1x PBS. The sections were embedded using Moviol embedding solution supplemented with DAPI-fluorescent stain (Carl Roth) at a final concentration of 1 μ g/ml.

2.12 Protein techniques

2.12.1 Preparation of protein extracts from MCF7 cells

Cells were washed with cold TBS and scraped in 0.5 ml TBS from the surface of the 6-well culture plate. Cells were transferred into a 1.5 ml reaction tube and centrifuged for 10 minutes at 3000 rpm and 4 °C. The supernatant was discarded and the pellet was lysed in lysis buffer (800 μ l of lysis buffer for Co-IP analyses, 100 μ l of lysis buffer for analytical protein samples) by pushing it 5 times through a 30 G syringe. After centrifugation for 15 minutes at 13000 rpm at 4 °C, the supernatant was transferred into a new reaction tube and used for Co-IP analyses or mixed 1:5 with 6x Laemmli buffer and denatured for 3 minutes at 95 °C. Protein extract was directly loaded on an SDS-PAGE gel or frozen at -20 °C.

2.12.2 Preparation of protein extracts from *Xenopus* embryos

Xenopus embryos were collected and lysed in lysis buffer. 10 μ l of lysis buffer were applied per embryo. Homogenization was done by pipetting the embryos 5 times through

a 30 G syringe. The lysate was centrifuged at 130000 rpm at 4 °C and the supernatant was transferred into a new reaction tube. The appropriate amount of 6x Laemmli buffer was added to the protein extract to get 1x Laemmli buffer in the solution. The samples were denatured for 3 minutes at 95 °C and frozen or loaded on a SDS-PAGE.

2.12.3 SDS - polyacrylamide gel electrophoresis

SDS - polyacrylamide gel electrophoresis (SDS-PAGE) was performed to separate proteins according to their size in an electric field (LAEMMLI, 1970). Discontinuous 10% or 12% polyacrylamide gels were prepared using standard protocols (Russel, 2001). The BioRad Mini Protean Tetra Cell system (Bio-Rad) was used for SDS-PAGE according to the manufacturer's protocol. The protein extracts were loaded into the chambers of the SDS polyacrylamide gels with a maximal volume of 25 µl. Further, 5 µl protein marker were loaded in one of the chambers (PageRuler Plus Prestained Protein ladder, Thermo Scientific). The proteins were separated for 1 - 2 hours at 70 - 120 V in a running chamber filled with Laemmli buffer.

2.12.4 Western blot

The protein extracts, separated by a polyacrylamide gel electrophoresis, were transferred by electro-blotting onto a nitrocellulose membrane. The blotting procedure was performed using the BioRad wet blot cell (Bio-Rad), containing transfer buffer, at 100 V for 1 - 2 hour on ice or overnight (15 h) at 30 V and room temperature. The membrane was stained for 2 minutes in PonceauS solution to visualize the protein bands. For blocking unspecific binding sites the membrane was incubated in TBST buffer supplemented with 5% milk powder (w/v) for 1 hour at room temperature on a shaker. The respective primary antibodies were diluted (according to table 4) in TBST buffer + milk powder and incubated on the membrane overnight at 4 °C. Afterwards the membrane was washed three times for 10 minutes with TBST buffer + 5% milk powder. Horseradish peroxidase coupled secondary antibodies were incubated on the membrane for 1 hour at room temperature. The membrane was washed three times with TBST buffer in intervals of 10 minutes prior to detection with the chemiluminescent substrate Pierce™ ECL Western Blotting Substrate (Thermo Scientific) according to the protocol. The chemiluminescent signal was detected by exposure of the membrane X-Ray film in time periods of several seconds and minutes. Protein intensities were analysed using Image J and calculated in arbitrary units [AU].

2.12.5 Co-Immunoprecipitation (Co-IP)

MCF7 cells were transfected into six-well plates 48 hours prior to co-immunoprecipitation analysis. To obtain a high concentration of protein extract, cells from two wells of a six-well plate were collected for each condition. For preparation of cell extract Co-IP lysis buffer was supplemented with SDS to a final concentration of 0.1% to disrupt membrane and lipid raft fractions. This buffer was used throughout the whole Co-IP experiment. The protein extracts were pre-cleared for 1 hour with 30 µl Protein A Sepharose CL-4B beads (GE Healthcare) at 4 °C with end-over-end mixing on a rotator. After pre-clearing 50 µl of the lysates were collected as input control. For antigen-antibody coupling, the pre-cleared lysate was centrifuged for 2 minutes at 2000 rpm, the supernatant was transferred into a new reaction tube and incubated with the respective antibodies for two hours at 4 °C with gentle rotation. Afterwards, 30 µl Protein A Sepharose beads were added to precipitate protein complexes and incubated further one hour at 4 °C on a rotator. Beads were washed 5 times with Co-IP lysis buffer, boiled in 15 µl 6x Laemmli buffer for 5 minutes at 95 °C and frozen at -20 °C or directly analyzed by Western blot.

2.12.6 Cell surface biotinylation

MCF7 cells cultured in six-well plates were cross-linked with 0.25 mg/ml EZ-Link-Sulpho-NHS-SS-biotin for 30 minutes (Thermo Scientific) and subsequently quenched using Quenching solution (Thermo Scientific). Cells were washed in TBS, scraped and lysed in 800 µl Co-IP lysis buffer. 50 µl of each sample were collected as input control. Cell surface proteins were affinity-purified using NeutrAvidin Agarose beads (Thermo Scientific) for 2 hours with end-over-end mixing on a rotator. Beads were washed five times for 5 minutes with Co-IP lysis buffer, boiled at 95 °C for 5 minutes in 6 x Laemmli loading buffer and loaded on 10% or 12% SDS-PAGE gels.

2.12.7 *In vitro* coupled transcription/translation reactions

For the coupled transcription and translation of eukaryotic proteins from DNA plasmids the TnT® Quick Coupled Transcription/Translation System (Promega) was used. According to the manufacturer's instructions.

2.13 Whole-mount in situ hybridization (WISH)

Whole-mount in situ hybridization was carried out as described (Harland, 1991).

WISH - day 1

Rehydration

Embryos that were stored in 100% ethanol were rehydrated prior to WISH according to table 7.

Table 8: Rehydration of embryos

Solution	Incubation time
100% ethanol	3 minutes
75% ethanol in water	3 minutes
50% ethanol in water	3 minutes
25% ethanol in PTw	3 minutes
PTw	3 minutes

Proteinase K treatment

Embryos were treated with proteinase K (0.15 U/ml, Merck) in PTw buffer to facilitate the accessibility of the RNA probe to the tissue. The following table gives the proteinase K incubation times according to the developmental stages of the embryos.

Table 9: Proteinase K treatment

Developmental stage of <i>Xenopus</i> embryos	Incubation time (minutes)	Temperature
9 - 10.5	6 - 8	room temperature
14 - 16	8 - 10	room temperature
20 - 25	15 - 18	room temperature
36	22 - 25	room temperature
40	17 - 20	37 °C
42 - 43	27 - 30	37 °C
46	32 - 35	37 °C

Acetylation and refixation

Table 10: Acetylation of embryos

Solution	Incubation time
1M Triethanolamine chlorid, pH 7.0 (TEA)	2 x 5 minutes
1M TEA with 0.3% acetic anhydride	5 minutes
1M TEA with 0.6% acetic anhydride	5 minutes
PTw	5 minutes

After acetylation, the embryos were re-fixed for 20 minutes in PTw buffer containing 4% (v/v) formaldehyde and were subsequently washed 5 times in PTw buffer.

Hybridization

Approximately 1 ml of PTw was left in the tubes and mixed with 250 µl Hyb-Mix. The solution was replaced immediately by 500 µl of fresh Hyb-Mix and incubated for 10 minutes at 60 °C. The Hyb-Mix was exchanged for a second time and embryos were incubated 4 – 5 hours at 60 °C in a shaking waterbath. The Hyb-Mix was replaced with the desired labeled RNA probe, diluted in Hyb-Mix solution. The hybridization was performed overnight at 60 °C.

WISH - day 2

Washing and RNase treatment

To remove unbound RNA probes, the samples were washed and digested with RNase A/RNase T1 mix (0.2 µg/ml and 0.5 U/ml respectively, Thermo Scientific).

Table 11: Washing steps and RNase treatment

Solution	Incubation temperature and time
Hyb Mix	60 °C, 10 minutes
2x SSC	60 °C, 3 x 15 minutes
RNases in 2x SSC	37 °C, 60 minutes
2x SSC	room temperature, 5 minutes
0.2x SSC	60 °C, 2 x 30 minutes
MAB	room temperature, 2x 15 minutes

Blocking and antibody reaction

To block unspecific binding sites embryos were incubated in MAB buffer containing the Boehringer Mannheim Blocking Reagent (BMB) and horse serum prior to incubation with Sheep Alkaline phosphatase-coupled anti-Dig antibody (Roche).

Table 12: Blocking and antibody reaction

Solution	Incubation temperature and time
MAB/2% BMB	10 minutes, room temperature
MAB/2% BMB/20% Horse serum	30 minutes, room temperature
MAB/2% BMB/20% Horse serum 1:5000 α -DIG antibodies	4 hours, room temperature
MAB	3 x 10 minutes, room temperature
MAB	overnight, 4 °C

WISH day 3

Staining reaction

Embryos were washed several times to remove unbound antibodies and subsequently incubated with the NBT/BCIP staining solution for alkaline phosphatase mediated staining reaction according to the following table.

Table 13: Washing and staining reaction

Solution	Incubation time
MAB	5 x 5 minutes, room temperature
APB	3 x 5 minutes, room temperature
APB with 80 μ g/ml NBT, 175 μ g/ml BCIP	Up to three days, 4 °C

2.14 Immunofluorescence

Cells were seeded on 10 mm glass coverslips (Menzel-Gläser, Thermo Scientific) for confocal laser-scanning fluorescence microscopy or 42 mm glass coverslips (H. Saur Laborbedarf) for total internal reflection (TIRF) microscopy. The cells were washed with PBS and fixed in 4% paraformaldehyde in PBS for 20 minutes at room temperature. For permeabilization, cells were incubated in 0.2% Triton-X100 in PBS. Afterwards the cells were washed for three times in PBS and blocked in blocking buffer for one hour.

Incubation with the first antibodies was carried out overnight at 4 °C. Cells were washed with blocking buffer and subsequently incubated with Alexa Fluor-conjugated secondary antibodies (life technologies) for one hour at room temperature. For confocal microscopy cells were mounted using fluorescence mounting medium (Dako, Agilent Technology) supplemented with DAPI to a final concentration of 1 µg/ml. Stained cells were imaged by confocal laser-scanning fluorescence microscopy (LSM 780, Carl-Zeiss or TCS SP5, Leica Microsystems). For TIRF microscopy, cells on the glass coverslips were covered with PBS and analyzed using a TIRF microscope (Leica DMI6000 B TIRF) with a HCX Plan-Apochromat 100x, NA 1.47 oil objective.

For life cell imaging cells were seeded in 2- or 4-well Lab-Tek Chambers (Nunc™ Lab-Tek™ Chambered Coverglass, Thermo Scientific). Life cell imaging was performed using a spinning disc confocal microscope (AxioObserver Z1, Zeiss) with a Plan-Apochromat 63x, NA 1.40 oil objective. Protein co-localization was quantified using ImageJ software (coloc 2 plugin).

3 Results

3.1 PTK7 changes its cellular localization in response to canonical Wnt proteins

3.1.1 Wnt3a stimulation mediates PTK7 translocation

PTK7 functions as a Wnt co-receptor in the regulation of both canonical and non-canonical Wnt signaling pathways. Interestingly, previous data revealed that PTK7 binds canonical but not non-canonical Wnt proteins (Peradziryi et al., 2011). As PTK7 inhibits canonical Wnt signaling, it remains unclear if conversely canonical Wnt ligands might affect the localization or stability of the PTK7 protein. To analyze this PTK7-GFP was stably expressed in MCF7 cells and its localization in the presence or absence of Wnt proteins was analyzed by confocal microscopy. In the absence of Wnt ligands PTK7 is mainly localized at the cell membrane (Figure 22 A). However, in the presence of recombinant human Wnt3a (rhWnt3a), a canonical Wnt ligand that interacts with PTK7 (Peradziryi et al., 2011), the PTK7 protein shifted from the membrane to the cytoplasm (Figure 22 B). This translocation did not occur in the presence of rhWnt5a protein (Figure 22 C), a non-canonical Wnt ligand, which does not interact with PTK7 in co-immunoprecipitation assays (Peradziryi et al., 2011). As PTK7 strongly accumulates at cell-cell contact sites, Wnt dependent PTK7 translocation was additionally analyzed in single cells. Similar to cells having cell-cell contacts, PTK7 shifts from the membrane to the cytoplasm in single cells after stimulation with rhWnt3a but not with rhWnt5a (Figure 22 D-F). For quantification of the PTK7 localization pattern, it was distinguished between membrane localization, cytoplasmic localization and the combination of both. The graph includes quantification of single cells as well as cells having cell-cell contacts (Figure 23). Before Wnt treatment, PTK7 localized in 51% of the cells to the plasma membrane, in 44% to both membrane and cytoplasm, while cytoplasmic localization was observed in only 5% of the cells analyzed. However, after rhWnt3a stimulation, membrane localization of PTK7 significantly decreased to only 2%, membrane and cytoplasmic localization decreased slightly to 36%, but cytoplasmic localization increased to over 62%. In contrary, no significant differences to untreated conditions were observed in the presence of rhWnt5a. These findings show that in the presence of canonical Wnt3a, PTK7 changes its cellular localization from the plasma membrane to the cytoplasm.

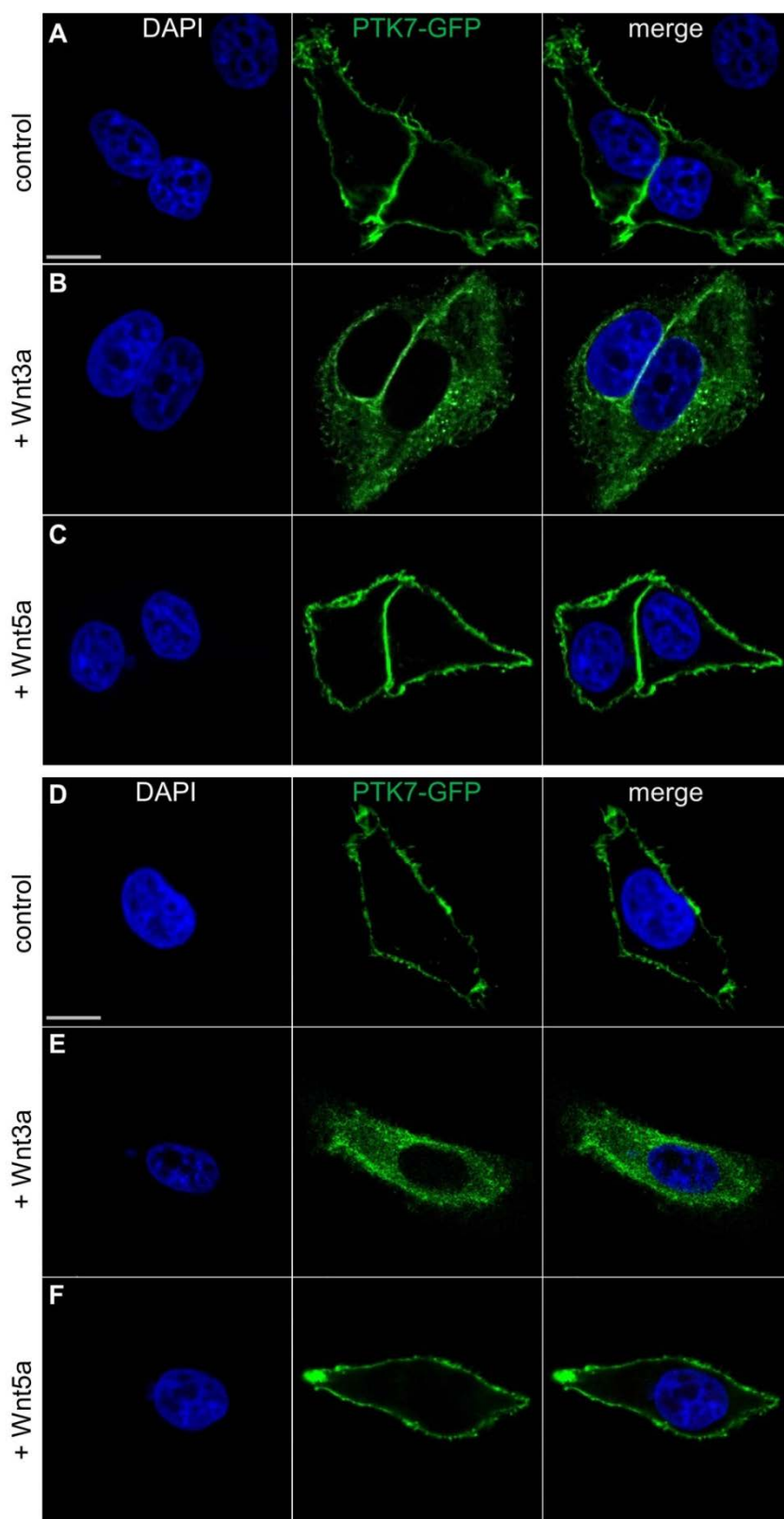


Figure 22: Canonical, but not non-canonical Wnt ligands, induce PTK7 internalization.

PTK7-GFP expression in stably transfected MCF7 cells was induced by the addition of doxycycline in a final concentration of 1 $\mu\text{g/ml}$ for 15 hours. Cells expressing PTK7-GFP were treated without Wnt protein, with rhWnt3a or rhWnt5a protein (50 ng) for 1 hour. **(A)** In cells having cell-cell contacts, PTK7 is localized at the plasma membrane before Wnt treatment and **(C)** after rhWnt5a treatment. **(B)** In the presence of rhWnt3a PTK7 is mainly localized to the cytoplasm. **(D-E)** In MCF7 single cells PTK7 translocates from the membrane to the cytoplasm only in the presence of the canonical Wnt ligand Wnt3a. Scale bars, 10 μm .

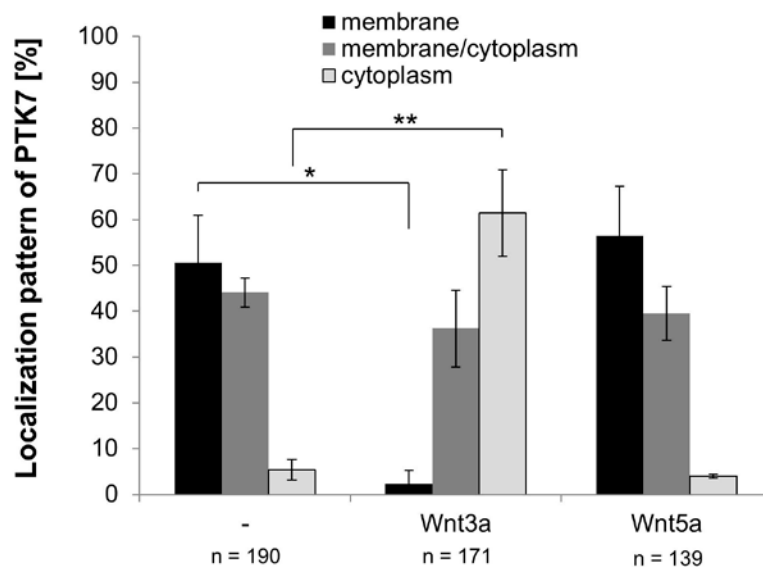


Figure 23: Quantification of PTK7 cellular localization in response to canonical or non-canonical Wnt proteins.

Quantification of the PTK7 localization pattern of three independent experiments. Single cells and cells with cell-cell contacts were analyzed. +/- standard errors are given. Numbers of cells (n) are indicated for each condition. * $p < 0.001$, ** $p < 0.005$ in a Student's t-test.

3.1.2 Wnt3a-dependent PTK7 internalization is independent of its kinase homology domain

As the kinase homology domain of PTK7 is required for membrane-recruitment of Dishevelled and necessary for PTK7 function in activating non-canonical PCP/Wnt signaling (Shnitsar and Borchers, 2008; Wehner et al., 2011), we analyzed if this domain plays a role in the Wnt3a-mediated translocation of PTK7. Therefore, a PTK7 deletion mutant lacking the kinase homology domain (Δ kPTK7) was stably expressed in MCF7 cells. In the absence of recombinant Wnt protein Δ kPTK7 is predominantly localized at the membrane (Figure 24 A). The same result can be seen after stimulation with rhWnt5a (Figure 24 C). However, in presence of rhWnt3a, the Δ kPTK7 protein is translocated to the cytoplasm (Figure 24 B). Similar results were observed in MCF7 single cells expressing Δ kPTK7 protein (Figure 24 D-F). Thus, the Wnt-mediated translocation of the PTK7 protein is independent of its kinase-homology domain. The quantification of the Δ kPTK7 localization pattern revealed that in the absence of recombinant Wnt ligands Δ kPTK7 was present at the membrane in 57% of the cells. A similar localization pattern was detected in Δ kPTK7-expressing cells treated with rhWnt5a, where in 64% of the cells Δ kPTK7 is localized to the plasma membrane, while 3% show a cytoplasmic localization. However, in the presence of rhWnt3a membrane localization of Δ kPTK7 significantly decreased to only 10%, while the cytoplasmic Δ kPTK7 localization increased from 3% under untreated conditions to 42% after rhWnt3a stimulation (Figure 25).

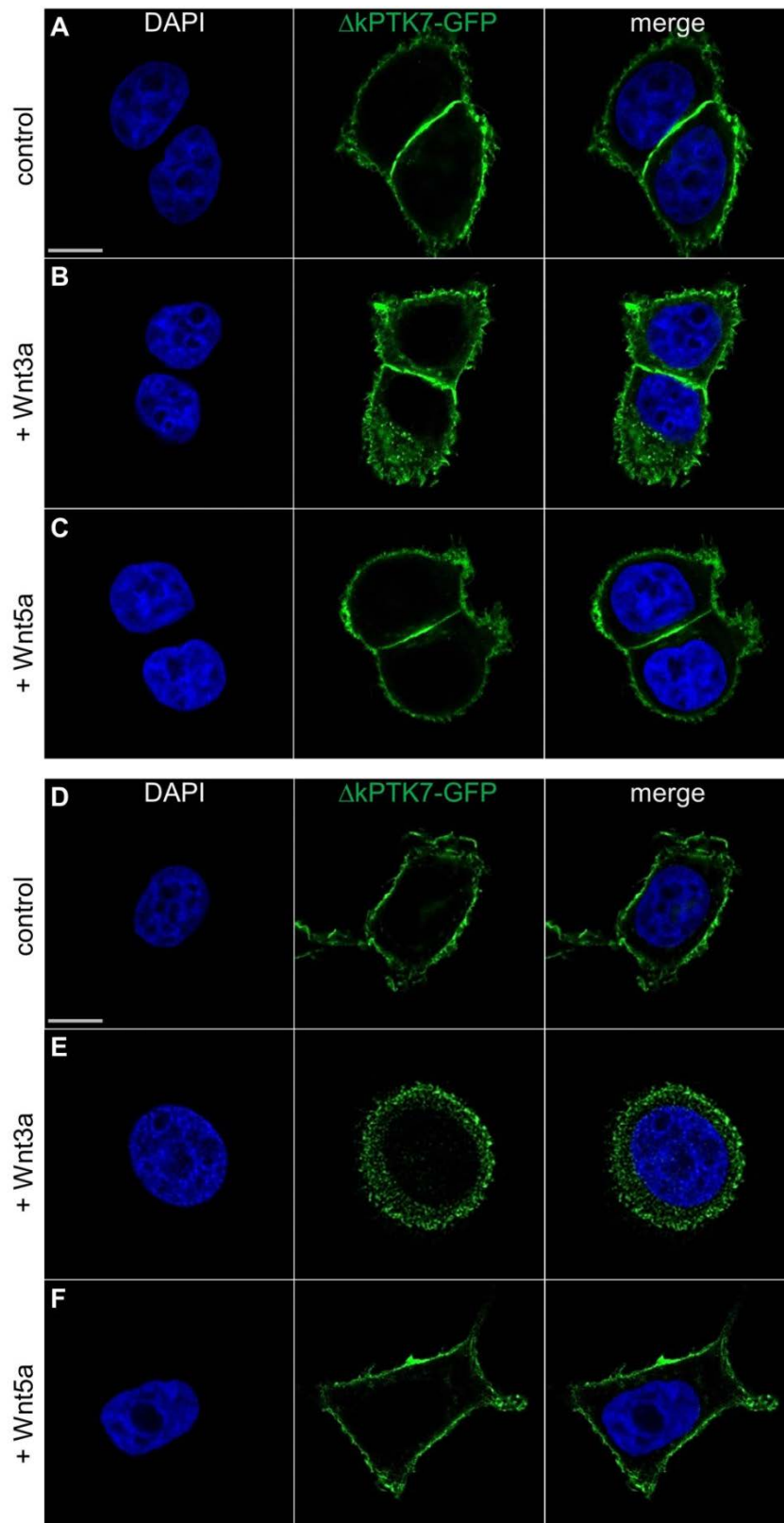


Figure 24: Wnt3a-dependent Δ kPTK7 translocation is independent of its kinase domain.

In MCF7 cells Δ kPTK7-GFP expression was induced by the addition of doxycycline in a final concentration of 1 μ g/ml for 15 hours. The cells were treated without or with the indicated Wnt proteins for 1 hour. **(A)** In untreated cells as well as in **(C)** rhWnt5a-treated cells Δ kPTK7 localizes to the plasma membrane. **(B)** In the presence of the canonical Wnt ligand rhWnt3a Δ kPTK7 is strongly localized to the cytoplasm. **(D-F)** Single cells expressing Δ kPTK7-GFP show similar localization pattern of Δ kPTK7 as observed for cells having cell-cell contacts. Scale bars, 10 μ m.

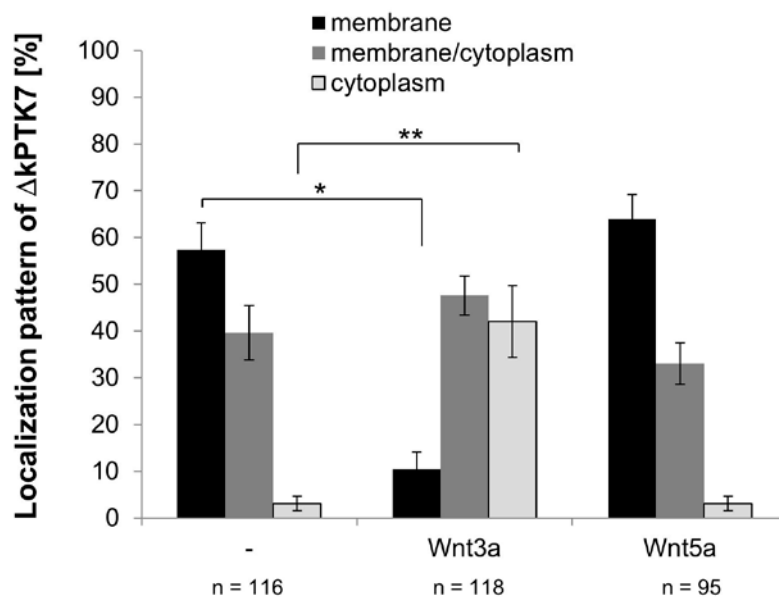


Figure 25: Quantification of Wnt3a-dependent Δ kPTK7 translocation.

Quantification of Δ kPTK7 localization. The graph shows three independent experiments, +/- standard errors are shown. Numbers of cells (n) are indicated for each condition. * $p < 0.005$, ** $p < 0.01$ in a Student's t-test.

3.1.3 Cell surface levels of PTK7 decrease in the presence of canonical Wnt ligands

To further confirm the Wnt3a-dependent clearance of the PTK7 receptor from the plasma membrane in a biochemical assay, cell-surface biotinylation analyses were performed. The concentration of biotinylated cell surface PTK7-GFP was determined before and after Wnt stimulation. Therefore, cell surface proteins were labeled with sulfo-NHS-SS-Biotin and affinity-purified using neutravidin agarose beads. Isolated cell surface PTK7-GFP and total PTK7-GFP were detected using an anti-GFP antibody. Consistent with the previous findings in fluorescently labeled cells, cell surface PTK7 protein levels significantly decreased after rhWnt3a treatment, but remained unchanged after rhWnt5a stimulation (Figure 26 A, C). Similar to full length PTK7-GFP, the cell-surface concentration of the Δ kPTK7-GFP protein also decreased after treatment with rhWnt3a (Fig 26 B, C). These experiments show that the PTK7 receptor is removed from the plasma membrane in the presence of canonical Wnt3a and that this process is independent of its kinase homology domain.

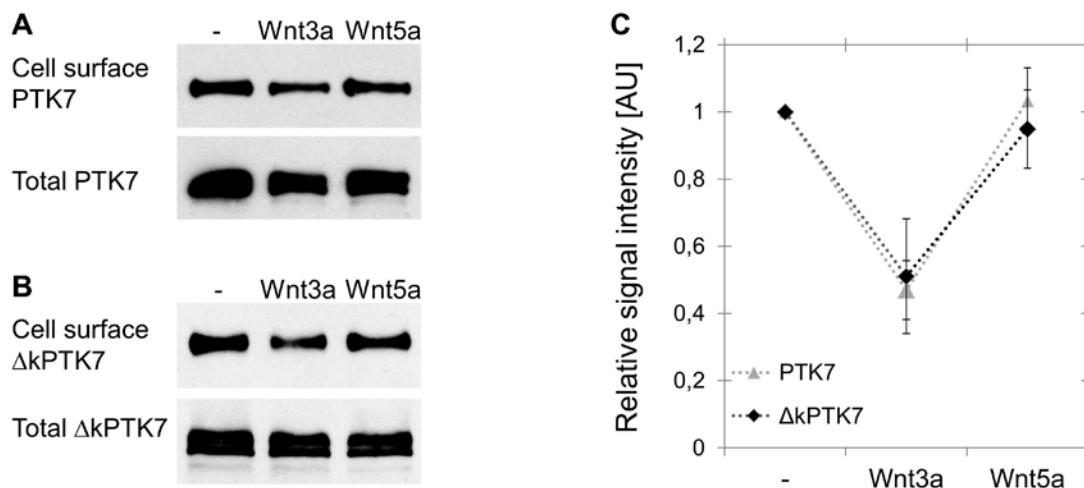


Figure 26: Cell surface PTK7 and Δ kPTK7 concentrations decrease after rhWnt3a treatment.

PTK7-GFP or Δ kPTK7-GFP expression was induced by doxycycline in MCF7 cells. The cells were treated with rhWnt3a or rhWnt5a for 1 hour. The cell surface proteins were biotinylated and precipitated using neutravidin beads. Cell surface and total PTK7-GFP or Δ kPTK7-GFP levels were detected using anti-GFP antibodies. **(A)** Cell surface PTK7 protein levels decreased in the presence of rhWnt3a but not in the presence of rhWnt5a or under untreated conditions in comparison to total PTK7 levels. **(B)** The signal intensity of Δ kPTK7 at the cell membrane decreased significantly in the presence of rhWnt3a, compared to the signal intensity in the presence of rhWnt5a or absence of Wnt proteins. **(C)** The graph summarizes three independent experiments with \pm standard errors. The intensities of the protein bands were analyzed using ImageJ. The ratio of cell surface to total protein levels is given in arbitrary units [AU]. Values of the control condition without Wnt treatment were set to 100%.

3.2 Proteolytic cleavage of PTK7 is not induced in response to canonical Wnt proteins

PTK7 is a known target for proteolytic processing by several proteases including MT1-MMP, ADAM and γ -secretase. Cleavage of PTK7 by γ -secretase leads to the generation of a soluble cytoplasmic PTK7 fragments (Golubkov and Strongin, 2012). As PTK7 constructs with a C-terminal GFP-tag were used for Wnt-dependent PTK7 translocation analyses, it is important to clarify if PTK7 shifts from the membrane to the cytoplasm or if the cytoplasmic part of PTK7, including the GFP-tag, is cleaved and released into the cytoplasm in response to rhWnt3a stimulation. To analyze this MCF7 cells expressing PTK7-GFP were treated with rhWnt3a for one hour or overnight. PTK7 protein from lysates of these cells was detected by either anti-PTK7 antibodies which recognize the extracellular N-terminal part or by anti-GFP antibodies which recognize the GFP-tag at the intracellular C-terminal domain of PTK7 (Figure 27 A). This double antibody staining can distinguish between the full-length and the cleaved C-terminal PTK7 fragments. Only the full-length PTK7 fragment was detected by the anti-PTK7 antibody, while the full-length

and plus potentially cleaved C-terminal PTK7 fragments were detected by the anti-GFP antibody. The number of detected PTK7 fragments remained unchanged in Wnt treated or untreated cells. Thus, rhWnt3a treatment neither led to the generation of additional PTK7 fragments nor to an increase in their protein concentration (Figure 27 B), demonstrating that rhWnt3a stimulation does not induce PTK7 cleavage. Interestingly, a general decrease in protein levels of the full length as well as the cleaved PTK7 fragments was detected in the presence of rhWnt3a, indicating a function of Wnt in PTK7 degradation. This issue will be picked up later in this study.

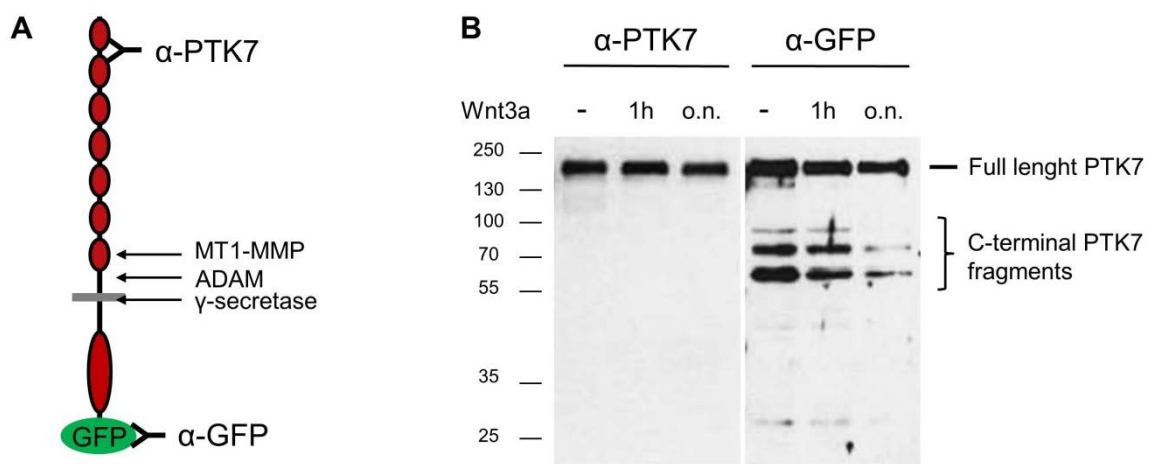


Figure 27: rhWnt3a treatment does not induce PTK7 proteolysis.

(A) Model of PTK7 with MT1-MMP, ADAM and γ -secretase cleavage sites and recognition sites of the anti-PTK7 and the anti-GFP antibody. **(B)** Full-length PTK7 is detected by both anti-PTK7 and anti-GFP antibodies. Cleaved C-terminal fragments were detected only by the anti-GFP antibody. No changes in the expression of cleaved PTK7 fragments due to rhWnt3a treatment were detected.

3.3 PTK7 translocates from the membrane to the cytoplasm together with canonical Wnt2b

As PTK7 binds canonical Wnt ligands (Peradziryi et al., 2011) and is internalized by a Wnt-dependent mechanism, one would expect the Wnt/PTK7 complex to be internalized together. To analyze whether Wnt and PTK7 internalize as a complex, MCF7 cells expressing PTK7-RFP were cultured together with cells expressing and secreting canonical Wnt2b-GFP or non-canonical Wnt5a-GFP (Figure 28 A). These GFP-tagged Wnt constructs had previously been shown to be functionally active in canonical and non-canonical Wnt signaling, respectively (Holzer et al., 2012; Wallkamm et al., 2014). After 4 hours of incubation secreted Wnt2b-GFP was found to co-localize with PTK7-RFP to the same vesicle-like structures in the cytoplasm (Figure 28 B). 66% of the counted PTK7 puncta in the responding cells co-localize with Wnt2b (Figure 28 E). These results indicate that Wnt2b and PTK7 form a ligand/receptor complex that is internalized together. Z-stack imaging with an orthogonal cell view further demonstrates that these PTK7-Wnt2b-positive vesicles are located in the cytoplasm (Figure 28 D). In contrast, although secreted Wnt5a-GFP was detected in the cytoplasm of the PTK7-RFP expressing cells no significant co-localization with PTK7-RFP was observed (Figure 28 C). The internalization of Wnt5a-GFP occurred possibly by a PTK7-independent mechanism.

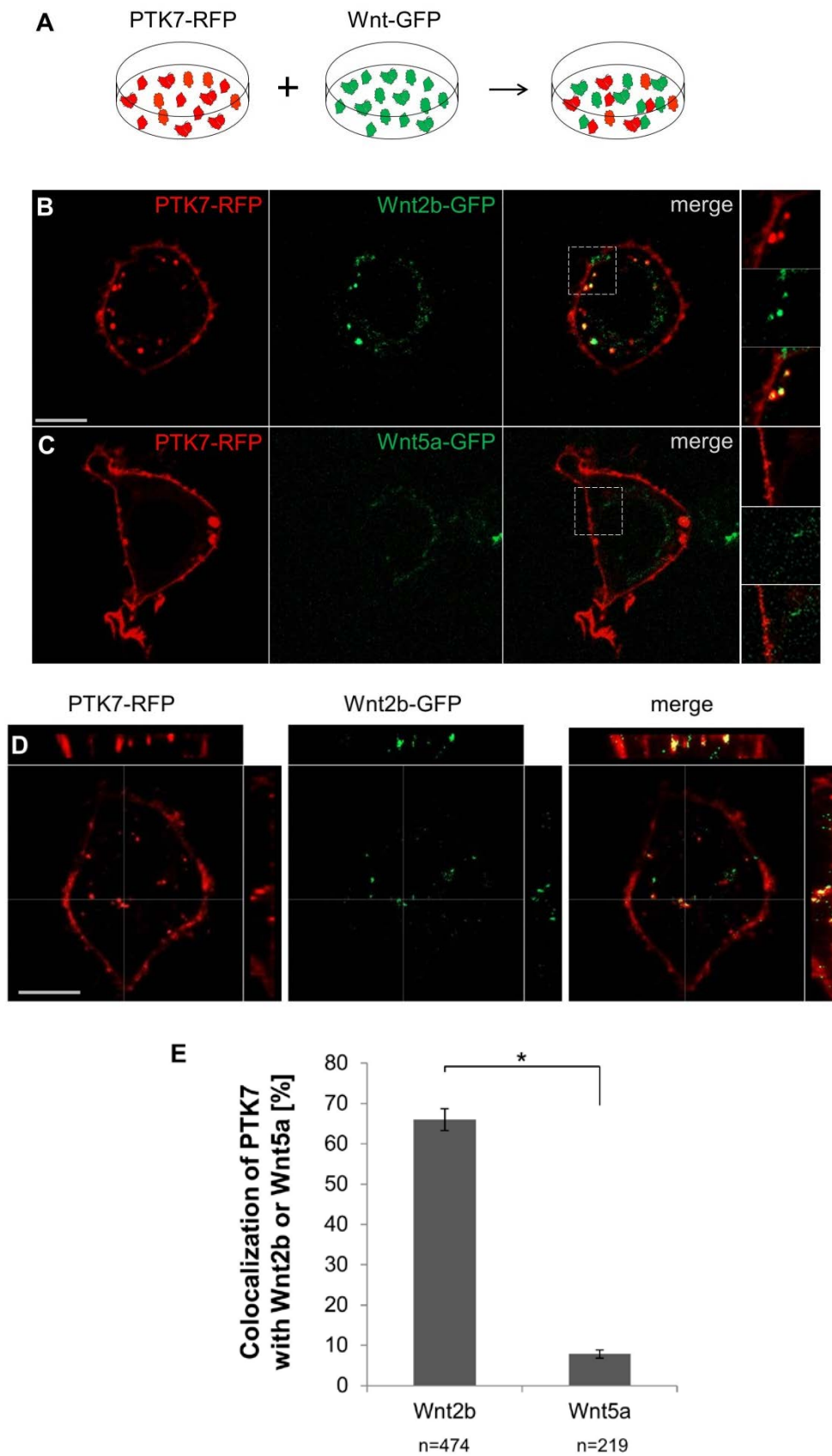


Figure 28: Wnt2b and PTK7 are translocated together to the cytoplasm.

(A) Scheme of experimental procedure. MCF7 cells were transfected with either PTK7-RFP or Wnt-GFP, respectively. After 2 days the differently transfected cell populations were co-cultured together 1:1 in one chamber slide. After 4 hours live-cell imaging was performed using spinning disc confocal microscopy. (B) Secreted Wnt2b-GFP accumulates together with PTK7-RFP in the

same vesicle-like structures. **(C)** Secreted Wnt5a-GFP localizes slightly to the cytoplasm of PTK7-RFP expressing cells, but the majority of the PTK7-RFP protein remains at the membrane. No PTK7-RFP and Wnt5a-GFP positive cytoplasmic puncta were detected. **(D)** Z-stack image with orthogonal sectioning of a MCF7 cell with PTK7-RFP and Wnt2b-GFP positive vesicles in the cytoplasm. 15 vertical sections per stack with a step size of 0.26 μm were taken. Scale bars, 10 μm . **(E)** The graph shows the percentage of cytoplasmic PTK7 puncta that co-localize with Wnt2b or Wnt5a. Three independent experiments are summarized and standard errors are given. Numbers of analyzed PTK7 puncta are indicated for each condition (n). 28 cells for PTK7-Wnt2b and 29 cells for PTK7-Wnt5a co-localization were analyzed. * $p < 0.0001$ in a Student's t-test.

3.4 PTK7 is endocytosed via a caveolin-dependent pathway

The data obtained so far show that in the presence of the canonical Wnt proteins, Wnt3a and Wnt2b, PTK7 localizes to vesicle-like structures in the cytoplasm. Moreover, upon canonical Wnt binding, canonical Wnt and PTK7 seem to be internalized together as a ligand/receptor complex. Receptor-mediated endocytosis via a clathrin- or caveolin-dependent pathway is a common process through which transmembrane proteins are transported to the cytoplasm. Thus, it is likely that the PTK7 translocation from the membrane into the cytoplasm is a result of receptor-mediated endocytosis.

3.4.1 PTK7 and caveolin-1 co-localize in vesicle-like structures in the cytoplasm in response to Wnt3a

To analyze whether PTK7 is endocytosed through a clathrin- or caveolin-mediated route, MCF7 cells expressing PTK7-GFP or $\Delta\text{kPTK7-GFP}$ were co-stained with antibodies detecting endogenous caveolin-1 or clathrin. In the presence of rhWnt3a, PTK7-GFP co-localized with caveolin-1 in vesicle-like structures in the cytoplasm in $59\% \pm 6\%$ of the analyzed cells (Figure 29 B, D). In contrast, in untreated cells or rhWnt5a stimulated cells, PTK7-GFP and caveolin-1 co-localized at the membrane, but cytoplasmic co-localization was rarely observed (Figure 29 A, C). This was the case in only $9\% \pm 6\%$ of the control cells and $18\% \pm 10\%$ of the rhWnt5a treated cells (Figure 29 D). To quantify the rate of co-localization between the two fluorophores used in this experiment, the Pearson correlation coefficient (PCC) was determined, which ranges between -1 and 1. A coefficient of 1 represents a perfect correlation, 0 means random correlation and -1 stands for perfect but negative correlation of all pixels of the 2 dyes analyzed (Adler and Parmryd, 2010). In untreated and rhWnt5a stimulated cells low PCC values were determined with 0.04 and -0.19, respectively. PCC is remarkably higher in the Wnt3a treated cell with a value of 0.61. Thus, the calculation of the PCC provides further evidence that there is a significant co-localization of caveolin-1 and PTK7-GFP upon rhWnt3a stimulation.

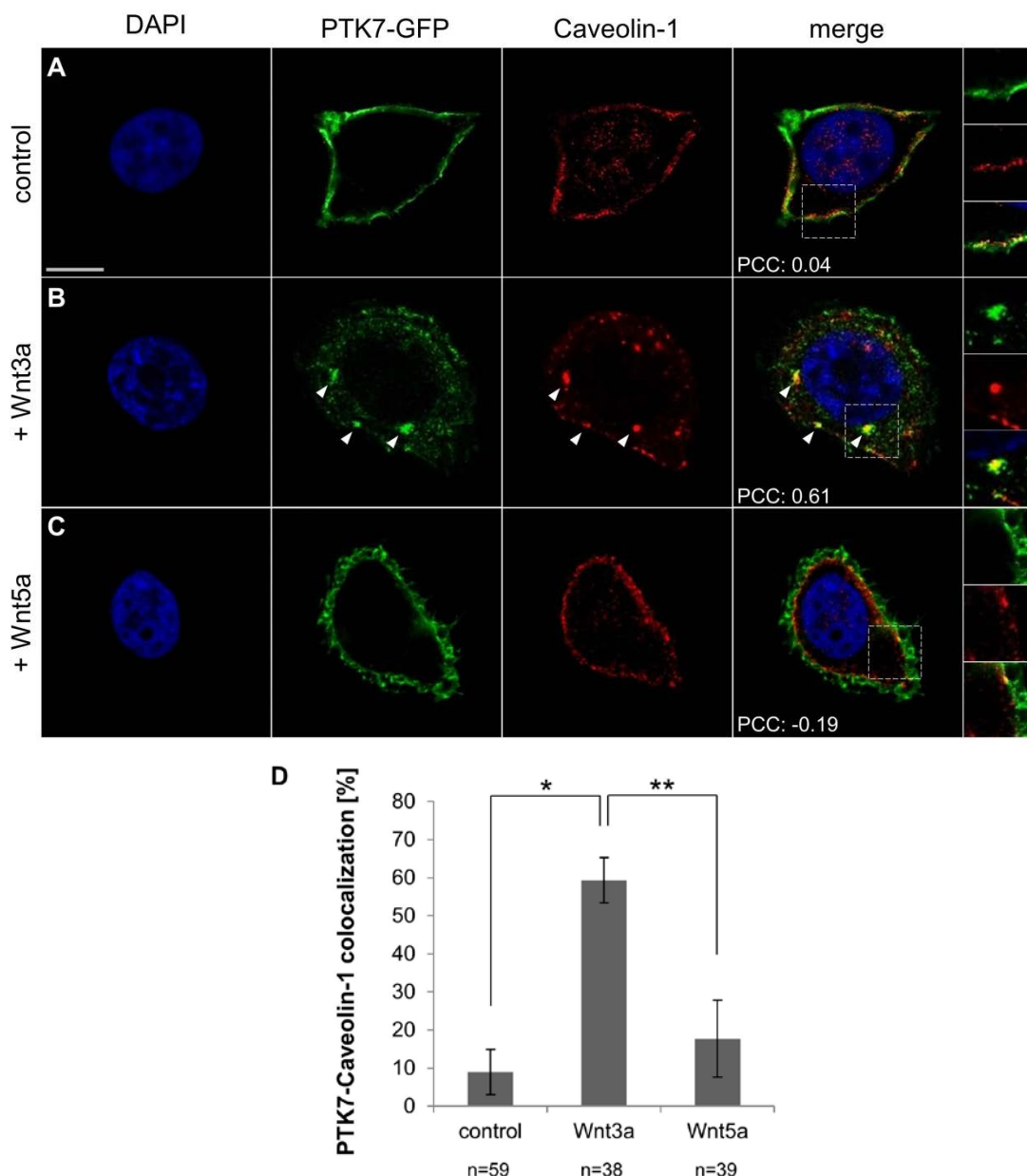


Figure 29: PTK7 endocytosis is mediated by caveolin-1.

(A-C) MCF7 cells stably expressing PTK7-GFP after doxycycline-induction were treated with rhWnt3a or rhWnt5a protein for 1 hour and co-stained with antibodies against endogenous caveolin-1. Overlay of green (PTK7-GFP) and red (caveolin-1) pixels are visible in the merged image in yellow. Cytoplasmic yellow puncta appear only in the presence of rhWnt3a (**B**). Pearson correlation coefficient (PCC) was calculated for the respective cells shown. Measurements of PCC were done with ImageJ (coloc2 plugin). Scale bar, 10 μ m. **(D)** Quantification of PTK7 and caveolin-1 co-localization based on the calculated PCCs. Each graph shows three independent experiments, +/- standard errors are given. Numbers of analyzed cells (n) are indicated for each condition. * $p < 0.001$, ** $p < 0.005$ in a Student's t-test.

As Wnt-dependent translocation of PTK7 into the cytoplasm was as well observed for the mutant PTK7 protein lacking the kinase homology domain, Δ kPTK7 was additionally analyzed for cytoplasmic co-localization with endogenous caveolin-1. Similar to the full length PTK7-GFP and caveolin-1 co-localization analyses, cytoplasmic co-localization of Δ kPTK7-GFP and caveolin-1 was detected rarely in only 10% of the untreated and 15% of

the rhWnt5a treated cells (Figure 30 A, C, D). rhWnt3a stimulation results in a significant increase in co-localization, which was detected in 52% of the cells (Figure 30 B, D). These results are further supported by the determined Pearson correlation coefficients of the Δ kPTK7-GFP and caveolin-1 co-localization. Low PCCs were calculated for untreated (PCC= 0.03) or rhWnt5a-treated cells (PCC= -0.11), while a high PCC of 0.51 was determined for the rhWnt3a-stimulated cell (Figure 30 A-C).

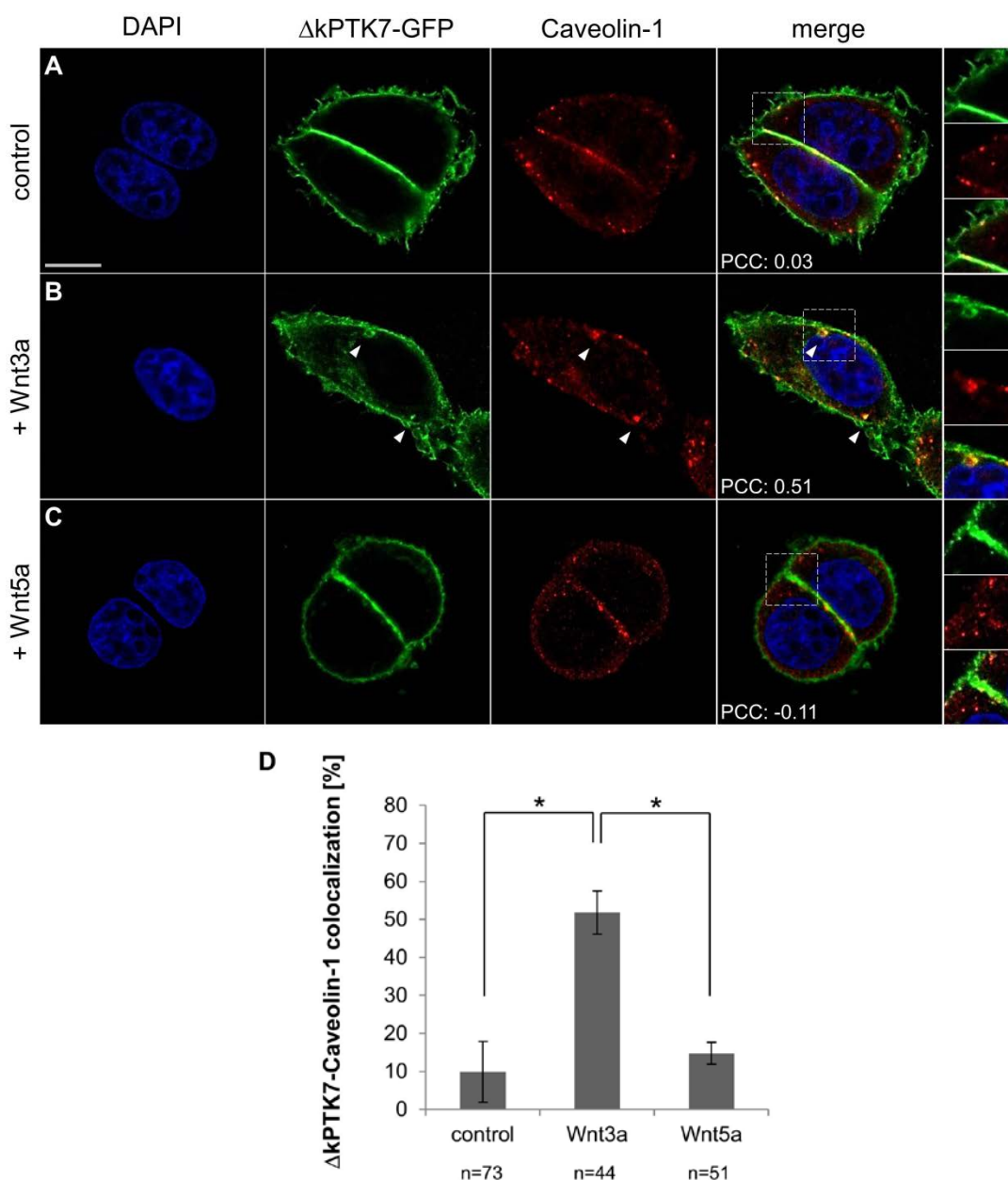


Figure 30: caveolin-1-mediated PTK7 endocytosis is independent of its kinase homology domain.

(A-C) MCF7 cells stably expressing a mutant PTK7 protein, lacking its kinase homology domain, Δ kPTK7-GFP, were treated with rhWnt3a or rhWnt5a protein for 1 hour and stained with anti caveolin-1 antibodies. Calculated PCC is given for each cell shown. Δ kPTK7-GFP and caveolin-1 co-localize in the cytoplasm after rhWnt3a treatment (B). In untreated cells (A) or rhWnt5a treated cells (C) Δ kPTK7 and caveolin-1 co-localize at the membrane but not in cytoplasmic structures. Scale bar, 10 μ m. (D) Quantification of Δ kPTK7 and caveolin-1 co-localization. Each graph shows three independent experiments with standard errors. Numbers of cells (n) are indicated for each condition. * $p < 0.005$ in a Student's t-test.

3.4.2 Inhibition of caveolin-mediated endocytosis prevents PTK7 endocytosis

Immunostaining experiments revealed that upon rhWnt3a stimulation the intracellular PTK7 pool co-localizes with caveolin-1 in vesicle-like structures, suggesting that PTK7 is endocytosed via a caveolin-mediated pathway. To further investigate the caveolin-1 dependent PTK7 internalization, caveolin-mediated endocytosis was inhibited in MCF7 cells using methyl- β -cyclodextrin (M β CD). M β CD is a cyclic oligosaccharide with a hydrophobic core, through which it binds cholesterol leading to the formation of soluble inclusion complexes. Thus, M β CD removes cholesterol from membranes resulting in a disruption of lipid raft microdomains and consequently destroys caveolae (Rodal et al., 1999). Inhibition of caveolin-mediated endocytosis by M β CD treatment prevented rhWnt3a induced PTK7 internalization in MCF7 cells (Figure 31 A-D). Quantification of PTK7 localization revealed that only 4% of the untreated cells showed a cytoplasmic PTK7 localization, similar to cells treated with M β CD (4%). As expected, in 54% of the cells PTK7 localizes to the cytoplasm after 1 hour of rhWnt3a treatment, but only in 10% of the cells treated with both, rhWnt3a and M β CD (Figure 31 E).

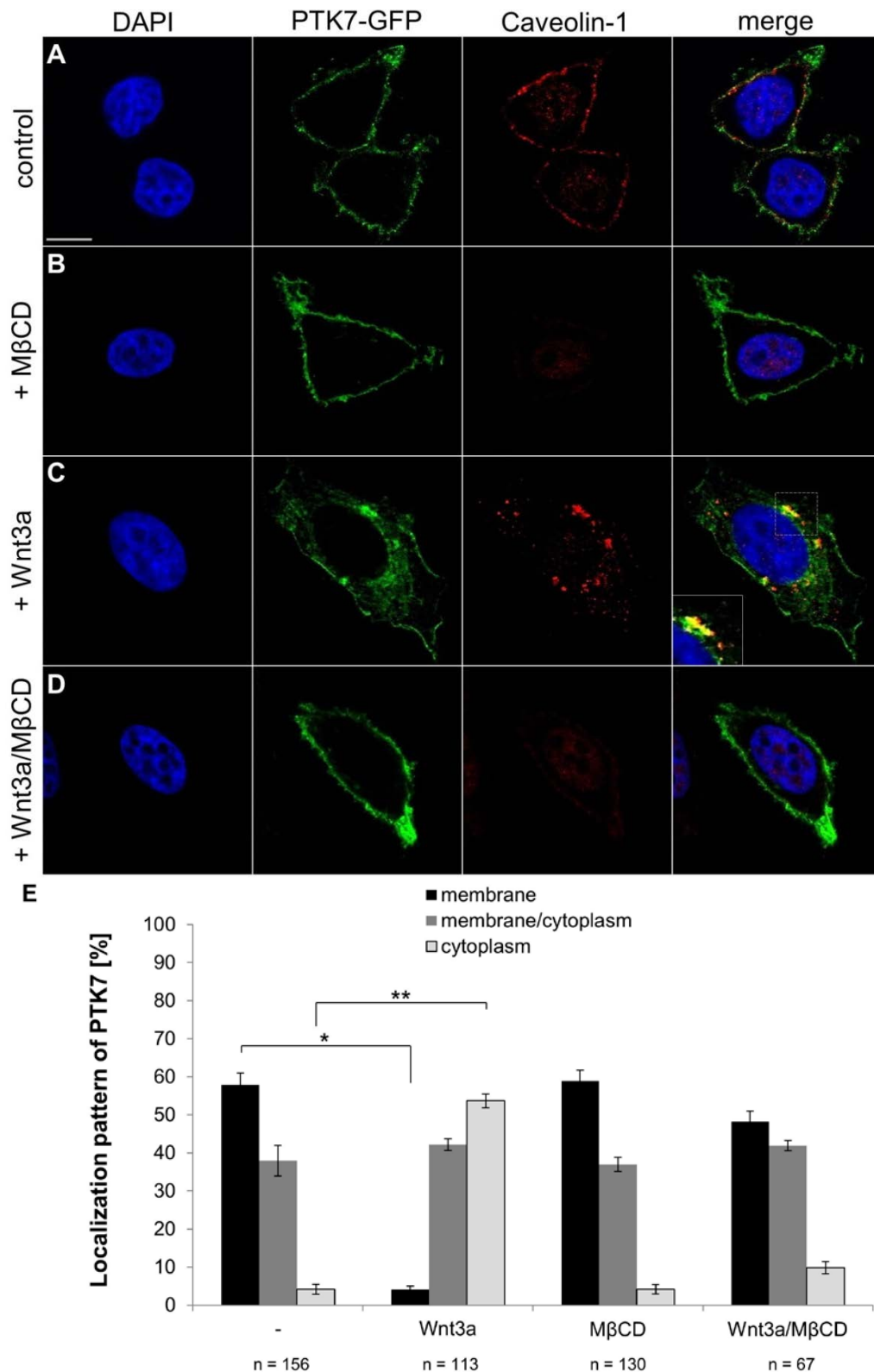


Figure 31: PTK7 internalization is prevented by MβCD treatment.

PTK7-GFP expressing MCF7 cells were cultured with methyl-β-cyclodextrin (MβCD) 4 hours prior to Wnt treatment. Cells were treated with rhWnt3a for 1 hour and co-stained with antibodies against endogenous caveolin-1. **(A-E)** PTK7 is localized to the membrane in untreated cells **(A)** and in cells treated with MβCD only **(B)**. In the presence of rhWnt3a PTK7 protein shifts to the cytoplasm and co-localizes with caveolin-1 **(C)**. MβCD prevents PTK7 translocation into the cytoplasm in cells treated with rhWnt3a **(D)**. Scale bars, 10 μm. **(E)** Quantification of the PTK7 localization pattern. Each graph shows three independent experiments with +/- standard errors. Numbers of analyzed cells (n) are shown. * p<0.0001 in a Student's t-test.

Similar results were obtained when caveolin-mediated endocytosis was inhibited by M β CD in cells expressing Δ kPTK7-GFP. As expected, cells with exclusive cytoplasmic localization of Δ kPTK7 were rarely, or not at all, found under untreated or M β CD treated conditions with 2.5% and 0% showing cytoplasmic PTK7 protein, respectively (Figure 32 A, B, E). In the presence of rhWnt3a 48% of the cells show a cytoplasmic Δ kPTK7 staining, but only 6% do so in the presence of rhWnt3a and M β CD (Figure 32 C, D). These data further proof that PTK7 is internalized by a caveolin-mediated pathway in a way that is independent of its kinase homology domain.

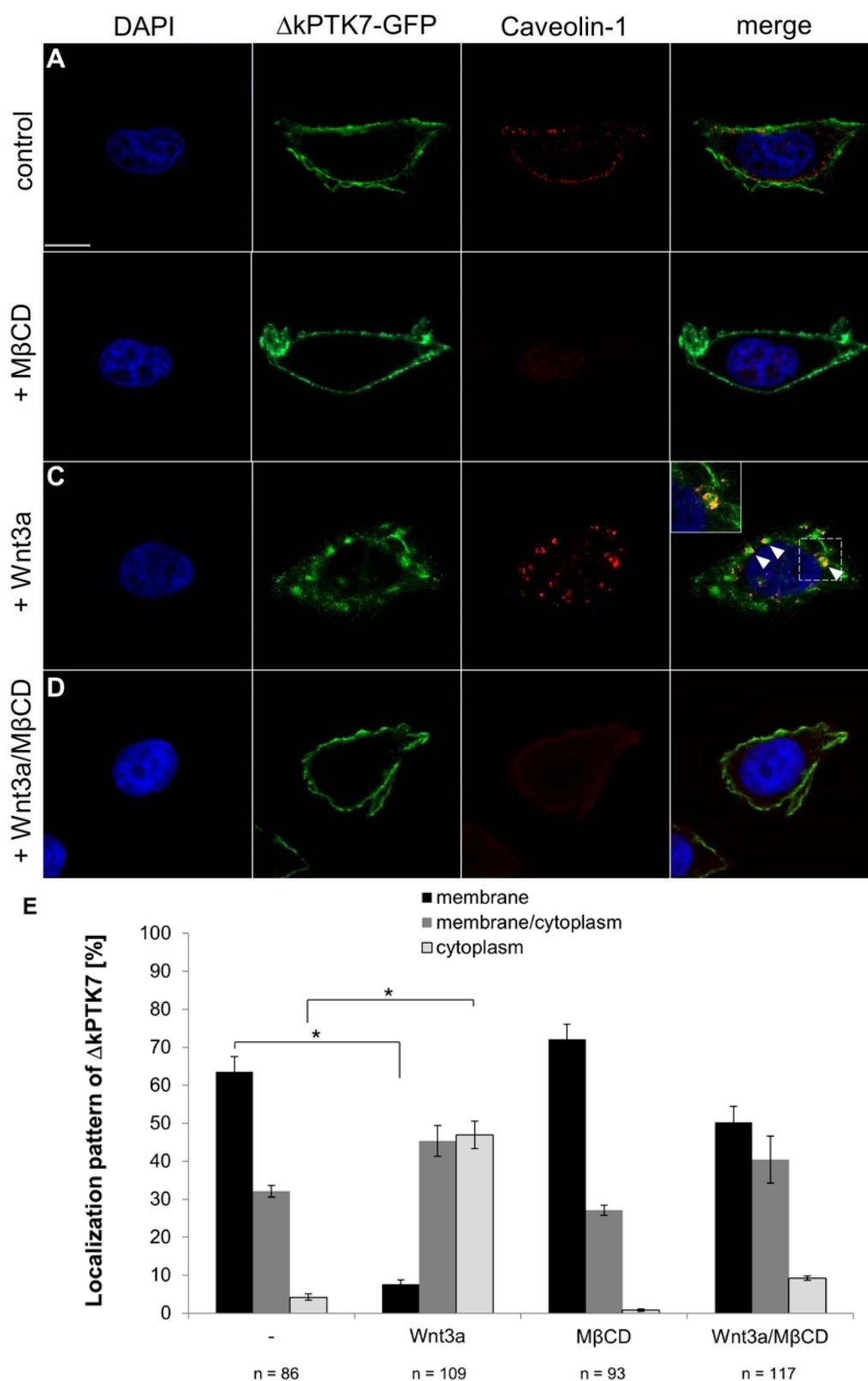


Figure 32: Δ kPTK7 internalization is prevented by M β CD treatment.

MCF7 cells expressing Δ kPTK7-GFP were cultured with methyl- β -cyclodextrin (M β CD), treated with rhWnt3a for 1 hour and co-stained with antibodies against endogenous caveolin-1. **(A)** Δ kPTK7 is present at the plasma membrane in the control and **(B)** M β CD-treated cells. **(C)** Δ kPTK7 translocates to the cytoplasm and co-localizes with caveolin-1 in rhWnt3a treated cells. **(D)** Δ kPTK7 localizes at the plasma membrane in the presence of M β CD and rhWnt3a-treated cells. **(E)** Quantification of the Δ kPTK7 localization pattern. Each graph shows three independent experiments with +/- standard errors. Numbers of cells analyzed (n) are shown. Scale bars, 10 μ m. * p < 0.001, ** p < 0.0001 in a Student's t-test.

3.4.3 PTK7 interacts with caveolin-1

Co-localization analyses of fluorescent PTK7-GFP and caveolin-1 suggest an interaction of the two proteins. To further verify these findings, biochemical interaction of PTK7 and caveolin-1 was examined in co-immunoprecipitation (Co-IP) analyses. MCF7 cells were co-transfected with an HA-tagged caveolin-1 construct and myc-tagged PTK7 constructs; full-length PTK7-MT and Δ kPTK7-MT. In lysates of these cells, PTK7 and Δ kPTK7 were immunoprecipitated using anti myc-antibodies. Both, the full-length PTK7-MT protein as well as the Δ kPTK7-MT mutant form, co-precipitate caveolin-1-HA (Figure 33 A). Single transfections of each construct served as a negative control. To verify this interaction Co-IP experiments were additionally performed in the reverse direction. Precipitation of caveolin-1 using anti-HA-antibodies, led to a co-precipitation of both PTK7 and Δ kPTK7 (Figure 33 B). In addition to the observed co-localization in fluorescently labeled cells, these findings indicate a biochemical interaction of PTK7 and caveolin-1, which is independent of the kinase homology domain.

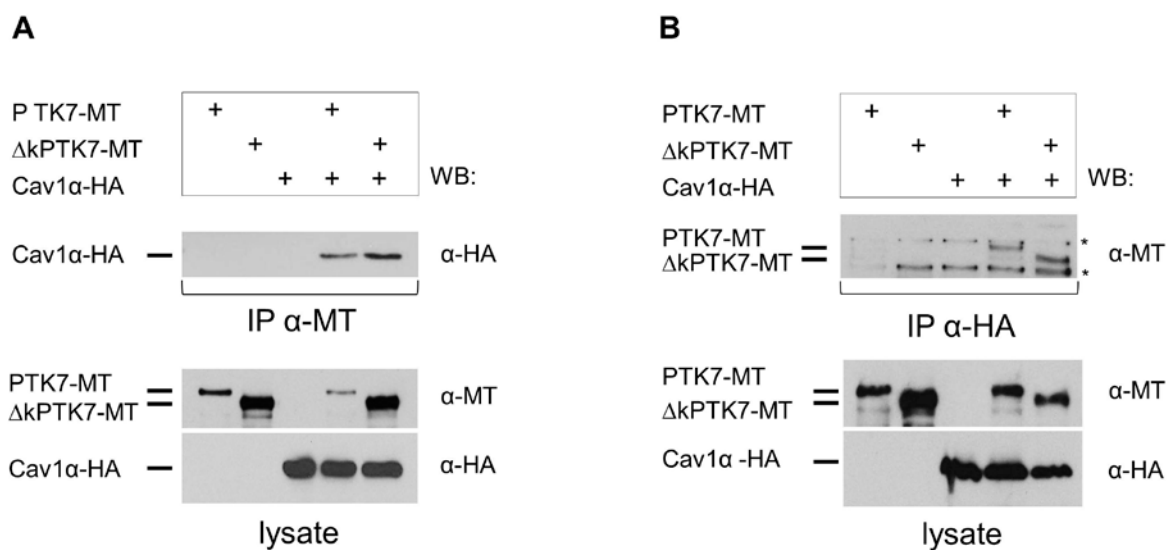


Figure 33: PTK7 and Δ kPTK7 interact with caveolin-1.

MCF7 cell were transfected with myc-tagged PTK7 constructs (PTK7-MT and Δ kPTK7-MT) and a HA-tagged caveolin-1 construct as displayed at the top. Co-precipitated proteins, probed with the antibodies indicated at the right, are shown in the upper blot and the lysates used for co-immunoprecipitation experiments in the lower blot. **(A)** PTK7 proteins were precipitated using anti-myc antibodies (IP α -MT). Myc-tagged PTK7 and myc-tagged Δ kPTK7 co-precipitate HA-tagged caveolin-1. **(B)** Vice versa, caveolin-1 proteins were precipitated with anti-HA antibodies (IP α -HA) and co-precipitated myc-tagged PTK7 and Δ kPTK7. * unspecific bands.

3.4.4 PTK7 endocytosis is independent of clathrin

To determine the role of clathrin-mediated endocytosis on PTK7 trafficking, MCF7 cells expressing PTK7-GFP or Δ kPTK7-GFP were co-stained with anti-clathrin antibodies to visualize endogenous clathrin expression. Cytoplasmic co-localization of PTK7-GFP with clathrin was rarely observed in untreated cells (9.2%) and in rhWnt5a treated cells (5.3%) (Figure 34 A,C,D). rhWnt3a stimulated cells show a slight but insignificant increase in PTK7-clathrin co-localization, which was detected in 17.6% of the analyzed cells (Figure 34 B,D). However, the magnified view of cells with fluorescently labeled PTK7 and clathrin clearly shows that PTK7 and clathrin do not localize to the same vesicle like structures in the cytoplasm (Figure 34 B). Similar to full length PTK7, Δ kPTK7-GFP showed an insignificant co-localization with clathrin. Co-localization was observed in 7.3% of the untreated, 9.5% of the rhWnt5a stimulated cells and 7.3% of the rhWnt3a treated cells co-localization of PTK7 and clathrin in the cytoplasm was observed (Figure 35). Further evidence was provided by the calculation of the Pearson correlation coefficients, which prove the low co-localization rates under all tested conditions (Figure 34, 35). These experiments indicate that rhWnt3a-induced PTK7 internalization largely seems to be independent of clathrin. However, as a slight increase in PTK7-clathrin co-localization in response to rhWnt3a was observed, a function of clathrin-mediated endocytosis on PTK7 trafficking cannot be ruled out completely.

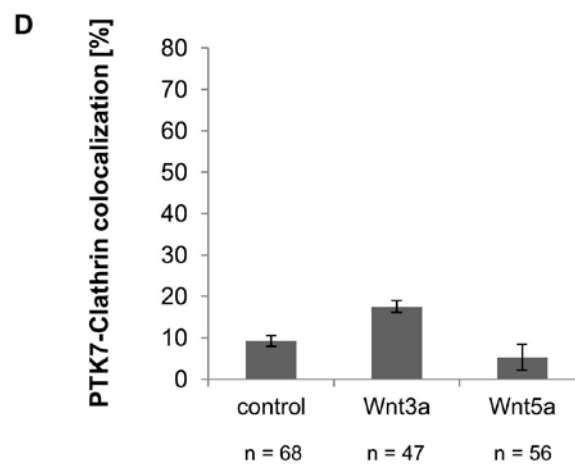
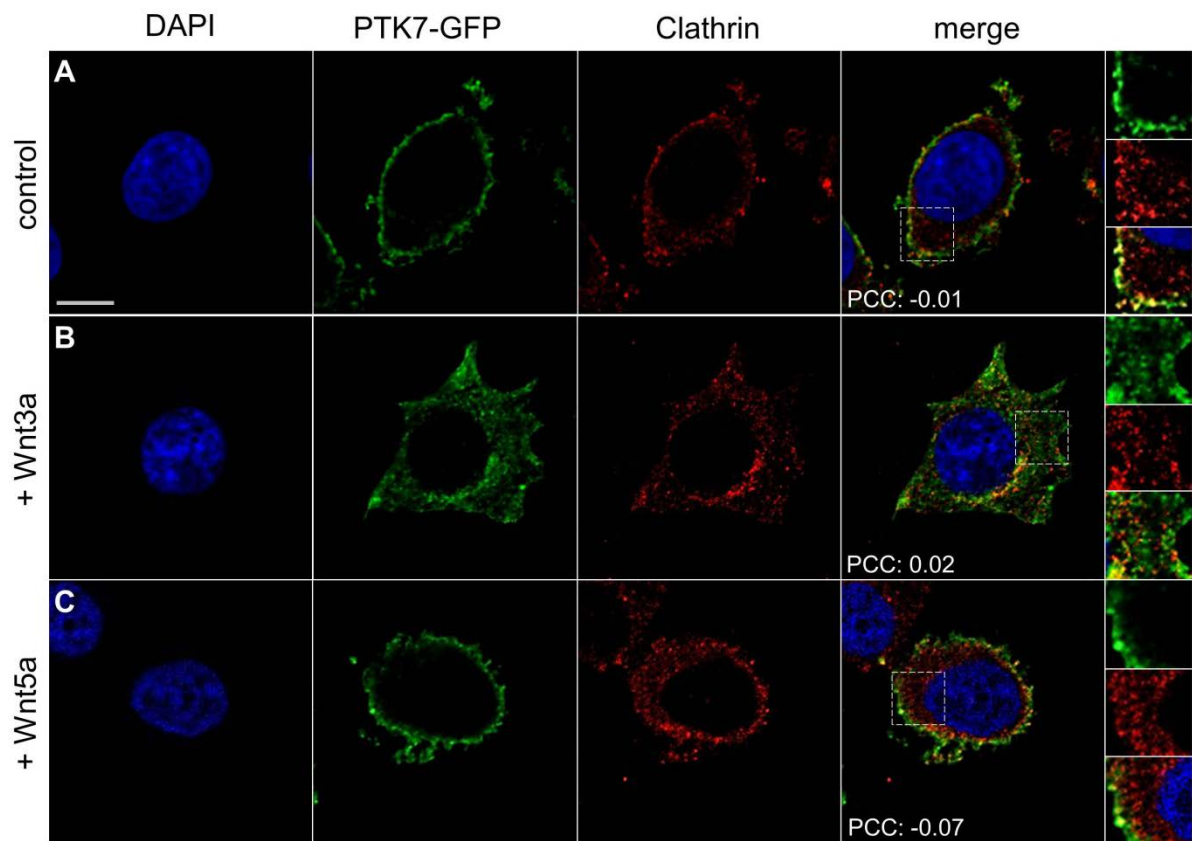


Figure 34: PTK7 infrequently co-localizes with clathrin.

(A-C) MCF7 cells stably expressing PTK7-GFP were treated with rhWnt3a or rhWnt5a protein for 1 hour and stained with anti-clathrin antibodies. PCCs for the respective cells are given. (D) Quantification of PTK7-GFP and clathrin co-localization based on calculated PCCs. The graph summarizes three independent experiments with +/- standard errors. Numbers of analyzed cells (n) are indicated for each condition. Scale bar, 10 μ m.

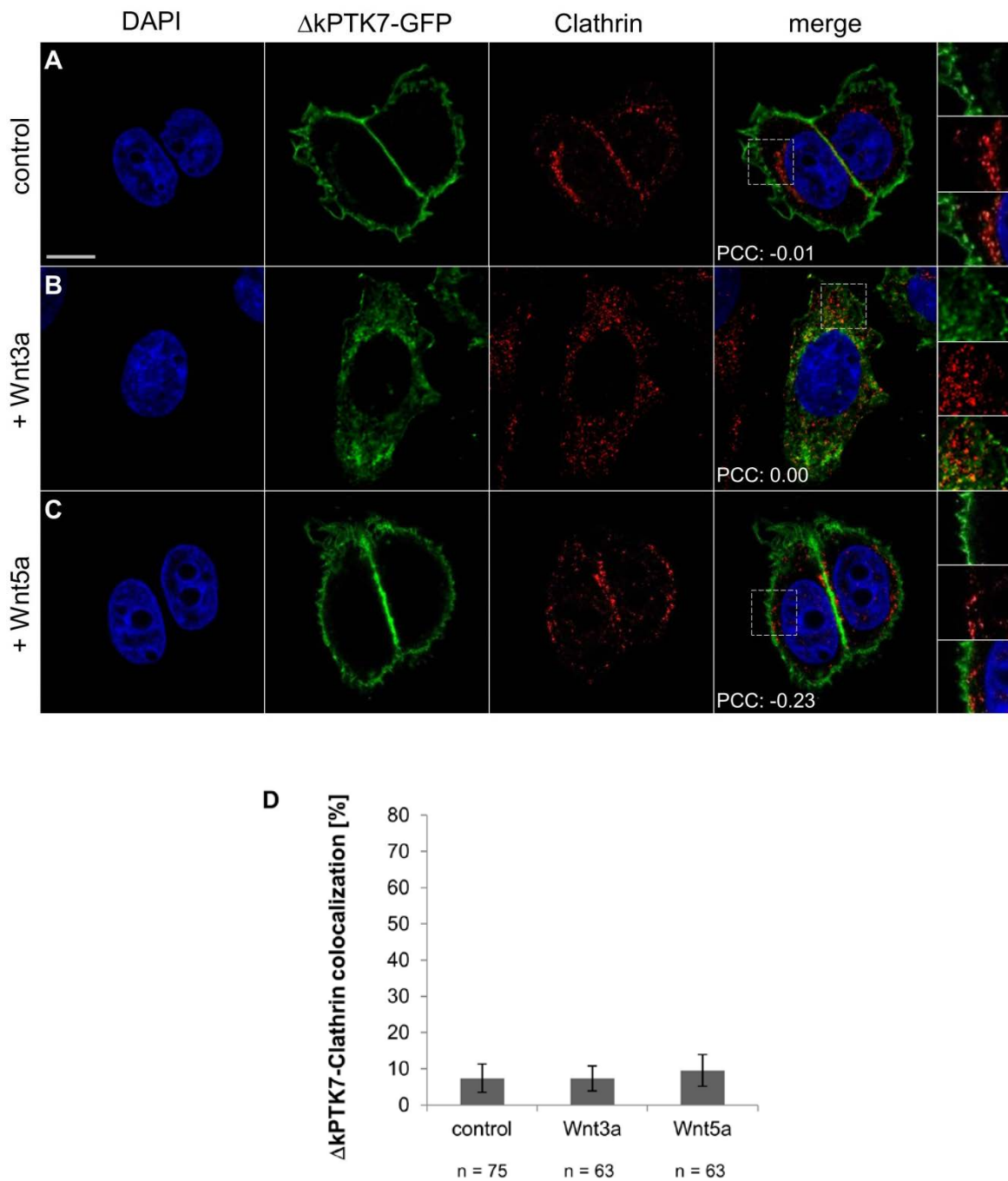


Figure 35: Δ kPTK7 hardly co-localizes with clathrin.

(A-C) MCF7 cells stably expressing Δ kPTK7-GFP were treated with rhWnt3a or rhWnt5a protein for 1 hour and stained with anti-clathrin antibodies. PCCs for the respective cells shown were calculated. (D) Quantification of Δ kPTK7-GFP and clathrin co-localization. Graph summarizes three independent experiments, +/- standard errors are shown. Numbers of cells (n) are indicated for each condition. Scale bar, 10 μ m.

3.4.5 PTK7 co-localizes with caveolin-1 but not with clathrin at the basal plasma membrane upon Wnt3a treatment

The findings, obtained by PTK7 and caveolin-1 or PTK7 and clathrin co-localization analyses, indicate that PTK7 endocytosis is mediated by caveolin-1 rather than by clathrin. However, in contrast to caveolin-1, which stably binds to the membrane, clathrin is dynamically associated with the plasma membrane and disassembles quickly after the vesicle has been released into the cytoplasm (Mundy et al. 2012; Parton and del Pozo, 2013). Thus, even if PTK7 endocytosis would be additionally mediated by clathrin, cytoplasmic co-localization of these two proteins might not have been observed due to fast disassembly of clathrin from the vesicles carrying the Wnt/PTK7 complex. To further analyze whether PTK7 co-localizes with clathrin or caveolin-1, the basal plasma membrane of the cells and the cytoplasmic regions immediately beneath the plasma membrane, where clathrin is most likely still attached to the vesicles were visualized using TIRF (Total Internal Reflection Fluorescence) microscopy. In MCF7 wild type cells endogenous PTK7, caveolin-1 and clathrin were stained using the respective antibodies. PTK7 dots were counted and analyzed for co-localization with either caveolin-1 or clathrin. As expected PTK7-caveolin-1 co-localization increased from 21.4% in untreated cells to 49.1% in rhWnt3a treated cells (Figure 36 A,B,E). In contrast, PTK7-clathrin co-localization remained largely unchanged in the presence or absence of rhWnt3a with 13% and 17.1%, respectively (Figure 36 C,D,E). These results further proof that PTK7 internalization is independent of the clathrin-mediated endocytosis pathway.

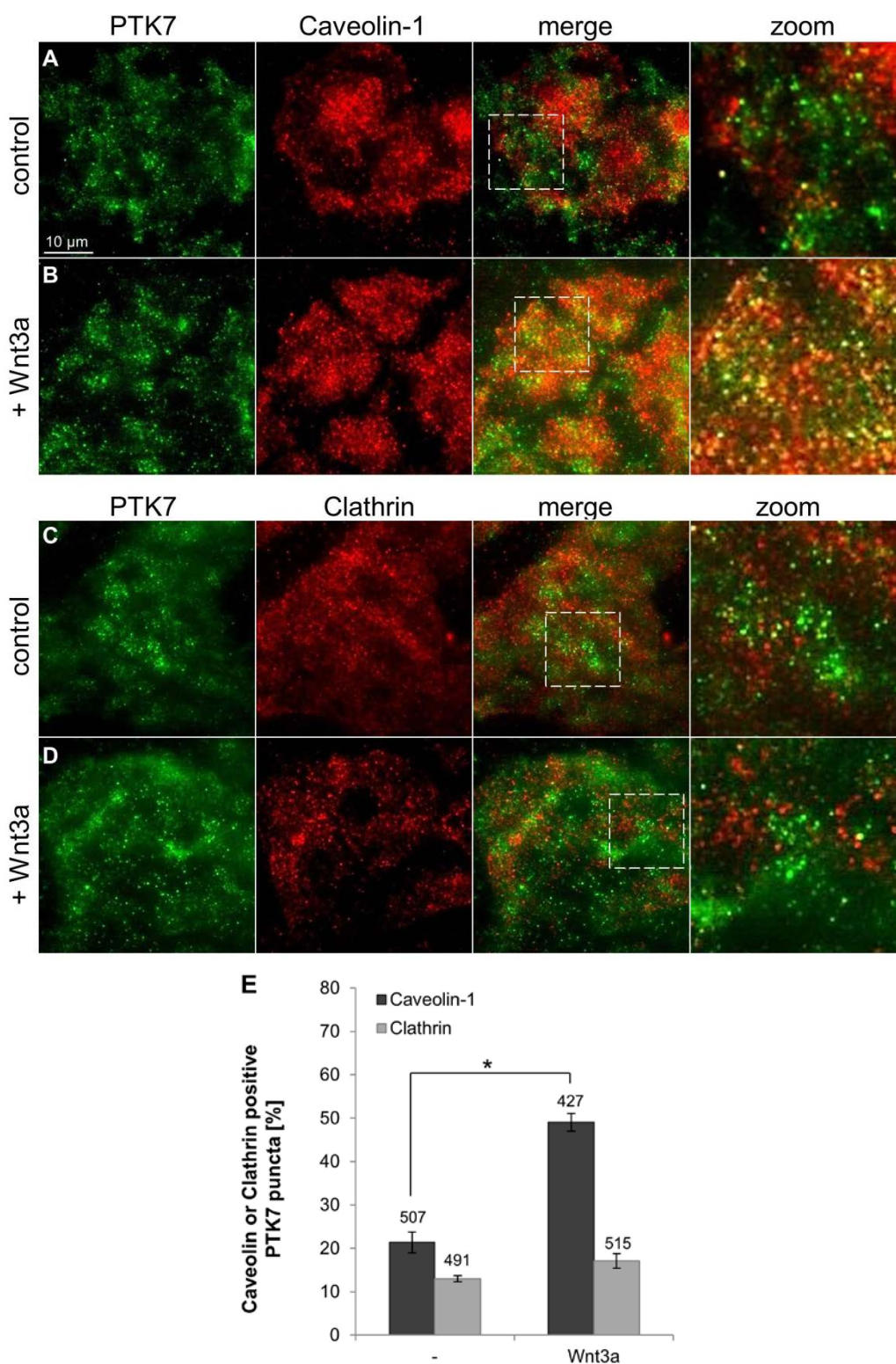


Figure 36: PTK7 and caveolin-1 co-localize at the basal plasma membrane after Wnt3a stimulation.

Endogenous PTK7, caveolin-1 or clathrin proteins were stained in wild type MCF7 cells using the respective antibodies and analyzed using TIRF microscopy. Resolution in Z-plane: ≤ 130 nm. **(A)** PTK7 co-localizes slightly with caveolin-1 in untreated cells. **(B)** Co-localization of PTK7 and caveolin-1 increased after rhWnt3a stimulation. **(C)** PTK7 hardly co-localizes with clathrin in the presence or **(D)** absence of rhWnt3a. **(E)** The graph summarizes the percentage of PTK7 puncta that co-localize with caveolin-1 or clathrin, based on the calculated PCCs. PCCs were determined for individual cells ($N \leq 24$), average values are summarized and standard errors are given. Numbers of analyzed PTK7 puncta (n) are indicated for each condition above the respective bar. * $p < 0.0001$ in a Student's t-test.

3.5 PTK7 is degraded in the lysosome in response to Wnt3a

3.5.1 PTK7 protein levels decrease upon Wnt3a treatment

Receptor-mediated endocytosis has a profound influence on the regulation of signaling pathways. Signal transduction can be terminated through internalization and subsequent transport of the receptor to the lysosome for degradation. However, endocytosis is not only important for signal termination but also for signal transduction, maintenance and amplification (Yamamoto et al., 2006; Kikuchi et al., 2009; Niehrs, 2012; Willert and Nusse, 2012; Feng and Gao, 2015). To examine if caveolin-1-mediated PTK7 endocytosis leads to lysosomal degradation of PTK7, MCF7 wild type cells were incubated with increasing concentrations of canonical rhWnt3a or non-canonical rhWnt5a. Subsequently, endogenous PTK7 protein levels were detected using Western blotting. PTK7 signal intensities were measured and normalized against actin signal intensities. Indeed, after 2 hours of Wnt-incubation, endogenous PTK7 protein intensity decreased with increasing concentrations of rhWnt3a, which mediates PTK7 endocytosis. Treatment of the cells with 25 or 50 ng of rhWnt3a had no significant effect on the PTK7 concentration. However, PTK7 protein intensity started to decrease at a concentration of 100 ng rhWnt3a and only faint PTK7 expression was detectable when cells were treated with 200 ng rhWnt3a (Figure 37 A). Compared to the untreated control with a signal intensity set to 100%, treatment of the cells with 100 ng rhWnt3a led to a decrease in PTK7 protein intensity to 81%, 150 ng rhWnt3a to 56% and 200 ng rhWnt3a decreased PTK7 intensity even to less than 40% (Figure 37 C). Non-canonical rhWnt5a does not mediate PTK7 endocytosis. Thus, as expected, PTK7 protein intensity did not change significantly after treating the cells with increasing concentrations of rhWnt5a protein (Figure 37 B). The calculated relative PTK7 signal intensities are in the range of 100% in the absence or presence rhWnt5a protein (Figure 37 C).

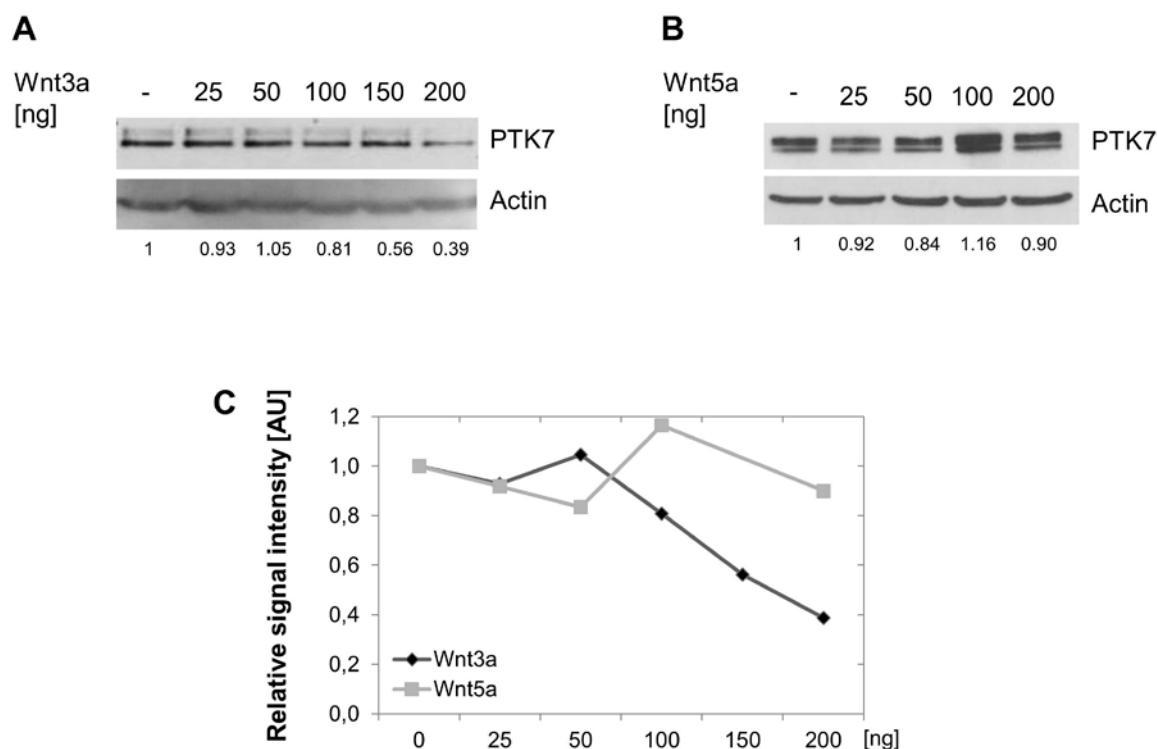


Figure 37: PTK7 protein concentrations decrease in response to canonical Wnt proteins.

(A, B) MCF7 wild type cells were incubated with increasing concentrations of rhWnt3a or rhWnt5a protein as indicated at the top. Cell lysates were probed using anti-PTK7 antibodies and anti-actin antibodies as loading control. PTK7 protein concentration decreases at increasing rhWnt3a concentrations. Endogenous PTK7 protein levels remain stable in the presence of increasing rhWnt5a concentrations. (C) PTK7 signal intensity was measured and normalized to signal intensity of actin internal control for each condition. The control condition without Wnt treatment was set to 1. The graph represents the relative signal intensities in arbitrary units [AU]. The graph summarizes three independent experiments + standard errors. Measurements of signal intensities were carried out using ImageJ.

3.5.2 Canonical Wnt proteins target PTK7 for proteasomal degradation via a caveolin-mediated pathway

The decrease of PTK7 protein in response to rhWnt3a, suggest that upon caveolin-1-dependent endocytosis, PTK7 is transported to the lysosome for degradation. To further analyze this, lysosomal degradation in MCF7 cells was inhibited using chloroquine. Chloroquine is a lysosomotropic agent that raises the lysosomal pH leading to an inhibition of lysosomal enzymes that require an acidic pH for their activity (Steinman et al., 1983). Endogenous PTK7 levels were determined upon rhWnt3a stimulation in the presence or absence of chloroquine. Chloroquine prevents the decrease of PTK7 in the presence of rhWnt3a (Figure 38 A). In comparison to the untreated control with the relative PTK7 signal intensity set to 100%, the relative PTK7 signal intensity drops slightly to 87% in the presence of 25 ng rhWnt3a and significantly to 54% in the presence of 200 ng rhWnt3a. However, no decrease of PTK7 protein was detected when lysosomal degradation was inhibited by chloroquine (Figure 38 B). These results indicate that

rhWnt3a leads to lysosomal degradation of PTK7 in a dose-dependent manner. To further prove that PTK7 is transported into the lysosome via a caveolin-mediated pathway, caveolin-dependent endocytosis was inhibited using methyl- β -cyclodextrin (M β CD) and PTK7 protein levels in response to rhWnt3a were analyzed. Under control conditions PTK7 protein concentration decreases significantly in the presence of 200 ng rhWnt3a as shown before. Conversely, endogenous PTK7 levels remained stable after inhibition of caveolin-mediated endocytosis (Figure 38 C,D). These findings show that Wnt3a triggers PTK7 lysosomal degradation by a caveolin-mediated endocytosis pathway.

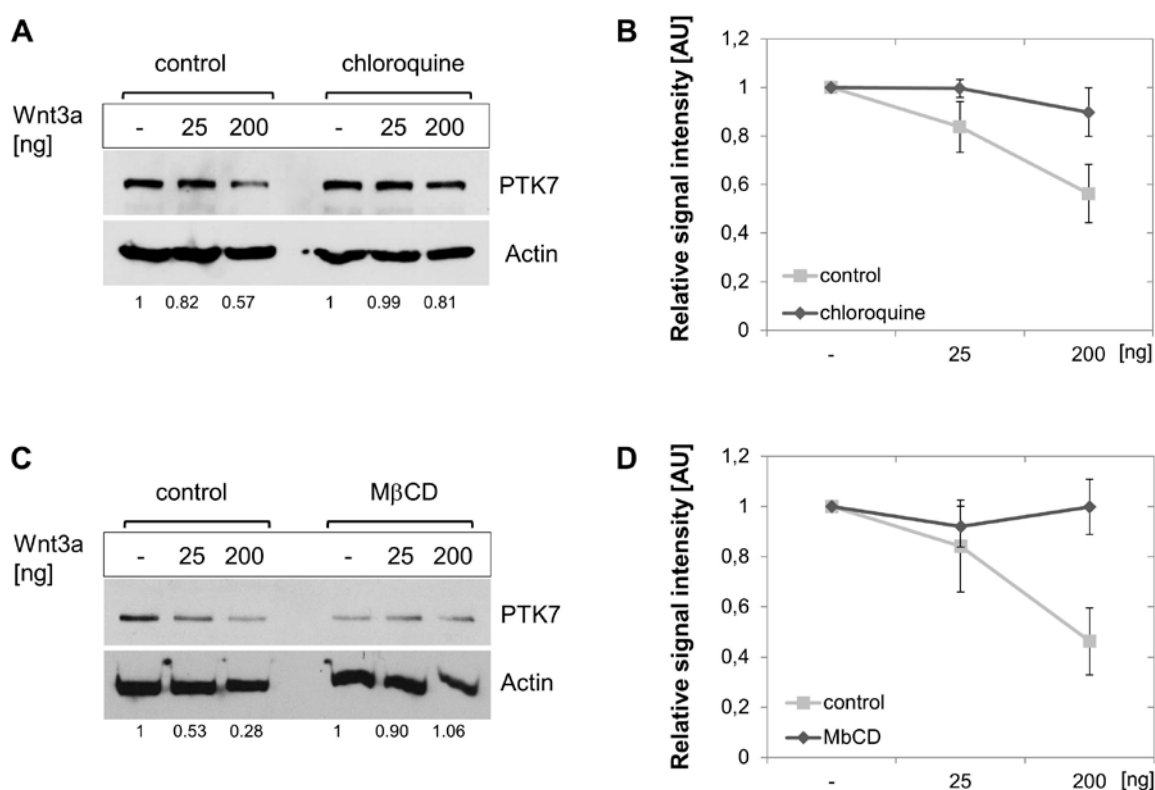


Figure 38: Inhibition of lysosomal degradation prevents Wnt3a-induced decrease of PTK7 protein.

MCF7 cells were incubated with 25 or 200 ng rhWnt3a in the presence or absence of the inhibitor of lysosomal degradation, chloroquine, or the inhibitor of caveolin-mediated endocytosis, methyl- β -cyclodextrin. Cell lysates were probed using anti-PTK7 antibodies. **(A)** In the absence of chloroquine, PTK7 protein concentration decreased after rhWnt3a stimulation. After inhibition of lysosomal degradation using chloroquine, PTK7 protein levels remained constant. **(B)** Relative signal intensity was calculated for each condition and plotted in arbitrary units. The graph included three independent experiments, \pm standard errors are given. **(C)** Under control conditions PTK7 protein levels decreased in response to rhWnt3a. In the presence of M β CD PTK7 protein remained stable. **(D)** The graph summarizes relative signal intensities in arbitrary units of three independent experiments, \pm standard errors are shown. Measurements of signal intensities were carried out using ImageJ.

3.6 Caveolin-1 loss-of-function decreases the inhibitory effect of PTK7 on canonical Wnt signaling

The Wnt co-receptor PTK7 inhibits canonical Wnt signaling. However, the molecular mechanism how PTK7 inhibits canonical Wnt signaling remains unclear. These data indicate that the Wnt/PTK7 complex is endocytosed via a caveolin-1 mediated pathway. Taking this in consideration, it is tempting to speculate that by this endocytic process PTK7 removes canonical Wnt ligands from the extracellular matrix, thereby inhibiting their function of activating canonical Wnt signaling. Thus, endocytosis mediated by caveolin-1 might be a key step in the PTK7-related inhibition of canonical Wnt signaling. The functional relevance of caveolin-1 mediated PTK7 endocytosis on canonical Wnt signaling was investigated in *Xenopus* second axis assays. *Xenopus* second axis analysis is a powerful tool to study whether a protein acts positively or negatively on canonical Wnt signaling. The ectopic activation of canonical Wnt signaling in the ventral part of the embryo by injection of canonical *Wnt8* mRNA, leads to the generation of embryos with an ectopic second axis. As PTK7 inhibits canonical Wnt signaling, co-injection of *PTK7* mRNA significantly inhibits second axis induction. Interestingly, after co-injection of *Wnt8*, *PTK7* and Cav1 α MO PTK7-induced inhibition of second axis induction was significantly reduced in comparison to second axis induction after co-injection of *Wnt8* and *PTK7* (Figure 39). Thus, co-injection of Cav1 α MO seems to reduce the inhibitory effect of PTK7 on canonical Wnt signaling. However, Cav1 α MO injection without *PTK7* as well reduced second axis induction. This is not surprising as a function of caveolin in activating canonical Wnt signaling by receptor endocytosis of LRP6 was described (Yamamoto et al., 2006). In the absence of PTK7, loss of caveolin might inhibit LRP6-related activation of canonical Wnt signaling. However, in the PTK7 context, caveolin-1 depletion seems to reduce PTK7-related inhibition of canonical Wnt signaling. These results indicate that caveolin-1 mediated endocytosis of the Wnt/PTK7 complex seems to be important for PTK7-related inhibition of canonical Wnt signaling.

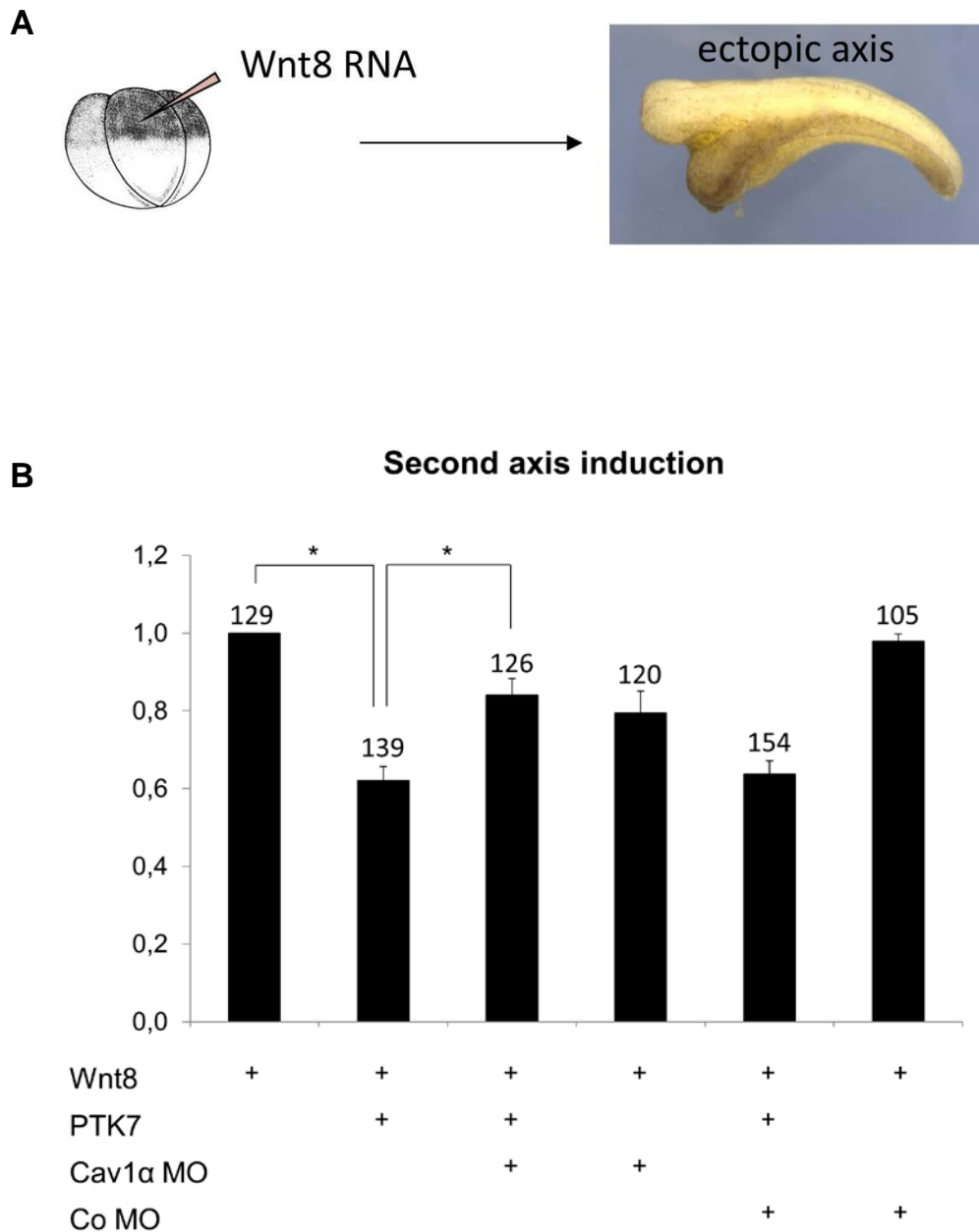


Figure 39: Caveolin-1 α loss-of-function prevents PTK7-mediated inhibition of canonical Wnt signaling in *Xenopus* second axis assay.

(A) 4-cell stage *Xenopus* embryos were injected with 5 pg *Wnt8* mRNA into one ventral blastomere to induce the generation of a second axis. (B) *Wnt8*-induced second axis development serves to normalize the data and was set to 1. *Wnt8*-induced second axis generation is significantly inhibited by co-injection of 250 pg *PTK7* mRNA. Co-injection of *PTK7* and 10 ng Caveolin-1 α MO reduced the inhibitory effect of *PTK7* on canonical Wnt signaling. The graph summarizes 4 independent experiments. Numbers of analyzed embryos (n) are shown for each condition above the respective bar. * $p < 0.0001$ in a Student's t-test.

3.7 The function of caveolin-1 in *Xenopus* development

3.7.1 Caveolin-1 knockdown leads to swimming defects, eye defects and bended *Xenopus* embryos

As PTK7 is endocytosed by a caveolin-dependent pathway in response to canonical Wnt proteins, we wondered how caveolin-1 itself affects embryonic development. To analyze the phenotypes caused by caveolin-1 depletion in *Xenopus*, both isoforms, caveolin-1 α and caveolin-1 β were knocked out by injection of the respective morpholinos in one blastomere of two-cell stage embryos. The injection in one of two blastomeres results in a knockdown of caveolin-1 in only one side of the embryo, while the uninjected side serves as a control. Embryos injected with 20 ng Cav1 α MO or Cav1 β MO exhibited a severely impaired swimming behavior. In contrast to control morpholino injected embryos, which are mobile and showed directed movement, caveolin-1 knockdown embryos exhibited tremors, spasms or even paralysis on the injected side resulting often in a circular swimming behavior. Apparently these embryos were not able to move the injected side properly (Movie S1). Swimming routes of control and caveolin-1 α knockdown embryos (embryos that were still able to move were selected) were tracked over a time of five seconds. The tracks clearly showed directed routes of the control embryos (Figure 40 B), while caveolin-1 α depleted embryos swam in circular routes (Figure 40 A) and some embryos did not move away from their spot (Figure 40 A, green track). In addition to the swimming defect, caveolin-1 α as well as caveolin-1 β morphants exhibited eye developmental defects on the injected side and also kinked tails (Figure 40 C, D). Nevertheless, the swimming defect was the predominant defect, as it can be detected in 91% of the caveolin-1 α and 87% in the caveolin-1 β injected embryos (Figure 40 F). Importantly, it should be pointed out that most of the embryos had a normal morphological appearance but were nevertheless not able to move normally.

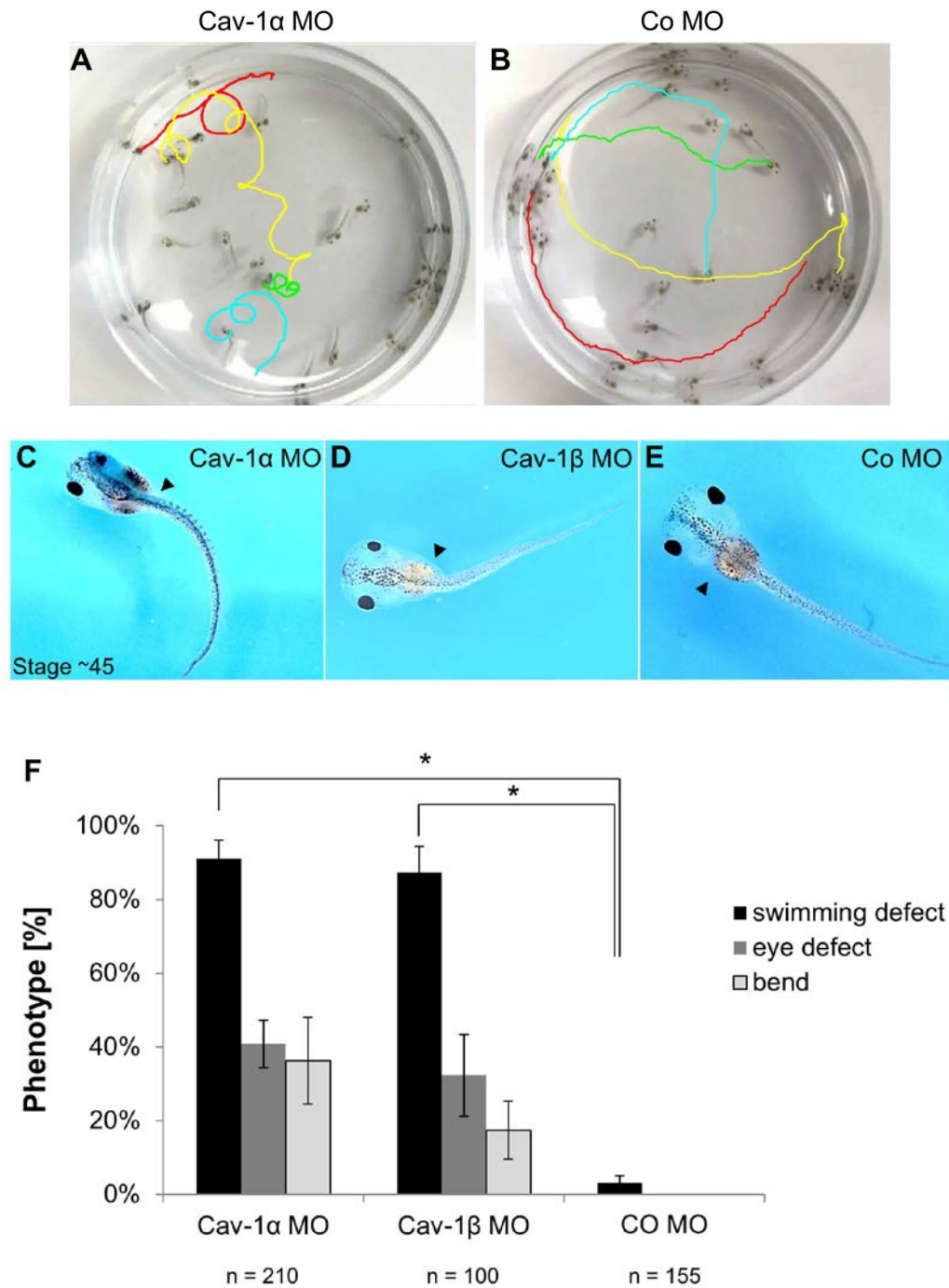


Figure 40: Caveolin-1 depletion leads to swimming defects, eye defects and bended embryos.

Two-cell stage *Xenopus* embryos were injected in one blastomere with 20 ng Cav-1α-MO or Co Mo together with 75 pg *lacZ* as lineage tracer. **(A, B)** Tracking of control or Cav-1α MO injected embryos (stage ~45) over five seconds. **(A)** Caveolin-1α knockdown embryos showed a circular swimming behavior. **(B)** Control embryos show directed movements. **(C)** Knockdown of caveolin-1α led to an underdeveloped eye on the injected side and kinked embryos. **(D)** Caveolin-1β knockdown embryos showed similar defects with a smaller eye at the injected side and a kinked tail. **(E)** Normal appearance of a control morpholino injected embryo. The injected sides are marked by an arrowhead. **(F)** Quantification of caveolin-1α and -1β knockdown phenotypes. The swimming defect is the predominant defect. The graph summarizes three independent experiments with +/- standard errors. Numbers of embryos (n) analyzed are shown. * $p < 0.005$ in a Student's t-test.

3.7.2 Co-injection of caveolin-1 α mRNA rescues the caveolin-1 α knockdown swimming defect

To prove that the observed swimming defect is specific for caveolin-1 depletion, it was analyzed whether co-injection of *caveolin-1 α* mRNA together with Cav-1 α MO can rescue this phenotype. As the Cav-1 α MO binds to the coding region of the gene, beginning at the start codon, a specific caveolin-1 α construct was generated containing a shifted ATG start codon, to prevent the binding of the morpholino to this rescue construct (Figure 41 A). Injection of 7.5 ng Cav-1 α MO results in a swimming defect observed in 71% of the embryos. This defect was rescued by co-injection of the caveolin-1 α rescue construct in a dose-dependent manner (Figure 41 B).

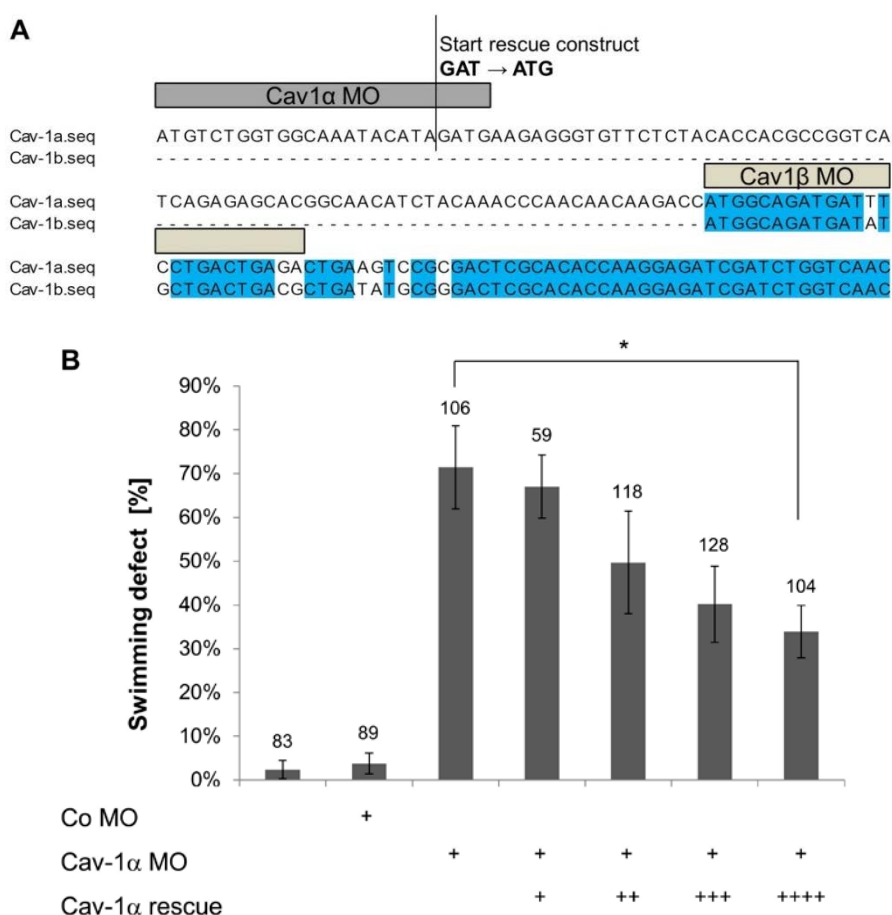


Figure 41: Caveolin-1 α mRNA rescues the Cav-1 α MO induced swimming defect.

(A) Partial alignment of the *caveolin-1 α* and *-1 β* mRNA sequences with the respective morpholino binding sites. Cav-1 α MO binds 25 base pairs beginning at the start codon of *caveolin-1 α* mRNA. The caveolin-1 α rescue construct has a shifted ATG, which replaces GAT at position 22-24, and is truncated by 21 base pairs. **(B)** Cav-1 α -induced swimming defect is rescued dose-dependently by co-injection of the caveolin-1 α rescue construct. Three independent experiments are summarized in the graph. Numbers of analyzed embryos (n) are given above each bar. * $p < 0.05$ in a Student's t-test.

3.7.3 Caveolin-1 α protein expression is inhibited by Cav-1 α MO, but not by Cav-1 β MO

Interestingly, the depletion of both caveolin-1 isoforms led to similar phenotypes. These two isoforms arise through alternate translation start sites, thus caveolin-1 β is truncated by 31 residues, while the remaining sequence is highly identical (Scherer et al., 1995). Although Cav-1 β MO contains 4 mismatch base pairs compared to the caveolin-1 α mRNA sequence (Figure 41 A), it cannot be ruled out that Cav-1 β MO affects caveolin-1 α protein expression, which might lead to the same observed phenotypes. To test this caveolin-1 α protein expression was detected *in vitro* in the presence of Cav-1 α MO, Cav-1 β MO, Co MO and the caveolin-1 α rescue construct using the TnT[®] Quick Coupled Transcription/Translation System (Promega). Control MO does not affect *in vitro* caveolin-1 α expression, but as expected the expression is inhibited in the presence of Cav-1 α MO. In the presence of Cav-1 β MO the caveolin-1 α protein is indeed expressed at similar levels as under control conditions, proving that the Cav-1 β MO does not bind to the *caveolin-1 α* mRNA sequence (Figure 42).

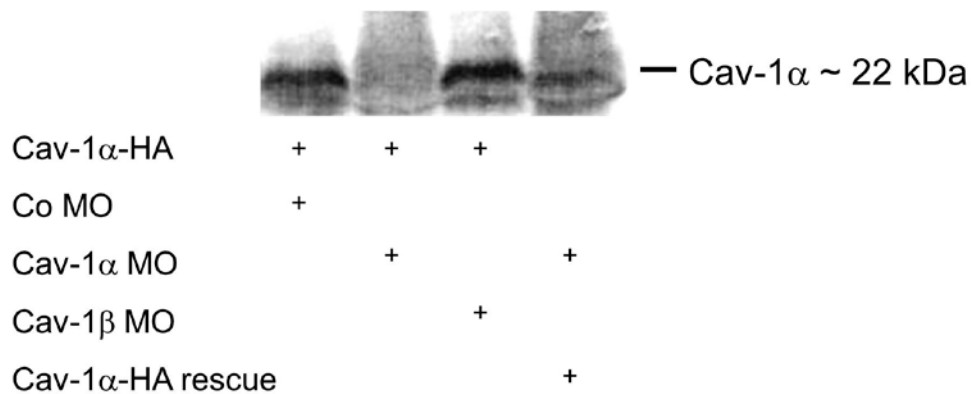


Figure 42: Cav-1 β MO does not affect caveolin-1 α protein expression.

HA-tagged caveolin-1 α protein was expressed *in vitro* in the presence of control MO, Cav-1 α MO, Cav-1 β MO or the Cav-1 α rescue construct using the TnT[®] Quick Coupled Transcription/Translation System (Promega). Caveolin-1 α expression was detected by Western blotting with anti-HA antibodies. Protein expression is inhibited only in the presence of Cav-1 α MO, but not in the presence of Co Mo, Cav-1 β MO or the caveolin-1 α rescue construct containing a shifted translation start site.

3.7.4 Caveolin-1 α is localized to the notochord of *Xenopus* embryos

The observed swimming defect might result from muscular or neuronal developmental defects, thus it was tested by whole mount *in situ* hybridization if caveolin-1 α might be expressed in these tissues in developing *Xenopus* embryos.

Prior studies in *Xenopus* embryos indicate that caveolin-1 α is expressed with no discrete localization until neural stages. At early tadpole stages, expression was detected in dorsal tissues, including the notochord, somites, the cement gland, the eye vesicle and the posterior tailbud (Razani et al., 2002a). However, here, caveolin-1 α expression was found to be restricted only to the notochord with a very strong staining during neural and tadpole stages. Hybridization with a sense control probe as negative control did not lead to any staining (Figure 43). Thus, no caveolin-1 α expression was detected in the somites or neuronal structures. However, the notochord is a known signaling center and the strong expression of caveolin-1 α in this tissue, suggests that caveolin-1 might have functions in the regulation of developmental signaling in the notochord.

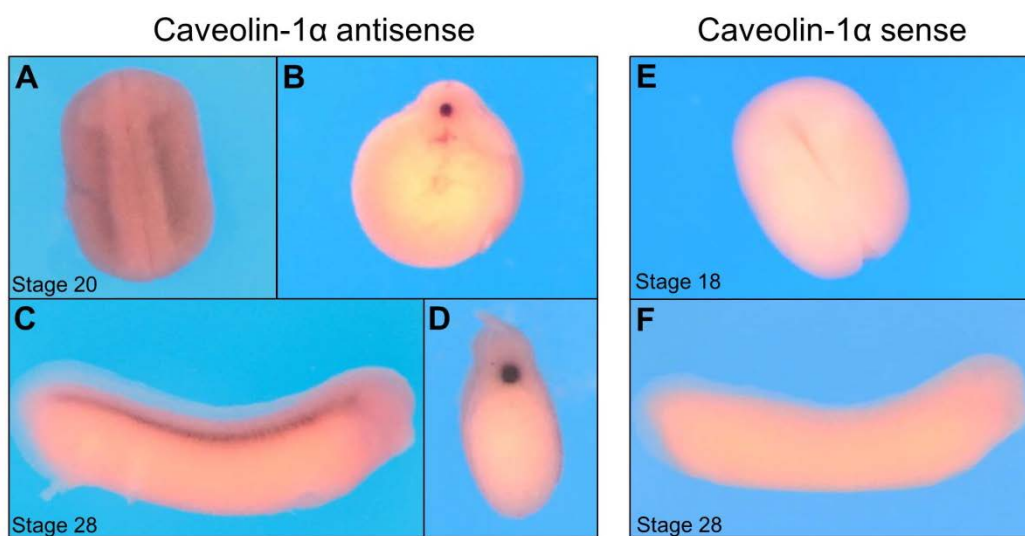


Figure 43: Caveolin-1 α is localized in the notochord in *Xenopus* embryos.

Whole mount *in situ* hybridization analysis of *caveolin-1 α* mRNA in wild type albino *Xenopus* embryos. **(A-D)** caveolin-1 α is expressed in the notochord in neurula (stage 20) and tadpole (stage 28) embryos. **(B, D)** Cross-sections through the respective neurula or tadpole embryos. **(E, F)** Caveolin-1 α sense controls were negative.

3.7.5 Caveolin-1 α knockdown causes disruption of the actin filaments

Although no caveolin-1 α expression was detected in muscular or neuronal structures, the observed swimming defect might nevertheless be a result of aberrant muscles or neurons. Moreover, in zebrafish embryos caveolin-1 depletion leads to a disrupted actin cytoskeleton of the muscle cells in the somites (Fang et al., 2006). To analyze if the swimming defect in *Xenopus* embryos might result from defective muscle development, two cell stage embryos were injected with Cav-1 α or Cav-1 β MO and *lacZ* mRNA as a tracer. At stage 45 these embryos were sectioned and the actin cytoskeleton of the muscle cells was stained using phalloidin. Co Mo injected embryos exhibit properly arranged actin bundles (Figure 44 A), while the actin cytoskeleton of the somites is

strongly disrupted in caveolin-1 α morphant embryos (Figure 44 B). Knockdown of caveolin-1 β leads to a slight disruption of the actin cytoskeleton (Figure 44 C).

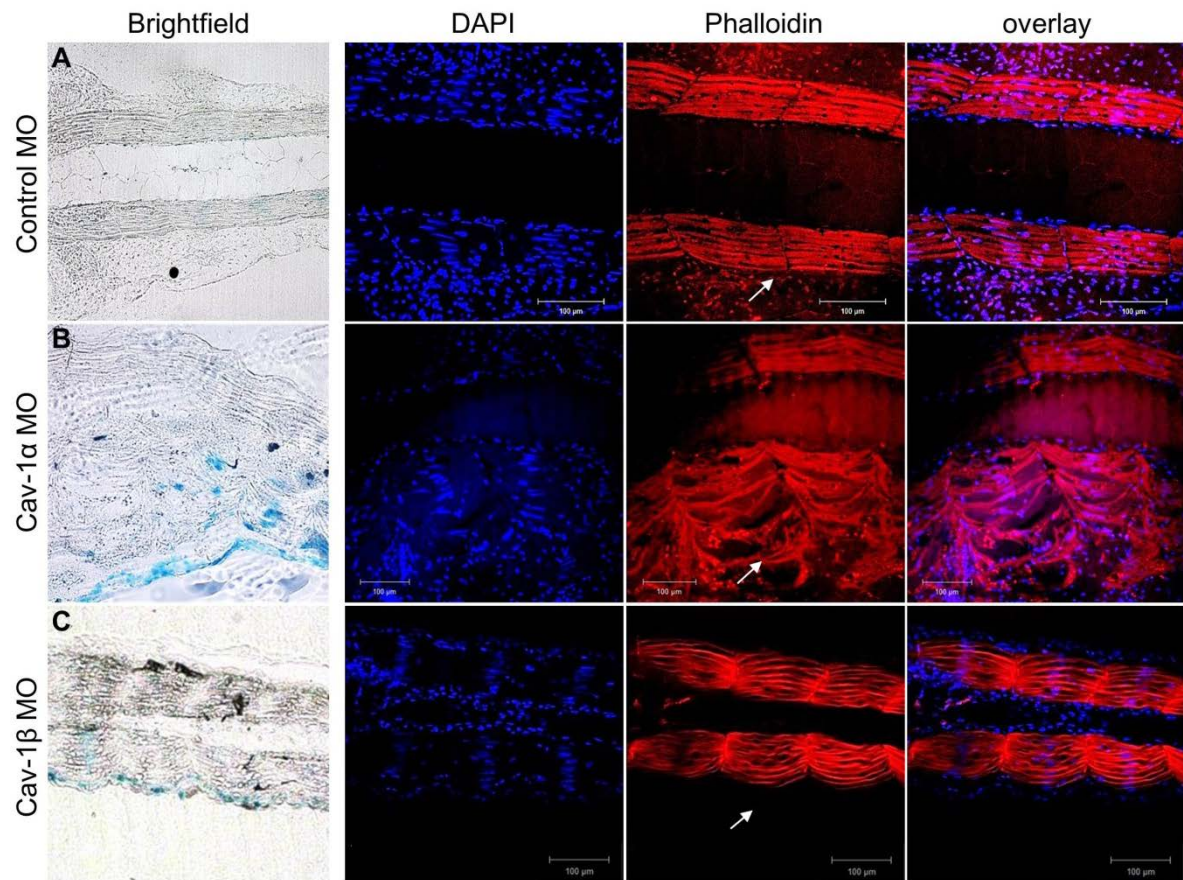


Figure 44: Caveolin-1 depletion leads to a disruption of the actin cytoskeleton.

Xenopus embryos at the two-cell stage were injected in one blastomere with 20 ng Co Mo, Cav-1 α -MO or Cav-1 β Mo together with 75 pg *lacZ* as lineage tracer and sectioned at stage ~ 45. 30 μ m sections were stained with DAPI and Tetramethylrhodamine (TRITC)-conjugated phalloidin. The injected sides are shown by blue *lacZ* staining in the brightfield images (left panel) and marked by a white arrow in the phalloidin stained image. (A) Co Mo injected embryos show a parallel arrangement of actin microfilaments in the somites. (B) Cav-1 α MO injected embryos exhibit severely disrupted actin filaments in the muscle cells. (C) Slight impairment of the actin cytoskeleton observed in Cav-1 β MO injected embryos. Scale bars 100 μ m.

3.7.6 Caveolin-1 α depletion has no effect on *Twist*, *Xbra* or *MyoD* patterning, but leads to aberrant *Pax2* expression

In zebrafish a reduced expression of neural markers, including *Pax2* and the muscle differentiation marker *MyoD* was observed in caveolin-1 α and caveolin-1 β morphant embryos (Fang et al., 2006). To study if caveolin-1 α depletion might lead to an aberrant expression of neural tissues in *Xenopus*, *Pax2* and the neural crest marker *Twist* were analyzed in Cav-1 α MO injected embryos. No differences in *Twist* expression were detected between control and caveolin-1 α knockout embryos (Figure 45 A-D). *Pax2* did not show any difference in staining at the midbrain-hindbrain boundary, but reduced

staining of the otic vesicle, the epibranchial placodes and the pronephric kidney (Figure 45 E-H). As the epibranchial placodes give rise to neurons and further structures of the sensory nervous system (Baker and Bronner-Fraser, 2001), caveolin-1 α might affect neural tissues in *Xenopus* as shown in zebrafish.

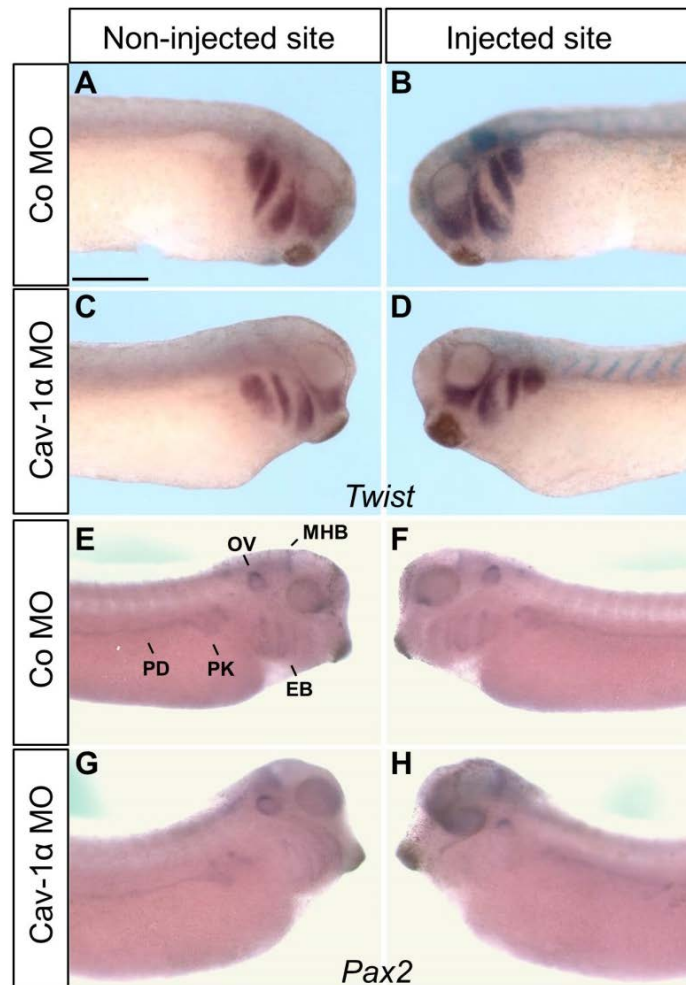


Figure 45: Caveolin-1 α depletion has no effect on *Twist* patterning, but leads to aberrant *Pax2* expression.

Two-cell stage *Xenopus* embryos were injected in one blastomere with 20 ng Cav-1 α MO or Co Mo together with 75 pg *lacZ* as lineage tracer and analyzed by whole-mount *in situ* hybridization using *Twist* and *Pax2* antisense probes. **(A, B)** Co Mo injected embryos show migrating neural crest cells at the control and the injected sites. **(C, D)** Cav-1 α MO injected embryos have normally migrating neural crest cells. **(E, F)** Normal expression of *Pax2* in the Co Mo injected embryos. **(G)** At the uninjected site *Pax2* expression is unchanged, while **(H)** at the Cav-1 α MO injected site *Pax2* is weaker expressed in the otic vesicle (OV), the pronephric kidney (PK) and the epibranchial placodes (EP), but not in the midbrain-hindbrain boundary (MHB) or the pronephric duct (PD). Scale bar: 500 μ m.

In contrast to the findings in zebrafish *MyoD* staining did not show any differences in expression between control and Cav-1 α MO injected embryos (Figure 46 A,B). Caveolin-1 α was found to be expressed in the notochord in *Xenopus* embryos (Figure 43), thus the notochord marker *Xbra* was analyzed. However, no difference in staining was detected between control and caveolin-1 α depleted embryos (Figure 43 C, D).

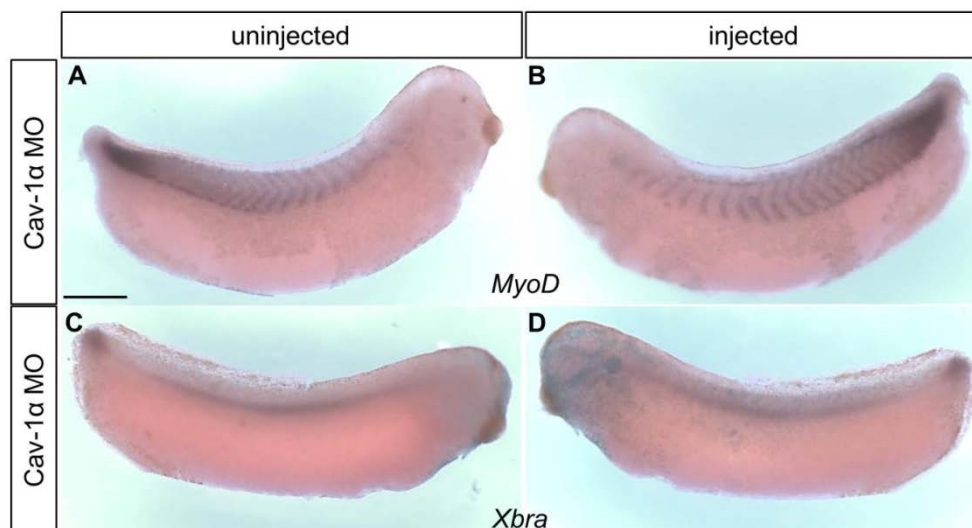


Figure 46: Caveolin-1 α depletion has no effect on *Xbra* or *MyoD* patterning.

Two-cell stage *Xenopus* embryos were injected in one blastomere with 20 ng Cav-1 α -MO or Co Mo together with 75 pg *lacZ* as lineage tracer and analyzed by whole-mount *in situ* hybridization using *MyoD* and *Xbra* antisense probes. **(A, B)** Normal expression of *MyoD* and **(C, D)** *Xbra* at injected and uninjected sites of the embryo. Scale bar: 500 μ m.

4 Discussion

Endocytosis of ligand/receptor complexes is a mechanism that has been described to control the specificity of downstream signaling (Chen et al., 2001; Blitzer and Nusse, 2006; Yamamoto et al., 2006; Bilic et al., 2007; Bryja et al., 2007; Yu et al., 2007; Sato et al., 2010; Taelman et al., 2010; Jiang et al., 2012) and may also play an important role in the regulation of Wnt signaling. Wnt signaling pathways, generally subdivided into canonical and non-canonical Wnt signaling, are involved in various biological processes, including cell proliferation, cell polarity and cell fate specification. Aberrant activation of Wnt signaling pathways leads to diverse diseases including birth defects and cancer (MacDonald et al., 2009; Niehrs, 2012; Feng and Gao, 2015; Sokol, 2015). To avoid poor activation or overactivation, Wnt signaling pathways need to be tightly regulated and this regulation is ensured by the formation of specific ligand/receptor complexes at the cell surface, thereby triggering different signaling outcomes. Thus, the cellular context defined by the availability of specific Wnt ligands and Wnt receptors determines downstream signaling. However, after many years of studying Wnt signaling, the molecular mechanism of how signal specificity is achieved is still not completely clear. Ligand-induced endocytosis of cell-surface receptors has been reported for Wnt co-receptors, including LRP6, Fz4 and Fz2 (Yamamoto et al., 2006; Chen et al., 2003; Blitzer and Nusse, 2006; Sato et al., 2010), adding a higher level of complexity to the regulation of Wnt signaling.

4.1 PTK7 endocytosis and co-receptor context

Here we show that the Wnt co-receptor PTK7 is endocytosed in the presence of canonical, but not non-canonical Wnt ligands. PTK7 is endocytosed via a caveolin-mediated pathway and likely degraded in the lysosome in response to canonical Wnt proteins. However, the receptor context and the outcome of PTK7 internalization and degradation on Wnt signaling remain to be clarified. As the cellular context and receptor complexes that form in the cells are crucial to direct Wnt signaling to specific branches, it is important to analyze PTK7 signaling by studying PTK7 complex formation with further proteins regulating Wnt signaling. PTK7 has been reported to interact with different Wnt co-receptors, including Fz7 (Peradziryi et al., 2011; Linnemannstöns et al., 2014), LRP6 (Bin-Nun et al., 2014) and Ror2 (unpublished data), these interactions might direct signaling to different branches. Further experiments are necessary to determine the role of the receptor context. PTK7 interacts with Fz7 and Fz7 mediates PTK7 interaction with canonical Wnt proteins (Peradziryi et al., 2011; Linnemannstöns et al., 2014). Thus, it is very likely that Fz7 is a part of the Wnt/PTK7 complex. Fz7 loss-of-function should abolish

the formation of the Wnt/PTK7 complex. Hence, Fz7 loss-of-function and Wnt-mediated Fz7-PTK7 colocalization analyses are necessary to proof this hypothesis.

A recent study showed that PTK7 interacts with the canonical Wnt receptor LRP6, resulting in positive regulation of canonical Wnt signaling (Bin-Nun et al., 2014). These findings indicate that the receptor context might affect PTK7 function. Interestingly, LRP6 itself was found to be endocytosed via a caveolin-mediated pathway upon Wnt3a treatment (Yamamoto et al., 2006), similar to the results obtained in this study for the PTK7 receptor. Thus, it is tempting to suggest that PTK7 might be endocytosed together with LRP6 via a caveolin-dependent pathway upon Wnt3a stimulation. Further experiments are necessary for instance LRP6 loss-of-function studies to analyze PTK7/LRP6 complex formation and endocytosis. It further remains elusive if Wnt-mediated PTK7 endocytosis is important for PTK7 function in promoting non-canonical PCP signaling. As PTK7 interacts with the non-canonical Wnt receptor Ror2 (unpublished data), it is interesting to study if Ror2 might be a part of the Wnt/PTK7 complex to promote non-canonical Wnt signaling or if PTK7 and Ror2 function is independent of Wnt-mediated PTK7 internalization. Hence, further experiments are necessary to determine the receptor context and to study if PTK7 interacts with different Wnt co-receptors to direct Wnt signaling into different branches.

4.2 PTK7 is endocytosed via a caveolin-mediated pathway in response to canonical Wnt proteins

Caveolin-mediated endocytosis is a general mechanism to activate or inhibit downstream signaling (Le Roy and Wrana, 2005; Yamamoto et al., 2006). In this study PTK7 was identified to co-localize with caveolin-1 in fluorescently labeled cells and in co-immunoprecipitation analysis. Further PTK7 is internalized in response to canonical Wnt ligands via a caveolin-mediated pathway. The chemical inhibition of caveolin-mediated endocytosis by methyl- β -cyclodextrin (M β CD) treatment results in significantly reduced PTK7 internalization. Although the kinase homology domain of PTK7 was reported to have important functions in Dsh membrane recruitment and thus activation of PCP signaling, it seems not to be relevant for PTK7 internalization, because a PTK7 mutant protein lacking this domain (Δ kPTK7) is as well interacting with caveolin-1 and endocytosed in response to canonical Wnt proteins. Moreover, these findings indicate that the binding between caveolin-1 and PTK7 does not rely on the kinase homology domain, thus the transmembrane domain or the cytoplasmic region directly beneath the transmembrane domain must be important for caveolin-1 and PTK7 interaction.

Protein-protein interaction of caveolin-1 and PTK7 has been studied by ectopic protein expression in fluorescently labeled cells as well as in co-immunoprecipitation assays. However, ectopic protein levels do not necessarily reflect endogenous processes in the cells. Therefore, PTK7 and caveolin-1 interaction was as well studied on the endogenous level. For TIRF microscopy endogenous proteins were stained using the respective antibodies and similar results as for ectopic PTK7 expression were observed. Co-immunoprecipitation assays were additionally performed using wild type cells. Thereby endogenous PTK7 was precipitated using anti-PTK7 antibodies and endogenous caveolin-1 α was co-precipitated (data not shown). Thus, the PTK7-caveolin interaction and the caveolin-mediated removal of PTK7 from the plasma membrane seem to be endogenously relevant.

4.3 Mutual inhibition of PTK7 and canonical Wnt proteins

PTK7 interacts with a pool of different canonical Wnt proteins, including Wnt3a, Wnt8 (Peradziryi et al., 2011) and Wnt2b (data not shown). In this study it has been shown that the canonical Wnt ligand Wnt2b is internalized together with PTK7 into the cytoplasm. Thus, PTK7 seems to remove canonical Wnt ligands from the extracellular matrix and the plasma membrane by entering the caveolin-mediated endocytic route. As a consequence the ternary complex of Wnt, LRP6 and Frizzled cannot form to activate canonical Wnt signaling, because canonical Wnts are captured in a PTK7-complex in the cytoplasm. Thus, PTK7 likely inhibits canonical Wnt signaling through receptor competition with other Wnt co-receptors, such as LRP6, for Wnt binding. In fact not only the binding of Wnt ligands to PTK7 but the internalization of this Wnt/PTK7 ligand/receptor complex seems to be important for effective inhibition of canonical Wnt signaling. As it was shown in *Xenopus* double axis assays, PTK7 inhibits canonical Wnt signaling, but in the absence of caveolin-1 α the inhibitory effect of PTK7 decreased. Thus, it seems that binding of Wnt ligands to PTK7 already inhibits canonical Wnt signaling to a certain degree, but this inhibitory effect is even increased after endocytosis of the ligand-receptor complex into the cytoplasm, thereby removing the Wnt ligand from the extracellular matrix and the plasma membrane.

Moreover, canonical Wnt proteins were found to inhibit non-canonical PCP/Wnt signaling through competing with non-canonical Wnt ligands for Fz receptor binding (Grumolato et al., 2010). As Fz is involved in both, canonical and non-canonical Wnt signaling pathways, the binding of a Wnt ligand triggers the coupling of Fz with either canonical co-receptors, like LRP6, or non-canonical co-receptors, like Ror2, to activate the respective Wnt signaling pathway. It has been shown in mammalian cells that canonical and non-

canonical Wnts perform reciprocal pathway inhibition at the cell surface by ligand competition for Fz binding. Wnt5a antagonizes Wnt3a interaction with Fz in *in vitro* binding assays and inhibited the Wnt3a-induced activation of canonical Wnt signaling. Vice versa Wnt3a inhibited the ability of Wnt5a to activate non-canonical Wnt/PCP signaling (Grumolato et al., 2010). According to this, by binding of canonical Wnt proteins and removing them from the plasma membrane, PTK7 can fulfill both of its functions on Wnt signaling. First the removal of canonical Wnt proteins results in inhibition of canonical Wnt signaling and second inhibition of PCP/Wnt signaling by canonical Wnt proteins is prevented.

Interestingly, it has been shown here, that the PTK7 protein is degraded in the lysosome upon Wnt3a treatment. Treatment with increasing concentrations of Wnt3a results in a dose-dependent decrease in endogenous PTK7 protein levels. The Wnt-mediated PTK7 decrease is prevented by chloroquine, an inhibitor of lysosomal degradation. These data suggest a mutual inhibition between canonical Wnt signaling and PTK7 signaling.

According to these findings, we propose a mechanism of PTK7-related inhibition of canonical Wnt signaling by receptor competition and a reciprocal inhibition of PTK7 by canonical Wnt ligands. In this model PTK7 suppresses canonical Wnt signaling by binding canonical Wnt ligands and thereby preventing their interaction with Wnt co-receptors like LRP6. Conversely, canonical Wnt proteins induce PTK7 lysosomal degradation (Figure 47).

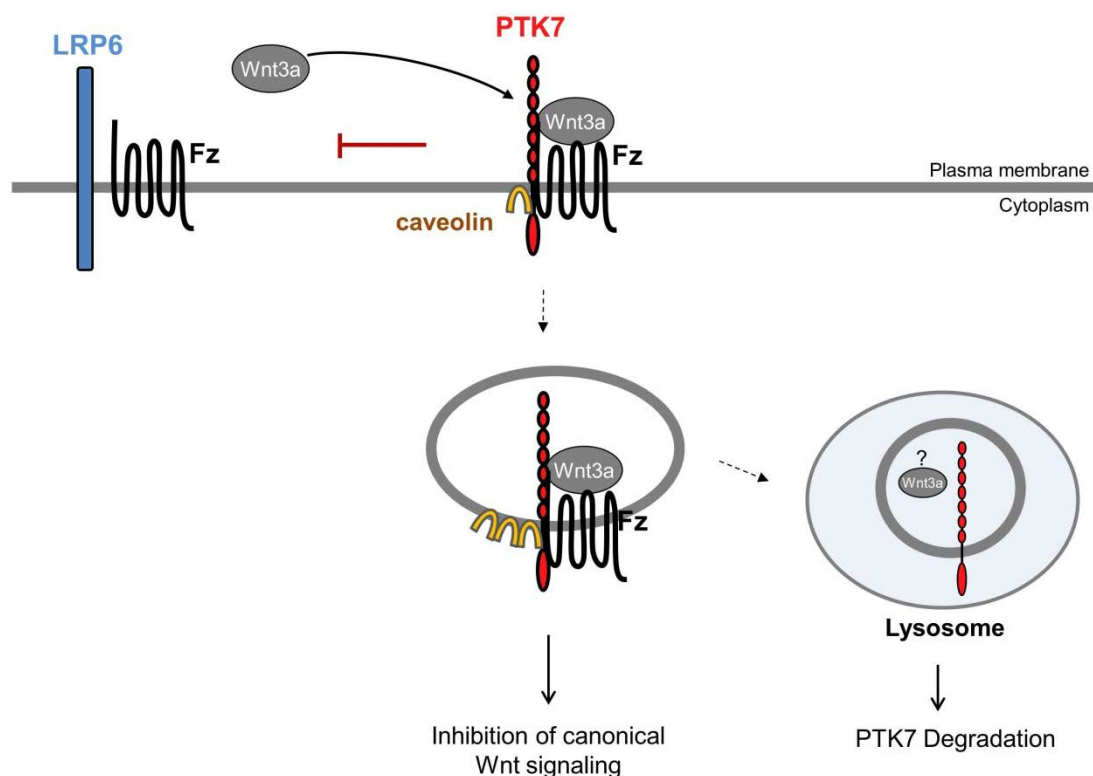


Figure 47: Molecular mechanism of PTK7 function.

PTK7 competes with other Wnt co-receptors, like LRP6 for Wnt binding, thus preventing activation of canonical Wnt signaling through Wnt/LRP6/Fz complex formation. PTK7 binds canonical Wnt ligands via its extracellular domain and this binding is mediated by Fz7. After interaction with Wnt, the Wnt/PTK7 complex is internalized via a caveolin-mediated endocytosis pathway, thereby removing Wnt proteins from the membrane and the extracellular matrix. Conversely, canonical Wnt proteins target PTK7 to lysosomal degradation. If Wnt proteins are as well degraded is not clear (indicated by ?).

Live cell imaging of MCF7 and neural crest cells expressing PTK7 indicated that PTK7 positive vesicles are not only internalized but also recycled back to the membrane (neural crest cell data not shown), suggesting that at least a fraction of PTK7 might be recycled and reused in response to canonical Wnt ligands. It is possible that canonical Wnt proteins increase the turnover rates of PTK7, leading to permanent cycles of ligand/receptor internalization and receptor recycling. These cycles would ensure a high efficiency of PTK7 to remove Wnt ligands from the cell surface. Further experiments are necessary to prove this hypothesis.

4.4 PTK7 modulates Wnt signaling

Contradictory data on how PTK7 functions in Wnt signaling had been described. On the one hand PTK7 was shown to activate PCP signaling as loss-of-function of PTK7 in vertebrates leads to phenotypes typical for a protein that activates PCP, including neural tube defects in mice, *Xenopus* and zebrafish, misoriented sensory hair cells of the inner

ear in the mouse and inhibition of neural crest cell migration in *Xenopus* (Lu et al., 2004; Paudyal et al., 2010; Hayes et al., 2013; Shnitsar and Borchers 2008). Further evidence of PTK7 function in activating PCP signaling was provided by the findings that its overexpression in *Xenopus* leads to nuclear localization of JNK (Shnitsar and Borchers, 2008) and transcriptional activation of ATF2 in luciferase reporter assays (Peradziryi et al., 2011). Furthermore, ectopic activation of PTK7 inhibits canonical Wnt signaling in double axis and luciferase reporter assays in *Xenopus*, *Drosophila* and mammalian cells. *Vice versa* loss of PTK7 increased Wnt/ β -catenin target gene expression (Peradziryi et al., 2011; Hayes et al., 2013).

On the other hand in further studies PTK7 was reported to activate canonical Wnt signaling. PTK7 was shown to interact with β -catenin, thereby activating the transcription of β -catenin-dependent genes in mammalian cells and *Xenopus* embryos. Additionally, PTK7 was shown to be required for Spemann's organizer formation and *Siamois* promoter activation (Lhoumeau et al., 2011; Puppo et al., 2011). However, these findings could not be confirmed in zebrafish or *Xenopus* embryos in later studies, where mRNA levels of organizer inducing genes were upregulated in PTK7 knockout embryos, indicating an inhibitory effect of PTK7 on organizer formation (Hayes et al., 2013; Bin-Nun et al., 2014). A further study indicated that PTK7 interacts with LRP6 to modulate LRP6 protein levels and thus positively regulates canonical Wnt signaling (Bin-Nun et al., 2014). In this study mainly PTK7 loss-of-function phenotypes by the use of morpholino oligonucleotides in *Xenopus* embryos have been analyzed. Unfortunately, no control morpholino has been used to exclude morpholino toxicity. Further, expression of the neural crest marker Snail2 was found to be inhibited in PTK7 loss-of-function embryos, indicating that PTK7 blocks neural crest cell induction, which depends on canonical Wnt signaling (Bin-Nun et al., 2014). In contrast, our group observed correctly induced neural crest cells, but impaired migration in PTK7 morphant embryos (Shnitsar and Borchers, 2008), which in turn rely on non-canonical PCP/Wnt signaling.

How can these differences in regulation of Wnt signaling by PTK7 be explained? PTK7 might have cell-type specific functions, thus, possibly behave differently in distinct systems. Wnt signaling pathways need to be tightly regulated to ensure correct signal transduction. Little changes in the cellular context might lead to aberrant downstream signaling. Thus, downstream Wnt signaling regulation depends on the cellular context and the availability of specific Wnt modulators, like Wnt receptors, co-receptors, Wnt ligands or Wnt antagonists in the cell and subsequently on the ligand/receptor complexes that are formed.

Regarding PTK7 and LRP6, the presence of both receptors in a particular cell might lead to Wnt/LRP6/PTK7 complex formation and possibly influence Wnt signaling in a different

way than in the absence of one of these receptors. During embryonic development PTK7 and LRP6 have overlapping but also distinct expression pattern. PTK7 is expressed in the neuroectoderm and in migrating cranial neural crest cells during gastrula and neurula stages (Lu et al., 2004; Shnitsar and Borchers, 2008). LRP6 is as well expressed in the neural plate and dorsal tissues but not in migrating neural crest cells (Houston and Wylie, 2002). Thus, PTK7 might function independently of LRP6 in neural crest cells.

4.5 Signaling function of PTK7

PTK7 is a Wnt co-receptor with functions in the regulation of both, canonical and non-canonical PCP/Wnt signaling (Peradziryi et al., 2012). In *Xenopus* PTK7 was indicated to activate PCP/Wnt signaling by recruiting Dsh to the plasma membrane, which is a prerequisite for the activation of vertebrate PCP (Shnitsar and Borchers, 2008; Wehner et al., 2011). Interestingly, PTK7 binds exclusively canonical Wnt ligands through its extracellular domain, but rather inhibits canonical Wnt signaling demonstrated by luciferase reporter and *Xenopus* double axis assays (Peradziryi et al., 2011; Hayes et al., 2013). Although the molecular mechanism how PTK7 functions in the activation of PCP signaling still needs to be clarified, analyzes in *Xenopus* indicated an important role of its kinase homology domain in Dsh membrane-recruitment, thereby promoting PCP signaling.

Further studies indicate that PTK7 regulates PCP signaling through interaction with a Src kinase (Andreeva et al., 2014). As the kinase homology domain of PTK7 is catalytically inactive, it has been suggested that PTK7 might interact with active kinases to promote signal transduction as it has been reported for other inactive receptor tyrosine kinases including the Ryk/Derailed receptor. In *Drosophila* Derailed interacts with the Src kinase SRC64B, leading to Derailed phosphorylation and promotion of Derailed function in axon guidance in the central nervous system (Wouda et al., 2008). Indeed a recent study indicates a similar mechanism for PTK7 as it was shown to regulate PCP through interaction with the non-receptor tyrosine kinase Src in MDCK cells and the auditory sensory epithelium of the mouse (Andreeva et al., 2014). PTK7 interact with Src via its kinase homology domain, which in turn is phosphorylated by Src. PCP signals through the small GTPase RhoA and its downstream effector ROCK to regulate changes in the actin cytoskeleton. PTK7-Src signaling was identified to regulate PCP through phosphorylation of ROCK2. However, how ROCK2 phosphorylation regulates changes in the actin cytoskeleton remains to be determined (Andreeva et al., 2014). Whether the interaction of PTK7 with Src kinases might also influence PTK7 function in inhibiting canonical Wnt signaling remains elusive. However, our proposed mechanism by which PTK7 inhibits

canonical Wnt signaling through binding canonical Wnt proteins is independent of the kinase homology domain of PTK7. As it has been shown that this domain is necessary for Src-binding (Andreeva et al., 2014), it is likely that PTK7-Src interaction is not important for PTK7 function in inhibiting canonical Wnt signaling.

Interestingly, in a further study it has been shown that cleavage of PTK7 by the protease MT1-MMP is required for its function on PCP signaling. PTK7 is cleaved by MT1-MMP in the seventh immunoglobulin domain, resulting in the generation of a secreted extracellular PTK7 fragment. In zebrafish inhibition of MT1-MMP-mediated cleavage led to convergent extension defects similar to those observed in PTK7 depleted embryos (Coyle et al., 2008; Golubkov et al., 2010). Additionally, classical PCP phenotypes have been identified in the mouse *chuhzoi* (*chz*) mutant, that carries a splice site mutation in the *ptk7* gene (Paudyal et al., 2010). This mutation leads to the insertion of an additional MT1-MMP cleavage site between the fifth and sixth extracellular immunoglobulin domain of PTK7, resulting in aberrant PTK7 proteolysis (Paudyal et al., 2010; Golubkov et al., 2011). Thus, inhibited and aberrant MT1-MMP-mediated PTK7 proteolysis impairs PCP-regulated processes in zebrafish and mice, indicating that correct PTK7 proteolysis seems to be crucial for PTK7 function in PCP signaling. In contrast, to PTK7 function in promoting PCP, it is not clear if MT1-MMP-mediated PTK7 proteolysis might have an effect on PTK7 function in inhibiting canonical Wnt signaling. In this study it has been shown that the binding of canonical Wnt proteins to PTK7 does not induce PTK7 proteolysis as no differences in the quantity of PTK7 proteolytic fragments were detected after Wnt-treatment. Further studies are necessary to unravel if PTK7 proteolysis might be important for PTK7 function in inhibiting canonical Wnt signaling.

4.6 PTK7 regulates diverse signaling pathways

Interestingly, PTK7 functions are not restricted to Wnt signaling, as PTK7 was additionally shown to play an important role in VEGF and Semaphorin signaling. PTK7 was identified to be expressed in vascular endothelial cells and to interact with Flt-1 (VEGFR1, vascular endothelial growth factor receptor type 1), a receptor which regulates angiogenesis (Shin et al., 2008; Lee et al., 2011). In the VEGF context, it has been shown that PTK7 is required for angiogenesis and VEGF-induced migration, invasion, and tube-formation of human umbilical vein endothelial cells (HUVEC) (Shin et al., 2008). Furthermore, PTK7 was implicated to form complexes with the Semaphorin transmembrane receptor Plexin. Plexins regulate axon guidance, cell shape, cell–cell interactions and cell motility (Winberg et al., 1998; Takahashi et al., 1999; Tamagnone et al., 1999). Interestingly, interaction of PTK7 with Plexins had been reported in different organisms, including *Drosophila*, chick

and *Xenopus*. In *Drosophila* Otk/Plexin A1 interaction mediates repulsive axon guidance in response to Sema1A (Winberg et al., 2001). In chick PTK7/KLG interacts with PlexinA1 in the heart ventricle segment to affect cell migration in response to Sema6D (Toyofuku et al., 2004). PTK7/PlexinA1 complex formation in *Xenopus* is involved in the regulation of cranial neural crest cells migration (Wagner et al., 2010). Although it has been shown in different organism that PTK7 interacts with Plexin and regulates Semaphorin signaling, the signaling mechanism remains elusive. We showed here that PTK7 is internalized in response to canonical Wnt proteins resulting most likely in inhibition of canonical Wnt signaling. It would be interesting to study if PTK7 endocytosis is restricted to its function in Wnt signaling or if PTK7-related regulation of VEGF and Semaphorin signaling also depends on its internalization, possibly mediated by VEGF or Semaphorin ligands. Thus, PTK7 seems to be broad regulator of different signaling pathways to regulate several dynamic processes.

4.7 Function of caveolin-1 during *Xenopus* development

4.7.1 Caveolin-1 depletion leads to impaired swimming behavior in *Xenopus*

The highly conserved caveolin protein family includes three members in vertebrates, caveolin-1 (with its two isoforms caveolin-1 α and -1 β), caveolin-2 and caveolin-3 (Rothberg et al., 1992; Way and Parton, 1995; Scherer et al., 1996; Tang et al., 1996; Williams and Lisanti, 2004; Parton and del Pozo, 2013). Mutations of *caveolin* genes in humans were found in various diseases like for example lipodystrophy, cardiac diseases, muscular dystrophies and cancer (Parton and del Pozo, 2013; Woodman et al., 2004).

Interestingly, caveolin-deficient mice exhibit phenotypes similar to the human counterparts. Mice depleted in caveolin-1 have lipid disorders, cardiac diseases and higher tumorigenicity when exposed to carcinogens. Caveolin-3 deficient mice comprise muscular defects with symptoms similar to limb-girdle muscular dystrophy in humans (Le Lay and Kurzchalia, 2005). Indeed in humans this syndrome is as well caused by a mutation in the *caveolin-3* gene (Hagiwara et al., 2000). These findings indicate a conserved function of the caveolin proteins. Interestingly, all caveolin deficient mice are viable and fertile (Le Lay and Kurzchalia, 2005), thus at least in mammals compensatory pathways might exist that balance the loss of caveolin. In contrast to the mouse, caveolin-1 depletion in zebrafish leads to lethality after approximately 5 days post fertilization and further results in morphological defects including eye and heart developmental defects and defects in muscular and neural tissues (Fang et al., 2006; Nixon et al., 2007).

In *Xenopus* caveolin loss-of-function studies have not been performed yet, thus in this study the function of caveolin-1 in early *Xenopus* development was analyzed. Knockdown of caveolin-1 α by Cav-1 α MO injection results in viable animals and led rather to mild morphological phenotypes, including eye developmental defects and kinked tails in up to 40% of the embryos. However, the predominant phenotype observed in caveolin-1 deficient embryos was a severely impaired swimming behavior. *In vitro* transcription/translation experiments evidenced the loss of caveolin-1 α expression in the presence of Cav-1 α MO; further the swimming defect phenotype was rescued by co-injection of caveolin-1 α mRNA, demonstrating the efficiency and specificity of the used Cav-1 α MO. As some of the embryos exhibited kinked tails, it is tempting to speculate that this morphological defect might be the result for the swimming defect. However, aberrant swimming behavior was as well observed in embryos with a normal morphological appearance. Thus, it seems not to be an outcome of the kinked-tail phenotype.

4.7.2 The loss of caveolin-1 leads to disrupted actin filaments in the somites

Interestingly, phalloidin-staining of the actin cytoskeleton in muscle cells of the somites revealed disrupted actin filaments in caveolin-1 deficient *Xenopus* embryos. Hence, rather these disrupted actin filaments appear to account for the swimming defect instead of the kinked-tail phenotype. These findings indicate that defective muscle development upon caveolin-1 depletion results in abnormal swimming behavior in *Xenopus*. Disrupted actin cytoskeleton of the somites was also observed in caveolin-1 depleted zebrafish embryos (Fang et al., 2006), this further proves a function of caveolin-1 in muscle development. However, no caveolin-1 expression was detected in the somites, but strong expression in the notochord. Similarly, in the notochord of chick, mouse and zebrafish embryos a strong caveolin-1 expression and extremely high abundance of caveolae was detected (Nixon et al., 2007), indicating a role of caveolin-1 in notochord function. The notochord in fact is a source of various signals important amongst others for somite patterning (Nixon et al., 2007). Additionally, caveolae were also found to serve as cellular signaling platforms, in which caveolin-1 was identified to bind many signaling proteins, thereby influences the activity of downstream signaling (Williams and Lisanti, 2004). Hence, caveolin-1, as strongly expressed in the notochord, might regulate developmental signaling pathways important for somite patterning, which might lead to the disruption of actin cytoskeletal arrangement if caveolin-1 is depleted.

Similar swimming defects as found in caveolin-1 knockdown embryos in this study were reported for *Xenopus* embryos treated with insecticides or pesticides as carbaryl

(Bacchetta et al., 2008) and chlorpyrifos (Colombo et al., 2005). Embryos treated with these chemicals exhibited impaired motility, tremors, spasms and paralysis due to disorganized muscle cells. Further development of an abnormal wavy or bent notochord was reported. These chemicals are known to inhibit the enzyme Acetylcholinesterase (AChE), which is important for the hydrolysis of the neurotransmitter acetylcholine in the synaptic cleft. Inhibition of AChE causes the accumulation of acetylcholine in the synapses and neuromuscular junctions and as a consequence leads to overstimulation of cholinergic receptors leading to symptoms like hyperexcitability, tremor and paralysis. Thus, the function of AChE is crucial for the development of neuromuscular junctions and the maintenance of muscle cell integrity (Colombo et al., 2005; Bacchetta et al., 2008). Furthermore, low AChE levels lead to skeletal muscle necrosis in rats, suggesting that Ach overstimulation leads to muscle degeneration (Bleecker et al., 1994).

4.7.3 Caveolin-1 loss-of-function might lead to neuronal disorders

In this study it was shown that muscle differentiation seems not to be influenced by caveolin-1 depletion as *MyoD* expression was unchanged between control and caveolin-1 depleted embryos. Therefore impaired innervation of motoneurons or defects in neuromuscular junction formation might be the reason for the disrupted actin cytoskeleton in muscle fibers upon caveolin-1 depletion. Indeed analysis of motoneurons and acetylcholine receptor clustering in caveolin-1 depleted *Xenopus* embryos revealed impaired axonal pathfinding of motoneurons and aberrant distribution acetylcholine receptors (Marlen Breuer, Master thesis). This leads to the hypothesis that caveolin might have a function in muscular innervation of motoneurons and impairment of this process might result in muscle development defects or muscle damage possibly through acetylcholine transmission. Further studies are necessary to clarify the influence of caveolin-1 in neuromuscular junction development, acetylcholine transmission and innervation of the muscles by motoneurons and most importantly to identify the underlying molecular mechanism leading to the observed phenotypes in caveolin-1 deficient *Xenopus* embryos.

Furthermore, expression of *Pax2*, a neural marker, was unchanged in the midbrain-hindbrain boundary, but reduced in the otic vesicle, the epibranchial placodes and the pronephric kidney of caveolin-1 knockdown embryos. The three epibranchial placodes give rise to neurons that innervate internal organs such as the heart, to transmit information about for example heart rate and blood pressure to the central nervous system (Baker and Bronner-Fraser, 2001). These findings indicate a role of caveolin-1 in affecting neural tissues as it was also shown in zebrafish. Interestingly, in humans and in

the mouse caveolin depletion leads to cardiac defects, like cardiomyopathy. Although depletion of caveolin-1 or caveolin-3 in the mouse results in the development of different phenotypes, heart defects were observed in loss-of-function studies of every *caveolin* gene (Le Lay and Kurzchalia, 2005). Further, caveolin-1/caveolin-3 double mutation in the mouse leads to even more severe cardiomyopathy (Park et al., 2002), indicating a high importance of caveolin in the heart. As the epibranchial placodes give rise to neurons that innervate the heart (Baker and Bronner-Fraser, 2001) and caveolin-depletion results in reduced or even loss of *Pax2* expression in the epibranchial placodes, possibly caveolin-1 depletion leads to heart defects due to impaired neuronal innervation. In this study heart defects were not analyzed in detail, but caveolin-1 depleted embryos often displayed ventral heart edema that got worse during development (data not shown), which is a typical phenotype of compromised heart function (Bartlett and Weeks, 2008). Thus, in further studies heart development in caveolin-1 deficient *Xenopus* embryos should be analyzed in more detail.

5 Conclusion

Previous findings from our lab revealed that PTK7 binds canonical Wnt proteins and inhibits canonical Wnt signaling (Peradziryi et al., 2011). However, it remains unclear how canonical Wnt ligands affect PTK7 function. Thus, the aim of this study was to analyze the effect of canonical Wnt ligands on the localization and stability of the PTK7 protein and consequently on its function regarding Wnt signaling. This study demonstrates that the localization of the Wnt co-receptor PTK7 is affected by canonical Wnt ligands. In the presence of canonical Wnt ligands, PTK7 changes its cellular localization from the plasma membrane to the cytoplasm in fluorescently labeled cells and cell surface biotinylation assays. Moreover, PTK7 is translocated together with bound canonical Wnt ligands as a ligand/receptor complex. The kinase homology domain of PTK7 is not involved in this process as a mutant form of PTK7 lacking its kinase homology domain, Δ kPTK7, changes its cellular localization after canonical Wnt stimulation similar to the full length PTK7 protein. Immunofluorescence and co-immunoprecipitation experiments revealed that PTK7 co-localizes and interacts with caveolin-1 and is endocytosed via a caveolin-mediated pathway in response to canonical Wnt stimulation. Chemical inhibition of caveolin-dependent endocytosis prevents Wnt-induced PTK7 internalization. In contrast clathrin-mediated endocytosis is not involved in the PTK7 translocation process.

It was further shown that canonical Wnt ligands induce a decrease in PTK7 protein concentration. Inhibition of lysosomal degradation prevents the Wnt3a-mediated reduction of PTK7 protein. Thus, canonical Wnt ligands trigger PTK7 degradation in the lysosome.

Additionally, this study demonstrates a function of caveolin-1 in early *Xenopus* development. It was shown that caveolin-1 loss-of-function leads to severe swimming defects in *Xenopus* embryos. These defects were rescued by co-injection of mRNA coding for caveolin-1. Analyzing the actin cytoskeleton of the somites in caveolin-1 morphant embryos revealed disrupted actin filaments of the muscle cells.

As MyoD staining was unchanged between control and caveolin-1 depleted embryos, muscle differentiation seems not to be affected.

6 References

- Aberle, H., Bauer, A., Stappert, J., Kispert, A., and Kemler, R. (1997). beta-catenin is a target for the ubiquitin-proteasome pathway. *The EMBO journal* *16*, 3797-3804.
- Acebron, S.P., Karaulanov, E., Berger, B.S., Huang, Y.-L., and Niehrs, C. (2014). Mitotic wnt signaling promotes protein stabilization and regulates cell size. *Mol Cell* *54*, 663-674.
- Adler, J., and Parmryd, I. (2010). Quantifying colocalization by correlation: The Pearson correlation coefficient is superior to the Mander's overlap coefficient. *Cytometry* *77A*, 733-742.
- Amit, S., Hatzubai, A., Birman, Y., Andersen, J.S., Ben-Shushan, E., Mann, M., Ben-Neriah, Y., and Alkalay, I. (2002). Axin-mediated CKI phosphorylation of beta-catenin at Ser 45: a molecular switch for the Wnt pathway. *Genes & Development* *16*, 1066-1076.
- Andreeva, A., Lee, J., Lohia, M., Wu, X., Macara, I.G., and Lu, X. (2014). PTK7-*Src* signaling at epithelial cell contacts mediates spatial organization of actomyosin and planar cell polarity. *Developmental cell* *29*, 20-33.
- Antic, D., Stubbs, J.L., Suyama, K., Kintner, C., Scott, M.P., and Axelrod, J.D. (2010). Planar cell polarity enables posterior localization of nodal cilia and left-right axis determination during mouse and *Xenopus* embryogenesis. *PLoS one* *5*, e8999.
- Axelrod, J.D., Miller, J.R., Shulman, J.M., Moon, R.T., and Perrimon, N. (1998). Differential recruitment of Dishevelled provides signaling specificity in the planar cell polarity and *Wingless* signaling pathways. *Genes & Development* *12*, 2610-2622.
- Bacchetta, R., Mantecca, P., Andrioletti, M., Vismara, C., and Vailati, G. (2008). Axial-skeletal defects caused by Carbaryl in *Xenopus laevis* embryos. *The Science of the total environment* *392*, 110-118.
- Baker, C.V., and Bronner-Fraser, M. (2001). Vertebrate cranial placodes I. Embryonic induction. *Developmental biology* *232*, 1-61.
- Banziger, C., Soldini, D., Schutt, C., Zipperlen, P., Hausmann, G., and Basler, K. (2006). *Wntless*, a conserved membrane protein dedicated to the secretion of Wnt proteins from signaling cells. *Cell* *125*, 509-522.
- Barrott, J.J., Cash, G.M., Smith, A.P., Barrow, J.R., and Murtaugh, L.C. (2011). Deletion of mouse *Porcn* blocks Wnt ligand secretion and reveals an ectodermal etiology of human focal dermal hypoplasia/Goltz syndrome. *Proc Natl Acad Sci U S A* *108*, 12752-12757.
- Bartlett, H.L., and Weeks, D.L. (2008). Lessons from the lily pad: Using *Xenopus* to understand heart disease. *Drug discovery today. Disease models* *5*, 141-146.
- Bartscherer, K., Pelte, N., Ingelfinger, D., and Boutros, M. (2006). Secretion of Wnt ligands requires Evi, a conserved transmembrane protein. *Cell* *125*, 523-533.
- Bastidas, F., Calisto, J. de, and Mayor, R. (2004). Identification of neural crest competence territory: role of Wnt signaling. *Developmental dynamics : an official publication of the American Association of Anatomists* *229*, 109-117.

- Bastock, R., Strutt, H., and Strutt, D. (2003). Strabismus is asymmetrically localised and binds to Prickle and Dishevelled during *Drosophila planar* polarity patterning. *Development (Cambridge, England)* *130*, 3007-3014.
- Bayly, R., and Axelrod, J.D. (2011). Pointing in the right direction: new developments in the field of planar cell polarity. *Nat. Rev. Genet.* *12*, 385-391.
- Behrens, J., Kries, J.P. von, Kuhl, M., Bruhn, L., Wedlich, D., Grosschedl, R., and Birchmeier, W. (1996). Functional interaction of beta-catenin with the transcription factor LEF-1. *Nature* *382*, 638-642.
- Belenkaya, T.Y., Wu, Y., Tang, X., Zhou, B., Cheng, L., Sharma, Y.V., Yan, D., Selva, E.M., and Lin, X. (2008). The retromer complex influences Wnt secretion by recycling wntless from endosomes to the trans-Golgi network. *Developmental cell* *14*, 120-131.
- Bhanot, P., Brink, M., Samos, C.H., Hsieh, J.C., Wang, Y., Macke, J.P., Andrew, D., Nathans, J., and Nusse, R. (1996). A new member of the frizzled family from *Drosophila* functions as a Wingless receptor. *Nature* *382*, 225-230.
- Biechele, S., Cox, B.J., and Rossant, J. (2011). Porcupine homolog is required for canonical Wnt signaling and gastrulation in mouse embryos. *Dev Biol* *355*, 275-285.
- Bilic, J., Huang, Y.-L., Davidson, G., Zimmermann, T., Cruciat, C.-M., Bienz, M., and Niehrs, C. (2007). Wnt induces LRP6 signalosomes and promotes dishevelled-dependent LRP6 phosphorylation. *Science (New York, N.Y.)* *316*, 1619-1622.
- Bin-Nun, N., Lichtig, H., Malyarova, A., Levy, M., Elias, S., and Frank, D. (2014). PTK7 modulates Wnt signaling activity via LRP6. *Development (Cambridge, England)* *141*, 410-421.
- Bleecker, J. de, Lison, D., van Den Abeele, K., Willems, J., and Reuck, J. de (1994). Acute and subacute organophosphate poisoning in the rat. *Neurotoxicology* *15*, 341-348.
- Blitzer, J.T., and Nusse, R. (2006). A critical role for endocytosis in Wnt signaling. *BMC cell biology* *7*, 28.
- Boutros, M., Paricio, N., Strutt, D.I., and Mlodzik, M. (1998). Dishevelled Activates JNK and Discriminates between JNK Pathways in Planar Polarity and wingless Signaling. *Cell* *94*, 109-118.
- Brannon, M., Gomperts, M., Sumoy, L., Moon, R.T., and Kimelman, D. (1997). A beta-catenin/XTcf-3 complex binds to the siamois promoter to regulate dorsal axis specification in *Xenopus*. *Genes & Development* *11*, 2359-2370.
- Bryja, V., Gradl, D., Schambony, A., Arenas, E., and Schulte, G. (2007). Beta-arrestin is a necessary component of Wnt/beta-catenin signaling in vitro and in vivo. *Proceedings of the National Academy of Sciences of the United States of America* *104*, 6690-6695.
- Caddy, J., Wilanowski, T., Darido, C., Dworkin, S., Ting, S.B., Zhao, Q., Rank, G., Auden, A., Srivastava, S., and Papenfuss, T.A., et al. (2010). Epidermal wound repair is regulated by the planar cell polarity signaling pathway. *Developmental cell* *19*, 138-147.
- Calisto, J. de, Araya, C., Marchant, L., Riaz, C.F., and Mayor, R. (2005). Essential role of non-canonical Wnt signalling in neural crest migration. *Development (Cambridge, England)* *132*, 2587-2597.

- Capelluto, D.G.S., Kutateladze, T.G., Habas, R., Finkielstein, C.V., He, X., and Overduin, M. (2002). The DIX domain targets dishevelled to actin stress fibres and vesicular membranes. *Nature* 419, 726-729.
- Capozza, F., Williams, T.M., Schubert, W., McClain, S., Bouzahzah, B., Sotgia, F., and Lisanti, M.P. (2003). Absence of caveolin-1 sensitizes mouse skin to carcinogen-induced epidermal hyperplasia and tumor formation. *The American journal of pathology* 162, 2029-2039.
- Carmona-Fontaine, C., Matthews, H., and Mayor, R. (2008). Directional cell migration in vivo: Wnt at the crest. *Cell adhesion & migration* 2, 240-242.
- Cavallo, R.A., Cox, R.T., Moline, M.M., Roose, J., Polevoy, G.A., Clevers, H., Peifer, M., and Bejsovec, A. (1998). Drosophila Tcf and Groucho interact to repress Wingless signalling activity. *Nature* 395, 604-608.
- Cha, S.-W., Tadjuidje, E., Tao, Q., Wylie, C., and Heasman, J. (2008). Wnt5a and Wnt11 interact in a maternal Dkk1-regulated fashion to activate both canonical and non-canonical signaling in *Xenopus* axis formation. *Development (Cambridge, England)* 135, 3719-3729.
- Chae, J., Kim, M.J., Goo, J.H., Collier, S., Gubb, D., Charlton, J., Adler, P.N., and Park, W.J. (1999). The Drosophila tissue polarity gene starry night encodes a member of the protocadherin family. *Development* 126, 5421-5429.
- Chen, W., Berge, D. ten, Brown, J., Ahn, S., Hu, L.A., Miller, W.E., Caron, M.G., Barak, L.S., Nusse, R., and Lefkowitz, R.J. (2003). Dishevelled 2 recruits beta-arrestin 2 to mediate Wnt5A-stimulated endocytosis of Frizzled 4. *Science (New York, N.Y.)* 301, 1391-1394.
- Chen, W., Hu, L.A., Semenov, M.V., Yanagawa, S., Kikuchi, A., Lefkowitz, R.J., and Miller, W.E. (2001). beta-Arrestin1 modulates lymphoid enhancer factor transcriptional activity through interaction with phosphorylated dishevelled proteins. *Proceedings of the National Academy of Sciences of the United States of America* 98, 14889-14894.
- Chou, Y.H., and Hayman, M.J. (1991). Characterization of a member of the immunoglobulin gene superfamily that possibly represents an additional class of growth factor receptor. *Proceedings of the National Academy of Sciences of the United States of America* 88, 4897-4901.
- Chung, H.M., and Malacinski, G.M. (1980). Establishment of the dorsal/ventral polarity of the amphibian embryo: use of ultraviolet irradiation and egg rotation as probes. *Developmental biology* 80, 120-133.
- Clevers, H., and Nusse, R. (2012). Wnt/beta-catenin signaling and disease. *Cell* 149, 1192-1205.
- Colombo, A., Orsi, F., and Bonfanti, P. (2005). Exposure to the organophosphorus pesticide chlorpyrifos inhibits acetylcholinesterase activity and affects muscular integrity in *Xenopus laevis* larvae. *Chemosphere* 61, 1665-1671.
- Coudreuse, D.Y.M., Roel, G., Betist, M.C., Destree, O., and Korswagen, H.C. (2006). Wnt gradient formation requires retromer function in Wnt-producing cells. *Science (New York, N.Y.)* 312, 921-924.

- Coyle, R.C., Latimer, A., and Jessen, J.R. (2008). Membrane-type 1 matrix metalloproteinase regulates cell migration during zebrafish gastrulation: evidence for an interaction with non-canonical Wnt signaling. *Experimental cell research* 314, 2150-2162.
- Cselenyi, C.S., Jernigan, K.K., Tahinci, E., Thorne, C.A., Lee, L.A., and Lee, E. (2008). LRP6 transduces a canonical Wnt signal independently of Axin degradation by inhibiting GSK3's phosphorylation of beta-catenin. *Proceedings of the National Academy of Sciences of the United States of America* 105, 8032-8037.
- Curtin, J.A., Quint, E., Tshipouri, V., Arkell, R.M., Cattanach, B., Copp, A.J., Henderson, D.J., Spurr, N., Stanier, P., and Fisher, E.M., et al. (2003). Mutation of *Celsr1* disrupts planar polarity of inner ear hair cells and causes severe neural tube defects in the mouse. *Current biology : CB* 13, 1129-1133.
- Dabdoub, A. (2003). Wnt signaling mediates reorientation of outer hair cell stereociliary bundles in the mammalian cochlea. *Development* 130, 2375-2384.
- Damianitsch, K., Melchert, J., and Pieler, T. (2009). XsFRP5 modulates endodermal organogenesis in *Xenopus laevis*. *Developmental biology* 329, 327-337.
- Dann, C.E., Hsieh, J.C., Rattner, A., Sharma, D., Nathans, J., and Leahy, D.J. (2001). Insights into Wnt binding and signalling from the structures of two Frizzled cysteine-rich domains. *Nature* 412, 86-90.
- Das, G., Jenny, A., Klein, T.J., Eaton, S., and Mlodzik, M. (2004). Diego interacts with Prickle and Strabismus/Van Gogh to localize planar cell polarity complexes. *Development* 131, 4467-4476.
- Davidson, G., Wu, W., Shen, J., Bilic, J., Fenger, U., Stannek, P., Glinka, A., and Niehrs, C. (2005). Casein kinase 1 gamma couples Wnt receptor activation to cytoplasmic signal transduction. *Nature* 438, 867-872.
- de Lau, Wim B M, Snel, B., and Clevers, H.C. (2012). The R-spondin protein family. *Genome biology* 13, 242.
- Dietzen, D.J., Hastings, W.R., and Lublin, D.M. (1995). Caveolin is palmitoylated on multiple cysteine residues. Palmitoylation is not necessary for localization of caveolin to caveolae. *The Journal of biological chemistry* 270, 6838-6842.
- Djiane, A., Riou, J., Umbhauer, M., Boucaut, J., and Shi, D. (2000). Role of frizzled 7 in the regulation of convergent extension movements during gastrulation in *Xenopus laevis*. *Development (Cambridge, England)* 127, 3091-3100.
- Drab, M., Verkade, P., Elger, M., Kasper, M., Lohn, M., Lauterbach, B., Menne, J., Lindschau, C., Mende, F., and Luft, F.C., et al. (2001). Loss of caveolae, vascular dysfunction, and pulmonary defects in caveolin-1 gene-disrupted mice. *Science (New York, N.Y.)* 293, 2449-2452.
- Du, S.J., Purcell, S.M., Christian, J.L., McGrew, L.L., and Moon, R.T. (1995). Identification of distinct classes and functional domains of Wnts through expression of wild-type and chimeric proteins in *Xenopus* embryos. *Molecular and cellular biology* 15, 2625-2634.
- Dubois, L., Lecourtois, M., Alexandre, C., Hirst, E., and Vincent, J.P. (2001). Regulated endocytic routing modulates wingless signaling in *Drosophila* embryos. *Cell* 105, 613-624.

- Easty, D.J., Mitchell, P.J., Patel, K., Florenes, V.A., Spritz, R.A., and Bennett, D.C. (1997). Loss of expression of receptor tyrosine kinase family genes PTK7 and SEK in metastatic melanoma. *International journal of cancer. Journal international du cancer* 71, 1061-1065.
- Fan, M.J., Gruning, W., Walz, G., and Sokol, S.Y. (1998). Wnt signaling and transcriptional control of Siamois in *Xenopus* embryos. *Proceedings of the National Academy of Sciences of the United States of America* 95, 5626-5631.
- Fang, P.-K., Solomon, K.R., Zhuang, L., Qi, M., McKee, M., Freeman, M.R., and Yelick, P.C. (2006). Caveolin-1alpha and -1beta perform nonredundant roles in early vertebrate development. *The American journal of pathology* 169, 2209-2222.
- Feiguin, F., Hannus, M., Mlodzik, M., and Eaton, S. (2001). The ankyrin repeat protein Diego mediates Frizzled-dependent planar polarization. *Dev Cell* 1, 93-101.
- Feng, Q., and Gao, N. (2015). Keeping wnt signalosome in check by vesicular traffic. *J Cell Physiol* 230, 1170-1180.
- Franch-Marro, X., Wendler, F., Guidato, S., Griffith, J., Baena-Lopez, A., Itasaki, N., Maurice, M.M., and Vincent, J.-P. (2008). Wingless secretion requires endosome-to-Golgi retrieval of Wntless/Evi/Sprinter by the retromer complex. *Nature cell biology* 10, 170-177.
- Fridolfsson, H.N., Roth, D.M., Insel, P.A., and Patel, H.H. (2014). Regulation of intracellular signaling and function by caveolin. *FASEB journal : official publication of the Federation of American Societies for Experimental Biology* 28, 3823-3831.
- Funayama, N., Fagotto, F., McCrea, P., and Gumbiner, B.M. (1995). Embryonic axis induction by the armadillo repeat domain of beta-catenin: evidence for intracellular signaling. *The Journal of cell biology* 128, 959-968.
- Galbiati, F., Engelman, J.A., Volonte, D., Zhang, X.L., Minetti, C., Li, M., Hou, H., JR, Kneitz, B., Edelmann, W., and Lisanti, M.P. (2001). Caveolin-3 null mice show a loss of caveolae, changes in the microdomain distribution of the dystrophin-glycoprotein complex, and t-tubule abnormalities. *The Journal of biological chemistry* 276, 21425-21433.
- Galbiati, F., Volonte, D., Brown, A.M., Weinstein, D.E., Ben-Ze'ev, A., Pestell, R.G., and Lisanti, M.P. (2000). Caveolin-1 expression inhibits Wnt/beta-catenin/Lef-1 signaling by recruiting beta-catenin to caveolae membrane domains. *The Journal of biological chemistry* 275, 23368-23377.
- Gerhart, J., Danilchik, M., Doniach, T., Roberts, S., Rowing, B., and Stewart, R. (1989). Cortical rotation of the *Xenopus* egg: consequences for the anteroposterior pattern of embryonic dorsal development. *Development (Cambridge, England)* 107 Suppl, 37-51.
- Glinka, A., Wu, W., Delius, H., Monaghan, A.P., Blumenstock, C., and Niehrs, C. (1998). Dickkopf-1 is a member of a new family of secreted proteins and functions in head induction. *Nature* 391, 357-362.
- Golubkov, V.S., Aleshin, A.E., and Strongin, A.Y. (2011). Potential relation of aberrant proteolysis of human protein tyrosine kinase 7 (PTK7) chuzhoi by membrane type 1 matrix metalloproteinase (MT1-MMP) to congenital defects. *The Journal of biological chemistry* 286, 20970-20976.
- Golubkov, V.S., Chekanov, A.V., Cieplak, P., Aleshin, A.E., Chernov, A.V., Zhu, W., Radichev, I.A., Zhang, D., Dong, P.D., and Strongin, A.Y. (2010). The Wnt/planar cell polarity protein-tyrosine kinase-7 (PTK7) is a highly efficient proteolytic target of

- membrane type-1 matrix metalloproteinase: implications in cancer and embryogenesis. *The Journal of biological chemistry* **285**, 35740-35749.
- Golubkov, V.S., and Strongin, A.Y. (2012). Insights into ectodomain shedding and processing of protein-tyrosine pseudokinase 7 (PTK7). *The Journal of biological chemistry* **287**, 42009-42018.
- Goodman, R.M., Thombre, S., Firtina, Z., Gray, D., Betts, D., Roebuck, J., Spana, E.P., and Selva, E.M. (2006). Sprinter: a novel transmembrane protein required for Wg secretion and signaling. *Development (Cambridge, England)* **133**, 4901-4911.
- Gray, R.S., Roszko, I., and Solnica-Krezel, L. (2011). Planar cell polarity: coordinating morphogenetic cell behaviors with embryonic polarity. *Dev. Cell* **21**, 120-133.
- Grumolato, L., Liu, G., Mong, P., Mudbhary, R., Biswas, R., Arroyave, R., Vijayakumar, S., Economides, A.N., and Aaronson, S.A. (2010). Canonical and noncanonical Wnts use a common mechanism to activate completely unrelated coreceptors. *Genes Dev* **24**, 2517-2530.
- Gubb, D., Green, C., Huen, D., Coulson, D., Johnson, G., Tree, D., Collier, S., and Roote, J. (1999). The balance between isoforms of the prickle LIM domain protein is critical for planar polarity in *Drosophila* imaginal discs. *Genes Dev* **13**, 2315-2327.
- Guo, N., Hawkins, C., and Nathans, J. (2004). Frizzled6 controls hair patterning in mice. *Proceedings of the National Academy of Sciences of the United States of America* **101**, 9277-9281.
- Habas, R., Kato, Y., and He, X. (2001). Wnt/Frizzled activation of Rho regulates vertebrate gastrulation and requires a novel Formin homology protein Daam1. *Cell* **107**, 843-854.
- Hagiwara, Y., Sasaoka, T., Araishi, K., Imamura, M., Yorifuji, H., Nonaka, I., Ozawa, E., and Kikuchi, T. (2000). Caveolin-3 deficiency causes muscle degeneration in mice. *Human molecular genetics* **9**, 3047-3054.
- Hamblet, N.S., Lijam, N., Ruiz-Lozano, P., Wang, J., Yang, Y., Luo, Z., Mei, L., Chien, K.R., Sussman, D.J., and Wynshaw-Boris, A. (2002). Dishevelled 2 is essential for cardiac outflow tract development, somite segmentation and neural tube closure. *Development (Cambridge, England)* **129**, 5827-5838.
- Harland, R., and Gerhart, J. (1997). Formation and function of Spemann's organizer. *Annual review of cell and developmental biology* **13**, 611-667.
- Harland, R.M. (1991). In situ hybridization: an improved whole-mount method for *Xenopus* embryos. *Methods in cell biology* **36**, 685-695.
- Hashimoto, M., Shinohara, K., Wang, J., Ikeuchi, S., Yoshida, S., Meno, C., Nonaka, S., Takada, S., Hatta, K., and Wynshaw-Boris, A., et al. (2010). Planar polarization of node cells determines the rotational axis of node cilia. *Nature cell biology* **12**, 170-176.
- Hayashi, K., Matsuda, S., Machida, K., Yamamoto, T., Fukuda, Y., Nimura, Y., Hayakawa, T., and Hamaguchi, M. (2001). Invasion activating caveolin-1 mutation in human scirrhous breast cancers. *Cancer research* **61**, 2361-2364.
- Hayer, A., Stoeber, M., Bissig, C., and Helenius, A. (2010). Biogenesis of caveolae: stepwise assembly of large caveolin and cavin complexes. *Traffic (Copenhagen, Denmark)* **11**, 361-382.

- Hayes, M., Naito, M., Daulat, A., Angers, S., and Ciruna, B. (2013). Ptk7 promotes non-canonical Wnt/PCP-mediated morphogenesis and inhibits Wnt/beta-catenin-dependent cell fate decisions during vertebrate development. *Development (Cambridge, England)* *140*, 1807-1818.
- He, T.C., Sparks, A.B., Rago, C., Hermeking, H., Zawel, L., da Costa, L.T., Morin, P.J., Vogelstein, B., and Kinzler, K.W. (1998). Identification of c-MYC as a target of the APC pathway. *Science (New York, N.Y.)* *281*, 1509-1512.
- He, X., Saint-Jeannet, J.P., Wang, Y., Nathans, J., Dawid, I., and Varmus, H. (1997). A member of the Frizzled protein family mediating axis induction by Wnt-5A. *Science (New York, N.Y.)* *275*, 1652-1654.
- Heasman, J., Crawford, A., Goldstone, K., Garner-Hamrick, P., Gumbiner, B., McCrea, P., Kintner, C., Noro, C.Y., and Wylie, C. (1994). Overexpression of cadherins and underexpression of beta-catenin inhibit dorsal mesoderm induction in early *Xenopus* embryos. *Cell* *79*, 791-803.
- Heisenberg, C.P., Tada, M., Rauch, G.J., Saude, L., Concha, M.L., Geisler, R., Stemple, D.L., Smith, J.C., and Wilson, S.W. (2000). Silberblick/Wnt11 mediates convergent extension movements during zebrafish gastrulation. *Nature* *405*, 76-81.
- Hikasa, H., and Sokol, S.Y. (2013). Wnt Signaling in Vertebrate Axis Specification. *Cold Spring Harbor perspectives in biology* *5*, a007955-a007955.
- Hill, M.M., Bastiani, M., Luetterforst, R., Kirkham, M., Kirkham, A., Nixon, S.J., Walser, P., Abankwa, D., Oorschot, V.M.J., and Martin, S., et al. (2008). PTRF-Cavin, a conserved cytoplasmic protein required for caveola formation and function. *Cell* *132*, 113-124.
- Hillen, W., and Berens, C. (1994). Mechanisms underlying expression of Tn10 encoded tetracycline resistance. *Annual review of microbiology* *48*, 345-369.
- Hillen, W., Gatz, C., Altschmied, L., Schollmeier, K., and Meier, I. (1983). Control of expression of the Tn10-encoded tetracycline resistance genes. Equilibrium and kinetic investigation of the regulatory reactions. *Journal of molecular biology* *169*, 707-721.
- Hofmann, K. (2000). A superfamily of membrane-bound O-acyltransferases with implications for wnt signaling. *Trends in biochemical sciences* *25*, 111-112.
- Holzer, T., Liffers, K., Rahm, K., Trageser, B., Ozbek, S., and Gradl, D. (2012). Live imaging of active fluorophore labelled Wnt proteins. *FEBS letters* *586*, 1638-1644.
- Hopwood, N.D., Pluck, A., and Gurdon, J.B. (1989a). A *Xenopus* mRNA related to *Drosophila* twist is expressed in response to induction in the mesoderm and the neural crest. *Cell* *59*, 893-903.
- Hopwood, N.D., Pluck, A., and Gurdon, J.B. (1989b). MyoD expression in the forming somites is an early response to mesoderm induction in *Xenopus* embryos. *The EMBO journal* *8*, 3409-3417.
- Houliston, E., and Elinson, R.P. (1992). Microtubules and cytoplasmic reorganization in the frog egg. *Current topics in developmental biology* *26*, 53-70.
- Houston, D.W., and Wylie, C. (2002). Cloning and expression of *Xenopus* Lrp5 and Lrp6 genes. *Mechanisms of development* *117*, 337-342.

- Huang, H.-C., and Klein, P.S. (2004). The Frizzled family: receptors for multiple signal transduction pathways. *Genome biology* 5, 234.
- Janda, C.Y., Waghray, D., Levin, A.M., Thomas, C., and Garcia, K.C. (2012). Structural basis of Wnt recognition by Frizzled. *Science* 337, 59-64.
- Jenny, A., Darken, R.S., Wilson, P.A., and Mlodzik, M. (2003). Prickle and Strabismus form a functional complex to generate a correct axis during planar cell polarity signaling. *The EMBO journal* 22, 4409-4420.
- Jesuthasan, S., and Stahle, U. (1997). Dynamic microtubules and specification of the zebrafish embryonic axis. *Current biology : CB* 7, 31-42.
- Jho, E.-h., Zhang, T., Domon, C., Joo, C.-K., Freund, J.-N., and Costantini, F. (2002). Wnt/ -Catenin/Tcf Signaling Induces the Transcription of Axin2, a Negative Regulator of the Signaling Pathway. *Molecular and cellular biology* 22, 1172-1183.
- Jiang, J., and Struhl, G. (1998). Regulation of the Hedgehog and Wingless signalling pathways by the F-box/WD40-repeat protein Slimb. *Nature* 391, 493-496.
- Jiang, Y., He, X., and Howe, P.H. (2012). Disabled-2 (Dab2) inhibits Wnt/beta-catenin signalling by binding LRP6 and promoting its internalization through clathrin. *The EMBO journal* 31, 2336-2349.
- Jung, J.-W., Shin, W.-S., Song, J., and Lee, S.-T. (2004). Cloning and characterization of the full-length mouse Ptk7 cDNA encoding a defective receptor protein tyrosine kinase. *Gene* 328, 75-84.
- Kadowaki, T., Wilder, E., Klingensmith, J., Zachary, K., and Perrimon, N. (1996). The segment polarity gene porcupine encodes a putative multitransmembrane protein involved in Wingless processing. *Genes & Development* 10, 3116-3128.
- Kelly, M., and Chen, P. (2007). Shaping the mammalian auditory sensory organ by the planar cell polarity pathway. *Int J Dev Biol* 51, 535-547.
- Kibar, Z., Torban, E., McDearmid, J.R., Reynolds, A., Berghout, J., Mathieu, M., Kirillova, I., Marco, P. de, Merello, E., and Hayes, J.M., et al. (2007). Mutations in VANGL1 associated with neural-tube defects. *N Engl J Med* 356, 1432-1437.
- Kiecker, C., and Niehrs, C. (2001). A morphogen gradient of Wnt/beta-catenin signalling regulates anteroposterior neural patterning in *Xenopus*. *Development (Cambridge, England)* 128, 4189-4201.
- Kikuchi, A., Yamamoto, H., and Sato, A. (2009). Selective activation mechanisms of Wnt signaling pathways. *Trends in cell biology* 19, 119-129.
- Kikuchi, A., Yamamoto, H., Sato, A., and Matsumoto, S. (2011). New insights into the mechanism of Wnt signaling pathway activation. *Int Rev Cell Mol Biol* 291, 21-71.
- Kilian, B., Mansukoski, H., Barbosa, F.C., Ulrich, F., Tada, M., and Heisenberg, C.P. (2003). The role of Ppt/Wnt5 in regulating cell shape and movement during zebrafish gastrulation. *Mechanisms of development* 120, 467-476.
- Kim, C.H., Oda, T., Itoh, M., Jiang, D., Artinger, K.B., Chandrasekharappa, S.C., Driever, W., and Chitnis, A.B. (2000). Repressor activity of Headless/Tcf3 is essential for vertebrate head formation. *Nature* 407, 913-916.

- Klein, T.J., and Mlodzik, M. (2004). A conserved signaling cassette regulates hair patterning from *Drosophila* to man. *Proceedings of the National Academy of Sciences of the United States of America* *101*, 9173-9174.
- Klingensmith, J., Noll, E., and Perrimon, N. (1989). The segment polarity phenotype of *Drosophila* involves differential tendencies toward transformation and cell death. *Dev Biol* *134*, 130-145.
- Klisch, T.J., Souopgui, J., Juergens, K., Rust, B., Pieler, T., and Henningfeld, K.A. (2006). Mxi1 is essential for neurogenesis in *Xenopus* and acts by bridging the pan-neural and proneural genes. *Developmental biology* *292*, 470-485.
- Komekado, H., Yamamoto, H., Chiba, T., and Kikuchi, A. (2007). Glycosylation and palmitoylation of Wnt-3a are coupled to produce an active form of Wnt-3a. *Genes Cells* *12*, 521-534.
- Kuhl, M., and Pandur, P. (2008). Dorsal axis duplication as a functional readout for Wnt activity. *Methods in molecular biology (Clifton, N.J.)* *469*, 467-476.
- Kurayoshi, M., Yamamoto, H., Izumi, S., and Kikuchi, A. (2007). Post-translational palmitoylation and glycosylation of Wnt-5a are necessary for its signalling. *Biochem J* *402*, 515-523.
- LaBonne, C., and Bronner-Fraser, M. (1998). Neural crest induction in *Xenopus*: evidence for a two-signal model. *Development (Cambridge, England)* *125*, 2403-2414.
- LAEMMLI, U.K. (1970). Cleavage of structural proteins during the assembly of the head of bacteriophage T4. *Nature* *227*, 680-685.
- Lajoie, P., and Nabi, I.R. (2010). Lipid Rafts, Caveolae, and Their Endocytosis. In (Elsevier), pp. 135–163.
- Larabell, C.A., Torres, M., Rowning, B.A., Yost, C., Miller, J.R., Wu, M., Kimelman, D., and Moon, R.T. (1997). Establishment of the dorso-ventral axis in *Xenopus* embryos is presaged by early asymmetries in beta-catenin that are modulated by the Wnt signaling pathway. *The Journal of cell biology* *136*, 1123-1136.
- Le, P.U., and Nabi, I.R. (2003). Distinct caveolae-mediated endocytic pathways target the Golgi apparatus and the endoplasmic reticulum. *Journal of cell science* *116*, 1059-1071.
- Le Lay, S., and Kurzchalia, T.V. (2005). Getting rid of caveolins: phenotypes of caveolin-deficient animals. *Biochimica et biophysica acta* *1746*, 322-333.
- Le Roy, C., and Wrana, J.L. (2005). Clathrin- and non-clathrin-mediated endocytic regulation of cell signalling. *Nature reviews. Molecular cell biology* *6*, 112-126.
- Lee, H., Park, D.S., Razani, B., Russell, R.G., Pestell, R.G., and Lisanti, M.P. (2002). Caveolin-1 mutations (P132L and null) and the pathogenesis of breast cancer: caveolin-1 (P132L) behaves in a dominant-negative manner and caveolin-1 (-/-) null mice show mammary epithelial cell hyperplasia. *The American journal of pathology* *161*, 1357-1369.
- Lee, H.K., Chauhan, S.K., Kay, E., and Dana, R. (2011). Flt-1 regulates vascular endothelial cell migration via a protein tyrosine kinase-7-dependent pathway. *Blood* *117*, 5762-5771.

- Lemaire, P., Garrett, N., and Gurdon, J.B. (1995). Expression cloning of Siamois, a *Xenopus* homeobox gene expressed in dorsal-vegetal cells of blastulae and able to induce a complete secondary axis. *Cell* 81, 85-94.
- Lhoumeau, A.-C., Puppo, F., Prebet, T., Kodjabachian, L., and Borg, J.-P. (2011). PTK7: a cell polarity receptor with multiple facets. *Cell cycle (Georgetown, Tex.)* 10, 1233-1236.
- Linnemannstöns, K., Ripp, C., Honemann-Capito, M., Brechtel-Curth, K., Hedderich, M., and Wodarz, A. (2014). The PTK7-related transmembrane proteins off-track and off-track 2 are co-receptors for *Drosophila* Wnt2 required for male fertility. *PLoS genetics* 10, e1004443.
- Liu, C., Kato, Y., Zhang, Z., Do, V.M., Yankner, B.A., and He, X. (1999). beta-Trcp couples beta-catenin phosphorylation-degradation and regulates *Xenopus* axis formation. *Proceedings of the National Academy of Sciences of the United States of America* 96, 6273-6278.
- Liu, C., Li, Y., Semenov, M., Han, C., Baeg, G.H., Tan, Y., Zhang, Z., Lin, X., and He, X. (2002a). Control of beta-catenin phosphorylation/degradation by a dual-kinase mechanism. *Cell* 108, 837-847.
- Liu, P., Rudick, M., and Anderson, R.G.W. (2002b). Multiple functions of caveolin-1. *The Journal of biological chemistry* 277, 41295-41298.
- Lu, X., Borchers, A.G.M., Jolicœur, C., Rayburn, H., Baker, J.C., and Tessier-Lavigne, M. (2004). PTK7/CCK-4 is a novel regulator of planar cell polarity in vertebrates. *Nature* 430, 93-98.
- MacDonald, B.T., Tamai, K., and He, X. (2009). Wnt/beta-catenin signaling: components, mechanisms, and diseases. *Dev Cell* 17, 9-26.
- Mao, J., Wang, J., Liu, B., Pan, W., Farr, G.H.3., Flynn, C., Yuan, H., Takada, S., Kimelman, D., and Li, L., et al. (2001). Low-density lipoprotein receptor-related protein-5 binds to Axin and regulates the canonical Wnt signaling pathway. *Molecular cell* 7, 801-809.
- Marcinkevicius, E., Fernandez-Gonzalez, R., and Zallen, J.A. (2009). Q&A: quantitative approaches to planar polarity and tissue organization. *Journal of biology* 8, 103.
- Marikawa, Y., and Elinson, R.P. (1998). beta-TrCP is a negative regulator of Wnt/beta-catenin signaling pathway and dorsal axis formation in *Xenopus* embryos. *Mechanisms of development* 77, 75-80.
- Matthews, H.K., Marchant, L., Carmona-Fontaine, C., Kuriyama, S., Larrain, J., Holt, M.R., Parsons, M., and Mayor, R. (2008). Directional migration of neural crest cells in vivo is regulated by Syndecan-4/Rac1 and non-canonical Wnt signaling/RhoA. *Development (Cambridge, England)* 135, 1771-1780.
- Mayor, R., and Theveneau, E. (2013). The neural crest. *Development (Cambridge, England)* 140, 2247-2251.
- McGrew, L.L., Takemaru, K., Bates, R., and Moon, R.T. (1999). Direct regulation of the *Xenopus* engrailed-2 promoter by the Wnt signaling pathway, and a molecular screen for Wnt-responsive genes, confirm a role for Wnt signaling during neural patterning in *Xenopus*. *Mechanisms of development* 87, 21-32.

- McNeill, H. (2010). Planar cell polarity: keeping hairs straight is not so simple. *Cold Spring Harbor perspectives in biology* 2, a003376.
- Miller, J.R., Rowning, B.A., Larabell, C.A., Yang-Snyder, J.A., Bates, R.L., and Moon, R.T. (1999). Establishment of the Dorsal-Ventral Axis in *Xenopus* Embryos Coincides with the Dorsal Enrichment of Dishevelled That Is Dependent on Cortical Rotation. *The Journal of cell biology* 146, 427-438.
- Miller, M.A., and Steele, R.E. (2000). Lemon encodes an unusual receptor protein-tyrosine kinase expressed during gametogenesis in *Hydra*. *Developmental biology* 224, 286-298.
- Mo, S., Wang, L., Li, Q., Li, J., Li, Y., Thannickal, V.J., and Cui, Z. (2010). Caveolin-1 regulates dorsoventral patterning through direct interaction with beta-catenin in zebrafish. *Developmental biology* 344, 210-223.
- Molenaar, M., van de Wetering, M., Oosterwegel, M., Peterson-Maduro, J., Godsave, S., Korinek, V., Roose, J., Destree, O., and Clevers, H. (1996). XTcf-3 transcription factor mediates beta-catenin-induced axis formation in *Xenopus* embryos. *Cell* 86, 391-399.
- Monier, S., Parton, R.G., Vogel, F., Behlke, J., Henske, A., and Kurzchalia, T.V. (1995). VIP21-caveolin, a membrane protein constituent of the caveolar coat, oligomerizes in vivo and in vitro. *Molecular Biology of the Cell* 6, 911-927.
- Montcouquiol, M., and Kelley, M.W. (2003). Planar and vertical signals control cellular differentiation and patterning in the mammalian cochlea. *The Journal of neuroscience : the official journal of the Society for Neuroscience* 23, 9469-9478.
- Montcouquiol, M., Rachel, R.A., Lanford, P.J., Copeland, N.G., Jenkins, N.A., and Kelley, M.W. (2003). Identification of *Vangl2* and *Scrb1* as planar polarity genes in mammals. *Nature* 423, 173-177.
- Mossie, K., Jallal, B., Alves, F., Sures, I., Plowman, G.D., and Ullrich, A. (1995). Colon carcinoma kinase-4 defines a new subclass of the receptor tyrosine kinase family. *Oncogene* 11, 2179-2184.
- Muller-Tidow, C., Schwable, J., Steffen, B., Tidow, N., Brandt, B., Becker, K., Schulze-Bahr, E., Halfter, H., Vogt, U., and Metzger, R., et al. (2004). High-throughput analysis of genome-wide receptor tyrosine kinase expression in human cancers identifies potential novel drug targets. *Clinical cancer research : an official journal of the American Association for Cancer Research* 10, 1241-1249.
- Mundy, Dorothy I.; Li, Wei Ping; Luby-Phelps, Katherine; Anderson, Richard G. W. (2012): Caveolin targeting to late endosome/lysosomal membranes is induced by perturbations of lysosomal pH and cholesterol content. In: *Molecular Biology of the Cell* 23 (5), S. 864-880. DOI: 10.1091/mbc.E11-07-0598.
- Nabi, I.R., and Le, P.U. (2003). Caveolae/raft-dependent endocytosis. *The Journal of cell biology* 161, 673-677.
- Navarro, A., Anand-Apte, B., and Parat, M.-O. (2004). A role for caveolae in cell migration. *FASEB journal : official publication of the Federation of American Societies for Experimental Biology* 18, 1801-1811.
- Niehrs, C. (2012). The complex world of WNT receptor signalling. *Nat. Rev. Mol. Cell Biol.* 13, 767-779.

- NIEUWKOOP, P.D. and FABER, J. (Eds.) (1956). Normal Table of *Xenopus laevis* (Daudin): A systematical and chronological survey of the development from the fertilized egg till the end of metamorphosis. North-Holland Publ. Co., Amsterdam.
- Nixon, S.J., Carter, A., Wegner, J., Ferguson, C., Floetenmeyer, M., Riches, J., Key, B., Westerfield, M., and Parton, R.G. (2007). Caveolin-1 is required for lateral line neuromast and notochord development. *Journal of cell science* *120*, 2151-2161.
- Nusse, R., and Varmus, H.E. (1982). Many tumors induced by the mouse mammary tumor virus contain a provirus integrated in the same region of the host genome. *Cell* *31*, 99-109.
- Oh, P., McIntosh, D.P., and Schnitzer, J.E. (1998). Dynamin at the neck of caveolae mediates their budding to form transport vesicles by GTP-driven fission from the plasma membrane of endothelium. *The Journal of cell biology* *141*, 101-114.
- Oishi, I., Suzuki, H., Onishi, N., Takada, R., Kani, S., Ohkawara, B., Koshida, I., Suzuki, K., Yamada, G., and Schwabe, G.C., et al. (2003). The receptor tyrosine kinase Ror2 is involved in non-canonical Wnt5a/JNK signalling pathway. *Genes Cells* *8*, 645-654.
- Palade, G.E. (1953). Fine structure of blood capillaries. *J. Appl. Phys.* *24*, 1424.
- Park, D.S., Cohen, A.W., Frank, P.G., Razani, B., Lee, H., Williams, T.M., Chandra, M., Shirani, J., Souza, A.P. de, and Tang, B., et al. (2003). Caveolin-1 null (-/-) mice show dramatic reductions in life span. *Biochemistry* *42*, 15124-15131.
- Park, D.S., Woodman, S.E., Schubert, W., Cohen, A.W., Frank, P.G., Chandra, M., Shirani, J., Razani, B., Tang, B., and Jelicks, L.A., et al. (2002). Caveolin-1/3 double-knockout mice are viable, but lack both muscle and non-muscle caveolae, and develop a severe cardiomyopathic phenotype. *The American journal of pathology* *160*, 2207-2217.
- Park, M., and Moon, R.T. (2002). The planar cell-polarity gene *stbm* regulates cell behaviour and cell fate in vertebrate embryos. *Nature cell biology* *4*, 20-25.
- Park, S.K., Lee, H.S., and Lee, S.T. (1996). Characterization of the human full-length PTK7 cDNA encoding a receptor protein tyrosine kinase-like molecule closely related to chick KLG. *Journal of biochemistry* *119*, 235-239.
- Parolini, I., Sargiacomo, M., Galbiati, F., Rizzo, G., Grignani, F., Engelman, J.A., Okamoto, T., Ikezu, T., Scherer, P.E., and Mora, R., et al. (1999). Expression of caveolin-1 is required for the transport of caveolin-2 to the plasma membrane. Retention of caveolin-2 at the level of the golgi complex. *The Journal of biological chemistry* *274*, 25718-25725.
- Parton, R.G., and del Pozo, M.A. (2013). Caveolae as plasma membrane sensors, protectors and organizers. *Nature reviews. Molecular cell biology* *14*, 98-112.
- Parton, R.G., and Simons, K. (2007). The multiple faces of caveolae. *Nature reviews. Molecular cell biology* *8*, 185-194.
- Paudyal, A., Damrau, C., Patterson, V.L., Ermakov, A., Formstone, C., Lalanne, Z., Wells, S., Lu, X., Norris, D.P., and Dean, C.H., et al. (2010). The novel mouse mutant, *chuzhoi*, has disruption of *Ptk7* protein and exhibits defects in neural tube, heart and lung development and abnormal planar cell polarity in the ear. *BMC Dev. Biol.* *10*, 87.

- Pelkmans, L., and Helenius, A. (2002). Endocytosis via caveolae. *Traffic* (Copenhagen, Denmark) *3*, 311-320.
- Pelkmans, L., and Zerial, M. (2005). Kinase-regulated quantal assemblies and kiss-and-run recycling of caveolae. *Nature* *436*, 128-133.
- Peradziryi, H., Kaplan, N.A., Podleschny, M., Liu, X., Wehner, P., Borchers, A., and Tolwinski, N.S. (2011). PTK7/Otk interacts with Wnts and inhibits canonical Wnt signalling. *EMBO J* *30*, 3729-3740.
- Peradziryi, H., Tolwinski, N.S., and Borchers, A. (2012). The many roles of PTK7: a versatile regulator of cell-cell communication. *Arch Biochem Biophys* *524*, 71-76.
- Petersen, C.P., and Reddien, P.W. (2009). Wnt signaling and the polarity of the primary body axis. *Cell* *139*, 1056-1068.
- Piao, S., Lee, S.-H., Kim, H., Yum, S., Stamos, J.L., Xu, Y., Lee, S.-J., Lee, J., Oh, S., and Han, J.-K., et al. (2008). Direct inhibition of GSK3beta by the phosphorylated cytoplasmic domain of LRP6 in Wnt/beta-catenin signaling. *PLoS one* *3*, e4046.
- Piper, R.C., and Katzmann, D.J. (2007). Biogenesis and function of multivesicular bodies. *Annual review of cell and developmental biology* *23*, 519-547.
- Pizzuti, A., Amati, F., Calabrese, G., Mari, A., Colosimo, A., Silani, V., Giardino, L., Ratti, A., Penso, D., and Calza, L., et al. (1996). cDNA characterization and chromosomal mapping of two human homologues of the *Drosophila* dishevelled polarity gene. *Human molecular genetics* *5*, 953-958.
- Port, F., Kuster, M., Herr, P., Furger, E., Banziger, C., Hausmann, G., and Basler, K. (2008). Wingless secretion promotes and requires retromer-dependent cycling of Wntless. *Nature cell biology* *10*, 178-185.
- Pulido, D., Campuzano, S., Koda, T., Modolell, J., and Barbacid, M. (1992). Dtrk, a *Drosophila* gene related to the trk family of neurotrophin receptors, encodes a novel class of neural cell adhesion molecule. *The EMBO journal* *11*, 391-404.
- Puppo, F., Thome, V., Lhoumeau, A.-C., Cibois, M., Gangar, A., Lembo, F., Belotti, E., Marchetto, S., Lecine, P., and Prebet, T., et al. (2011). Protein tyrosine kinase 7 has a conserved role in Wnt/beta-catenin canonical signalling. *EMBO reports* *12*, 43-49.
- Razani, B., Engelman, J.A., Wang, X.B., Schubert, W., Zhang, X.L., Marks, C.B., Macaluso, F., Russell, R.G., Li, M., and Pestell, R.G., et al. (2001). Caveolin-1 null mice are viable but show evidence of hyperproliferative and vascular abnormalities. *The Journal of biological chemistry* *276*, 38121-38138.
- Razani, B., Park, D.S., Miyana, Y., Ghatpande, A., Cohen, J., Wang, X.B., Scherer, P.E., Evans, T., and Lisanti, M.P. (2002a). Molecular cloning and developmental expression of the caveolin gene family in the amphibian *Xenopus laevis*. *Biochemistry* *41*, 7914-7924.
- Razani, B., Wang, X.B., Engelman, J.A., Battista, M., Lagaud, G., Zhang, X.L., Kneitz, B., Hou, H., JR, Christ, G.J., and Edelman, W., et al. (2002b). Caveolin-2-deficient mice show evidence of severe pulmonary dysfunction without disruption of caveolae. *Molecular and cellular biology* *22*, 2329-2344.

- Rodal, S.K., Skretting, G., Garred, Ø., Vilhardt, F., van Deurs, B., and Sandvig, K. (1999). Extraction of Cholesterol with Methyl- β -Cyclodextrin Perturbs Formation of Clathrin-coated Endocytic Vesicles. *Molecular Biology of the Cell* 10, 961–974,
- Roose, J., Molenaar, M., Peterson, J., Hurenkamp, J., Brantjes, H., Moerer, P., van de Wetering, M., Destree, O., and Clevers, H. (1998). The *Xenopus* Wnt effector XTcf-3 interacts with Groucho-related transcriptional repressors. *Nature* 395, 608-612.
- Rosso, S.B., Sussman, D., Wynshaw-Boris, A., and Salinas, P.C. (2005). Wnt signaling through Dishevelled, Rac and JNK regulates dendritic development. *Nature neuroscience* 8, 34-42.
- Rothbacher, U., Laurent, M.N., Deardorff, M.A., Klein, P.S., Cho, K.W., and Fraser, S.E. (2000). Dishevelled phosphorylation, subcellular localization and multimerization regulate its role in early embryogenesis. *The EMBO journal* 19, 1010-1022.
- Rothberg, K.G., Heuser, J.E., Donzell, W.C., Ying, Y.S., Glenney, J.R., and Anderson, R.G. (1992). Caveolin, a protein component of caveolae membrane coats. *Cell* 68, 673-682.
- Rupp, R.A., Snider, L., and Weintraub, H. (1994). *Xenopus* embryos regulate the nuclear localization of XMyoD. *Genes & Development* 8, 1311-1323.
- Russel, S.a., 2001. *Molecular Cloning: a laboratory manual* 3rd ed. Cold Spring Harbour Laboratory Press
- Saiki, R.K., Gelfand, D.H., Stoffel, S., Scharf, S.J., Higuchi, R., Horn, G.T., Mullis, K.B., and Erlich, H.A. (1988). Primer-directed enzymatic amplification of DNA with a thermostable DNA polymerase. *Science (New York, N.Y.)* 239, 487-491.
- Sakane, H., Yamamoto, H., and Kikuchi, A. (2010). LRP6 is internalized by Dkk1 to suppress its phosphorylation in the lipid raft and is recycled for reuse. *Journal of cell science* 123, 360-368.
- Sanger, F., Nicklen, S., and Coulson, A.R. (1977). DNA sequencing with chain-terminating inhibitors. *Proceedings of the National Academy of Sciences of the United States of America* 74, 5463-5467.
- Sato, A., Yamamoto, H., Sakane, H., Koyama, H., and Kikuchi, A. (2010). Wnt5a regulates distinct signalling pathways by binding to Frizzled2. *The EMBO journal* 29, 41-54.
- Scharf, S.R., and Gerhart, J.C. (1980). Determination of the dorsal-ventral axis in eggs of *Xenopus laevis*: complete rescue of uv-impaired eggs by oblique orientation before first cleavage. *Developmental biology* 79, 181-198.
- Scherer, P.E., Lewis, R.Y., Volonte, D., Engelman, J.A., Galbiati, F., Couet, J., Kohtz, D.S., van Donselaar, E., Peters, P., and Lisanti, M.P. (1997). Cell-type and tissue-specific expression of caveolin-2. Caveolins 1 and 2 co-localize and form a stable hetero-oligomeric complex in vivo. *The Journal of biological chemistry* 272, 29337-29346.
- Scherer, P.E., Okamoto, T., Chun, M., Nishimoto, I., Lodish, H.F., and Lisanti, M.P. (1996). Identification, sequence, and expression of caveolin-2 defines a caveolin gene family. *Proceedings of the National Academy of Sciences of the United States of America* 93, 131-135.

- Scherer, P.E., Tang, Z., Chun, M., Sargiacomo, M., Lodish, H.F., and Lisanti, M.P. (1995). Caveolin isoforms differ in their N-terminal protein sequence and subcellular distribution. Identification and epitope mapping of an isoform-specific monoclonal antibody probe. *The Journal of biological chemistry* 270, 16395-16401.
- Schier, A.F., and Talbot, W.S. (2005). Molecular genetics of axis formation in zebrafish. *Annual review of genetics* 39, 561-613.
- Schlegel, A., and Lisanti, M.P. (2000). A molecular dissection of caveolin-1 membrane attachment and oligomerization. Two separate regions of the caveolin-1 C-terminal domain mediate membrane binding and oligomer/oligomer interactions in vivo. *The Journal of biological chemistry* 275, 21605-21617.
- Schohl, A., and Fagotto, F. (2002). Beta-catenin, MAPK and Smad signaling during early *Xenopus* development. *Development (Cambridge, England)* 129, 37-52.
- Semenov, M.V., and Snyder, M. (1997). Human dishevelled genes constitute a DHR-containing multigene family. *Genomics* 42, 302-310.
- Sharp, P.A., Sugden, B., and Sambrook, J. (1973). Detection of two restriction endonuclease activities in *Haemophilus parainfluenzae* using analytical agarose-ethidium bromide electrophoresis. *Biochemistry* 12, 3055-3063.
- Shin, W.-S., Maeng, Y.-S., Jung, J.-W., Min, J.-K., Kwon, Y.-G., and Lee, S.-T. (2008). Soluble PTK7 inhibits tube formation, migration, and invasion of endothelial cells and angiogenesis. *Biochemical and biophysical research communications* 371, 793-798.
- Shnitsar, I., and Borchers, A. (2008). PTK7 recruits dsh to regulate neural crest migration. *Development* 135, 4015-4024.
- Shvets, E., Ludwig, A., and Nichols, B.J. (2014). News from the caves: update on the structure and function of caveolae. *Current opinion in cell biology* 29, 99-106.
- Simons, M., and Mlodzik, M. (2008). Planar cell polarity signaling: from fly development to human disease. *Annual review of genetics* 42, 517-540.
- Smart, E.J., and Anderson, R.G.W. (2002). Alterations in membrane cholesterol that affect structure and function of caveolae. *Methods in enzymology* 353, 131-139.
- Smith, J.C., Price, B.M., Green, J.B., Weigel, D., and Herrmann, B.G. (1991). Expression of a *Xenopus* homolog of Brachyury (T) is an immediate-early response to mesoderm induction. *Cell* 67, 79-87.
- Smith, W.C., and Harland, R.M. (1991). Injected Xwnt-8 RNA acts early in *Xenopus* embryos to promote formation of a vegetal dorsalizing center. *Cell* 67, 753-765.
- Sokol, S., Christian, J.L., Moon, R.T., and Melton, D.A. (1991). Injected Wnt RNA induces a complete body axis in *Xenopus* embryos. *Cell* 67, 741-752.
- Sokol, S.Y. (1999). Wnt signaling and dorso-ventral axis specification in vertebrates. *Current Opinion in Genetics & Development* 9, 405-410.
- Sokol, S.Y. (2015). Spatial and temporal aspects of Wnt signaling and planar cell polarity during vertebrate embryonic development. *Semin Cell Dev Biol*.
- Sokol, S.Y., Klingensmith, J., Perrimon, N., and Itoh, K. (1995). Dorsalizing and neuralizing properties of Xdsh, a maternally expressed *Xenopus* homolog of dishevelled. *Development (Cambridge, England)* 121, 3487.

- Steinman, R.M., Mellman, I.S., Muller, W.A., and Cohn, Z.A. (1983). Endocytosis and the recycling of plasma membrane. *J Cell Biol* 96, 1-27.
- Strigini, M., and Cohen, S.M. (2000). Wingless gradient formation in the *Drosophila* wing. *Current biology* : CB 10, 293-300.
- Sussman, D.J., Klingensmith, J., Salinas, P., Adams, P.S., Nusse, R., and Perrimon, N. (1994). Isolation and characterization of a mouse homolog of the *Drosophila* segment polarity gene *dishevelled*. *Developmental biology* 166, 73-86.
- Tada, M., and Smith, J.C. (2000). *Xwnt11* is a target of *Xenopus* Brachyury: regulation of gastrulation movements via *Dishevelled*, but not through the canonical Wnt pathway. *Development (Cambridge, England)* 127, 2227-2238.
- Taelman, V.F., Dobrowolski, R., Plouhinec, J.-L., Fuentealba, L.C., Vorwald, P.P., Gumper, I., Sabatini, D.D., and Robertis, E.M. de (2010). *Cell* 143, 1136-1148.
- Takada, R., Satomi, Y., Kurata, T., Ueno, N., Norioka, S., Kondoh, H., Takao, T., and Takada, S. (2006). Monounsaturated fatty acid modification of Wnt protein: its role in Wnt secretion. *Developmental cell* 11, 791-801.
- Takahashi, T., Fournier, A., Nakamura, F., Wang, L.-H., Murakami, Y., Kalb, R.G., Fujisawa, H., and Strittmatter, S.M. (1999). Plexin-Neuropilin-1 Complexes Form Functional Semaphorin-3A Receptors. *Cell* 99, 59-69.
- Tamagnone, L., Artigiani, S., Chen, H., He, Z., Ming, G.-l., Song, H.-j., Chedotal, A., Winberg, M.L., Goodman, C.S., and Poo, M.-m., et al. (1999). Plexins Are a Large Family of Receptors for Transmembrane, Secreted, and GPI-Anchored Semaphorins in Vertebrates. *Cell* 99, 71-80.
- Tamai, K., Zeng, X., Liu, C., Zhang, X., Harada, Y., Chang, Z., and He, X. (2004). A mechanism for Wnt coreceptor activation. *Molecular cell* 13, 149-156.
- Tanaka, K., Kitagawa, Y., and Kadowaki, T. (2002). *Drosophila* segment polarity gene product porcupine stimulates the posttranslational N-glycosylation of wingless in the endoplasmic reticulum. *The Journal of biological chemistry* 277, 12816-12823.
- Tang, Z., Okamoto, T., Boontrakulpoontawee, P., Katada, T., Otsuka, A.J., and Lisanti, M.P. (1997). Identification, sequence, and expression of an invertebrate caveolin gene family from the nematode *Caenorhabditis elegans*. Implications for the molecular evolution of mammalian caveolin genes. *The Journal of biological chemistry* 272, 2437-2445.
- Tang, Z., Scherer, P.E., Okamoto, T., Song, K., Chu, C., Kohtz, D.S., Nishimoto, I., Lodish, H.F., and Lisanti, M.P. (1996). Molecular cloning of caveolin-3, a novel member of the caveolin gene family expressed predominantly in muscle. *The Journal of biological chemistry* 271, 2255-2261.
- Tao, Q., Yokota, C., Puck, H., Kofron, M., Birsoy, B., Yan, D., Asashima, M., Wylie, C.C., Lin, X., and Heasman, J. (2005). Maternal *wnt11* activates the canonical wnt signaling pathway required for axis formation in *Xenopus* embryos. *Cell* 120, 857-871.
- Taylor, J., Abramova, N., Charlton, J., and Adler, P.N. (1998). Van Gogh: a new *Drosophila* tissue polarity gene. *Genetics* 150, 199-210.
- Tetsu, O., and McCormick, F. (1999). Beta-catenin regulates expression of cyclin D1 in colon carcinoma cells. *Nature* 398, 422-426.

- Theisen, H., Purcell, J., Bennett, M., Kansagara, D., Syed, A., and Marsh, J.L. (1994). Dishevelled is required during wingless signaling to establish both cell polarity and cell identity. *Development* 120, 347-360.
- Toyofuku, T., Zhang, H., Kumanogoh, A., Takegahara, N., Suto, F., Kamei, J., Aoki, K., Yabuki, M., Hori, M., and Fujisawa, H., et al. (2004). Dual roles of Semaphorin 6D in cardiac morphogenesis through region-specific association of its receptor, Plexin-A1, with off-track and vascular endothelial growth factor receptor type 2. *Genes & Development* 18, 435-447.
- Traub, L.M. (2009). Clathrin couture: fashioning distinctive membrane coats at the cell surface. *PLoS biology* 7, e1000192.
- Tree, D.R.P., Shulman, J.M., Rousset, R., Scott, M.P., Gubb, D., and Axelrod, J.D. (2002). Prickle mediates feedback amplification to generate asymmetric planar cell polarity signaling. *Cell* 109, 371-381.
- Umbhauer, M., Djiane, A., Goisset, C., Penzo-Mendez, A., Riou, J.F., Boucaut, J.C., and Shi, D.L. (2000). The C-terminal cytoplasmic Lys-thr-X-X-X-Trp motif in frizzled receptors mediates Wnt/beta-catenin signalling. *The EMBO journal* 19, 4944-4954.
- Usui, T., Shima, Y., Shimada, Y., Hirano, S., Burgess, R.W., Schwarz, T.L., Takeichi, M., and Uemura, T. (1999). Flamingo, a seven-pass transmembrane cadherin, regulates planar cell polarity under the control of Frizzled. *Cell* 98, 585-595.
- van den Heuvel, M., Nusse, R., Johnston, P., and Lawrence, P.A. (1989a). Distribution of the wingless gene product in *Drosophila* embryos: a protein involved in cell-cell communication. *Cell* 59, 739-749.
- van den Heuvel, M., Nusse, R., Johnston, P., and Lawrence, P.A. (1989b). Distribution of the wingless gene product in *Drosophila* embryos: a protein involved in cell-cell communication. *Cell* 59, 739-749.
- Verkaar, F., and Zaman, G.J.R. (2010). A model for signaling specificity of Wnt/Frizzled combinations through co-receptor recruitment. *FEBS Lett.* 584, 3850-3854.
- Vinson, C.R., and Adler, P.N. (1987a). Directional non-cell autonomy and the transmission of polarity information by the frizzled gene of *Drosophila*. *Nature* 329, 549-551.
- Vinson, C.R., and Adler, P.N. (1987b). Directional non-cell autonomy and the transmission of polarity information by the frizzled gene of *Drosophila*. *Nature* 329, 549-551.
- Vinson, C.R., Conover, S., and Adler, P.N. (1989). A *Drosophila* tissue polarity locus encodes a protein containing seven potential transmembrane domains. *Nature* 338, 263-264.
- Vinten, J., Johnsen, A.H., Roepstorff, P., Harpoth, J., and Tranum-Jensen, J. (2005). Identification of a major protein on the cytosolic face of caveolae. *Biochimica et biophysica acta* 1717, 34-40.
- Vladar, E.K., Antic, D., and Axelrod, J.D. (2009). Planar cell polarity signaling: the developing cell's compass. *Cold Spring Harb Perspect Biol* 1, a002964.
- Wagner, G., Peradziryi, H., Wehner, P., and Borchers, A. (2010). PlexinA1 interacts with PTK7 and is required for neural crest migration. *Biochemical and biophysical research communications* 402, 402-407.

- Wallingford, J.B. (2012). Planar cell polarity and the developmental control of cell behavior in vertebrate embryos. *Annu. Rev. Cell Dev. Biol.* 28, 627-653.
- Wallingford, J.B., and Habas, R. (2005). The developmental biology of Dishevelled: an enigmatic protein governing cell fate and cell polarity. *Development* 132, 4421-4436.
- Wallingford, J.B., and Harland, R.M. (2002). Neural tube closure requires Dishevelled-dependent convergent extension of the midline. *Development* 129, 5815-5825.
- Wallingford, J.B., Rowning, B.A., Vogeli, K.M., Rothbacher, U., Fraser, S.E., and Harland, R.M. (2000). Dishevelled controls cell polarity during *Xenopus* gastrulation. *Nature* 405, 81-85.
- Wallingford, J.B., Vogeli, K.M., and Harland, R.M. (2001). Regulation of convergent extension in *Xenopus* by Wnt5a and Frizzled-8 is independent of the canonical Wnt pathway. *The International journal of developmental biology* 45, 225-227.
- Wallkamm, V., Dörlich, R., Rahm, K., Klessing, T., Nienhaus, G.U., Wedlich, D., and Gradl, D. (2014). Live imaging of Xwnt5A-ROR2 complexes. *PloS one* 9, e109428.
- Wang, B., Sinha, T., Jiao, K., Serra, R., and Wang, J. (2011). Disruption of PCP signaling causes limb morphogenesis and skeletal defects and may underlie Robinow syndrome and brachydactyly type B. *Human molecular genetics* 20, 271-285.
- Wang, Y., Guo, N., and Nathans, J. (2006). The role of Frizzled3 and Frizzled6 in neural tube closure and in the planar polarity of inner-ear sensory hair cells. *J. Neurosci.* 26, 2147-2156.
- Wang, Y., Macke, J.P., Abella, B.S., Andreasson, K., Worley, P., Gilbert, D.J., Copeland, N.G., Jenkins, N.A., and Nathans, J. (1996). A large family of putative transmembrane receptors homologous to the product of the *Drosophila* tissue polarity gene frizzled. *The Journal of biological chemistry* 271, 4468-4476.
- Wang, Y., and Nathans, J. (2007). Tissue/planar cell polarity in vertebrates: new insights and new questions. *Development* 134, 647-658.
- Way, M., and Parton, R.G. (1995). M-caveolin, a muscle-specific caveolin-related protein. *FEBS letters* 376, 108-112.
- Weaver, C., and Kimelman, D. (2004). Move it or lose it: axis specification in *Xenopus*. *Development (Cambridge, England)* 131, 3491-3499.
- Wehner, P., Shnitsar, I., Urlaub, H., and Borchers, A. (2011). RACK1 is a novel interaction partner of PTK7 that is required for neural tube closure. *Development* 138, 1321-1327.
- Willert, K., Brown, J.D., Danenberg, E., Duncan, A.W., Weissman, I.L., Reya, T., Yates, J.R.3., and Nusse, R. (2003). Wnt proteins are lipid-modified and can act as stem cell growth factors. *Nature* 423, 448-452.
- Willert, K., and Nusse, R. (2012). Wnt proteins. *Cold Spring Harb Perspect Biol* 4, a007864.
- Williams, T.M., and Lisanti, M.P. (2004). The caveolin proteins. *Genome biology* 5, 214.
- Winberg, M.L., Noordermeer, J.N., Tamagnone, L., Comoglio, P.M., Spriggs, M.K., Tessier-Lavigne, M., and Goodman, C.S. (1998). Plexin A Is a Neuronal Semaphorin Receptor that Controls Axon Guidance. *Cell* 95, 903-916.

- Winberg, M.L., Tamagnone, L., Bai, J., Comoglio, P.M., Montell, D., and Goodman, C.S. (2001). The transmembrane protein Off-track associates with Plexins and functions downstream of Semaphorin signaling during axon guidance. *Neuron* *32*, 53-62.
- Winter, C.G., Wang, B., Ballew, A., Royou, A., Karess, R., Axelrod, J.D., and Luo, L. (2001). *Drosophila* Rho-associated kinase (Drok) links Frizzled-mediated planar cell polarity signaling to the actin cytoskeleton. *Cell* *105*, 81-91.
- Wolff, T., and Rubin, G.M. (1998). Strabismus, a novel gene that regulates tissue polarity and cell fate decisions in *Drosophila*. *Development* *125*, 1149-1159.
- Wong, G.T., Gavin, B.J., and McMahon, A.P. (1994). Differential transformation of mammary epithelial cells by Wnt genes. *Molecular and cellular biology* *14*, 6278-6286.
- Wong, H.-C., Bourdelas, A., Krauss, A., Lee, H.-J., Shao, Y., Wu, D., Mlodzik, M., Shi, D.-L., and Zheng, J. (2003). Direct binding of the PDZ domain of Dishevelled to a conserved internal sequence in the C-terminal region of Frizzled. *Molecular cell* *12*, 1251-1260.
- Woodman, S.E., Sotgia, F., Galbiati, F., Minetti, C., and Lisanti, M.P. (2004). Caveolinopathies: mutations in caveolin-3 cause four distinct autosomal dominant muscle diseases. *Neurology* *62*, 538-543.
- Wouda, R.R., Bansraj, Monique R K S, de Jong, Anja W M, Noordermeer, J.N., and Fradkin, L.G. (2008). Src family kinases are required for WNT5 signaling through the Derailed/RYK receptor in the *Drosophila* embryonic central nervous system. *Development (Cambridge, England)* *135*, 2277-2287.
- Wu, G., Huang, H., Garcia Abreu, J., and He, X. (2009). Inhibition of GSK3 phosphorylation of beta-catenin via phosphorylated PPPSPXS motifs of Wnt coreceptor LRP6. *PLoS one* *4*, e4926.
- Wu, J., Roman, A.-C., Carvajal-Gonzalez, J.M., and Mlodzik, M. (2013). Wg and Wnt4 provide long-range directional input to planar cell polarity orientation in *Drosophila*. *Nature cell biology* *15*, 1045-1055.
- Yamaguchi, T.P. (2001). Heads or tails. Wnts and anterior–posterior patterning. *Current Biology* *11*, R713-R724.
- Yamamoto, H., Komekado, H., and Kikuchi, A. (2006). Caveolin is necessary for Wnt-3a-dependent internalization of LRP6 and accumulation of beta-catenin. *Dev Cell* *11*, 213-223.
- Yamamoto, H., Sakane, H., Michiue, T., and Kikuchi, A. (2008). Wnt3a and Dkk1 regulate distinct internalization pathways of LRP6 to tune the activation of beta-catenin signaling. *Dev Cell* *15*, 37-48.
- Yost, C., Torres, M., Miller, J.R., Huang, E., Kimelman, D., and Moon, R.T. (1996). The axis-inducing activity, stability, and subcellular distribution of beta-catenin is regulated in *Xenopus* embryos by glycogen synthase kinase 3. *Genes & Development* *10*, 1443-1454.
- Yu, A., Rual, J.-F., Tamai, K., Harada, Y., Vidal, M., He, X., and Kirchhausen, T. (2007). Association of Dishevelled with the clathrin AP-2 adaptor is required for Frizzled endocytosis and planar cell polarity signaling. *Developmental cell* *12*, 129-141.
- Zeng, X., Tamai, K., Doble, B., Li, S., Huang, H., Habas, R., Okamura, H., Woodgett, J., and He, X. (2005). A dual-kinase mechanism for Wnt co-receptor phosphorylation and activation. *Nature* *438*, 873-877.

Zerial, M., and McBride, H. (2001). Rab proteins as membrane organizers. *Nature reviews. Molecular cell biology* 2, 107-117.

Curriculum Vitae

Personal data

Name Hanna Irena Berger
Date of Birth 02.07.1987
Place of Birth Katowice, Poland
Address Ockershäuserstraße 59, 35037 Marburg, Germany
Email hanna.berger@biologie.uni-marburg.de

Education

01/2012 – 12/2015 **Doctoral studies:** “PTK7 protein localization and stability is affected by canonical Wnt ligands”.
01.2012- 03.2013: Department of Developmental Biochemistry, Georg August University of Göttingen, Germany
04.2013-12.2015: Molecular Embryology, Philipps University of Marburg, Germany. Advisor: Prof. Dr. A. Borchers

10/2009-10/2011 **Master studies in Microbiology and Biochemistry (M.Sc.):**
“Characterization of putative transcription factors in *Aspergillus fumigatus*”. Department of Molecular Microbiology and Genetics, Georg August University of Göttingen, Germany. Advisor: Prof. Dr. G. Braus

10/2006-08/2009 **Bachelor studies in Biology (B.Sc.):** “The Analysis of α -Synuclein in *Saccharomyces cerevisiae*”. Department of Molecular Microbiology and Genetics, Georg August University of Göttingen, Germany. Advisor: Prof. Dr. G. Braus

06/2006 **Abitur**, Albert-Schweitzer-Schule Kassel, Germany